On Techno-economic Evaluation of Wind-based DG

by

Mohammed Hamdan Hamed Albadi

A thesis
presented to the University of Waterloo
in fulfillment of the
thesis requirement for the degree of
Doctor of Philosophy
in
Electrical and Computer Engineering

Waterloo, Ontario, Canada, 2010

AUTHOR'S DECLARATION

I hereby declare that I am the sole author of this thesis. This is a true copy of the thesis, including any required final revisions, as accepted by my examiners.

I understand that my thesis may be made electronically available to the public.

Abstract

The growing interest in small-scale electricity generation located near customers, known as Distributed Generation (DG), is driven primarily by emerging technologies, environmental regulations and concerns, electricity market restructuring, and growing customer demand for increased quality and reliability of the electricity supply. Wind turbines are one of the renewable DG technologies that have become an important source of electricity in many parts of the world. Wind power can be used in many places to provide a viable solution to rising demand, energy security and independence, and climate change mitigation. This research aims broadly at facilitating the integration of wind-based DG without jeopardizing the system's economics and reliability. To achieve this goal, the thesis tackles wind power from three perspectives: those of the policy maker, the investor, and the system operator.

Generally, the economic viability of a project is determined within the framework of relevant policies. Therefore, these policies influence the decisions of potential investors in wind power. From this perspective, chapters 3 and 4 investigate the influence of policies on the economic viability of wind-based DG projects. In chapter 3, the role of Ontario's taxation and incentive policies in the economic viability of wind-based DG projects is investigated. In this study, the effects of provincial income taxes, capital cost allowances, property taxes, and relevant federal incentives are considered. Net Present Value (NPV) and Internal Rate of Return (IRR) for different scenarios are used to assess the project's viability under the Ontario Standard Offer Program (SOP) for wind power.

In chapter 4, the thesis proposes the use of wind power as a source of electricity in a new city being developed in the Duqm area of Oman, where no policies supporting renewable energy exist. The study shows that the cost of electricity produced by wind turbines is higher than that of the existing generation system, due to the subsidized prices of domestically available natural gas. However, given high international natural gas prices, the country's long-term Liquefied Natural Gas (LNG) export obligations, and the expansion of natural gas-based industries, investments in wind power in Duqm can be justified. A feed-in tariff and capital cost allowance policies are recommended to facilitate investments in this sector.

From a wind-based DG investor's perspective, the optimal selection of wind turbines can make wind power more economical, as illustrated in chapters 5 and 6. In chapter 5, the thesis presents a new generic model for Capacity Factor (*CF*) estimation using wind speed characteristics at any site and the power performance curve parameters of any pitch-regulated wind turbine. Compared to the existing model, the proposed formulation is simpler and results in more accurate CF estimation. CF models can be used by wind-based DG investors for optimal turbine-site matching applications. However, in chapter 6, the thesis

demonstrates that using CF models as the sole basis for turbine-site matching applications tends to produce results that are biased towards higher towers but do not include the associated costs. Therefore, a novel formulation for the turbine-site matching problem, based on a modified CF formulation that does include turbine tower height, is introduced in chapter 6. The proposed universal Turbine-Site Matching Index ($TSMI$) also includes the effects of turbine rated power and tower height on the initial capital cost of wind turbines.

Chapter 7 tackles wind power from a power system operator's perspective. Despite wind power benefits, the effects of its intermittent nature on power systems need to be carefully examined as penetration levels increase. In this chapter, the thesis investigates the effects of different temporal wind profiles on the scheduling costs of thermal generation units. Two profiles are considered: synoptic-dominated and diurnal-dominated variations of aggregated wind power. To simulate wind profile impacts, a linear mixed-integer unit commitment problem is formulated in a GAMS environment. The uncertainty associated with wind power is represented using a chance constrained formulation. The simulation results illustrate the significant impacts of different wind profiles on fuel saving benefits, startup costs, and wind power curtailments. In addition, the results demonstrate the importance of the wide geographical dispersion of wind power production facilities to minimize the impacts of network constraints on the value of the harvested wind energy and the amount of curtailed energy.

Acknowledgements

I praise and thank Allah almighty for helping me through this work.

I would like to express my gratitude and appreciation to my advisor, Professor Ehab El-Saadany, for his guidance and support throughout my PhD studies.

I highly appreciate the constructive comments of my external examiner, Professor Mohamed E. El-Hawary.

I would like to thank my doctoral committee members, Professor Paul Parker, Professor Mehrdad Kazerani and Professor Kankar Bhattacharya, for their insightful comments and suggestions.

I gratefully appreciate the financial support received from my employer, Sultan Qaboos University, Muscat, Oman.

Finally, I would like to thank my parents, my wife, and my children for their understanding, encouragement and continuous support.

Dedication

To all those who are striving for a better future for Humanity and the Environment

Table of Contents

List of Figures

List of Tables

Nomenclature

A	Annuity
ACF	Annual cash flow
AD	Annual depreciation
ADB	Accelerated declining balance depreciation method
A_s	Swept rotor Area in (m^2)
B_{kj}	Line k-j charging susceptance in p.u.
c	Scale factor in (m/s)
CCA	Capital cost allowance
CF	Capacity factor
CPP	Critical Peak Pricing
CSC_i	Cold start costs of the i^{th} unit
CST_i	Number of U_{off} hours at which CSC_i would be incurred if the unit is started up
$C(v)$	Cumulative distribution function
COE	Cost of electricity in ($/kWh)
C_p	Turbine coefficient of performance
DB	Declining balance depreciation method
DCCF	Discounted cumulative cash flow
DCF	Discounted cash flow
DR	Demand response
dr	Discount rate
E_a	Annual energy yield of a wind turbine
EDF	Electricite De France
EDP	Extreme Day Pricing
ED-CPP	Extreme Day Critical Peak Pricing
$e_{ND,t}$	Forecast error of net demand during hour t
$e_{PD,t}$	Forecast error of demand during hour t
$e_{wind,t}$	Forecast error of wind power during hour t
EIA	Energy Information Administration
FC_{it}	Fuel cost of the i^{th} unit during hour t
FIT	Feed-in tariff
FV	Future value
$f(v_x)$	Probability of having a speed of v_x

g	Gravitational constant in (m/s^2)
GDB	Gross domestic product
h	Tower height in (m)
HSC_i	Hot start costs of the i^{th} unit
ICC	Initial capital cost ($/kW)
ICE	Internal combustion engine
IBP	Incentive Based Programs
IRR	Internal rate of return
J	Total generation costs
k	Shape factor
LMP	Locational marginal prices
LNG	Liquefied natural gas
LR	Long-range customers
LSF	Load scaling factor
MBP	Market Based Programs
MC	Maintenance cost ($/MW)
MIS	Main Interconnected System (of Oman)
MP	Market price for electricity
MR	Must-run units
MT	microturbines
MWS	Mean wind speed (m/s)
N	Number of years in the future
ND_t^f	Day-ahead forecasted net demand during hour t
NG	Number of generation units
NPV	Net present value
NYISO	New York independent system operator
OC	Operational costs
OMR	Omani Riyal (1 OMR = 2.59 US$)
OPF	Optimal power flow
O&M	Annual operational and maintenance cost
P_0	Standard sea level atmospheric pressure in (Pa)
PAEW	Public Authority for Electricity and Water (of Oman)
pdf	Probability density function

$PD_{k,t}$	Real power demand at bus k during hour t
PD_t^f	Day-ahead forecasted demand during hour t
P_e	Wind turbine output power
P_{it}	Output of the i^{th} unit during hour t
$P_{i,max}$	Upper limit of P_i
$P_{k,t}$	Output of the thermal units connected to bus k during hour t
P_{kj}^{max}	Capacity limit of the line kj
PV	Photovoltaic cells
Pr	Price of the asset
$P_{wind,t}$	Accommodated wind power during hour t
$P^f_{wind,t}$	Day-ahead forecasted wind power during hour t
PPA	Power purchase agreement
P_{rated}	Wind turbine rated output
PP	Payback period
PV	Present value
PV_A	Present value of the recurring annuity
Q_i	Reactive power output of generator i
QD_k	Reactive power demand at bus k
r	Specific gas constant for air in (J/kg.K)
RFP	Request for proposal
R_{kj}	Line k-j resistance in p.u
RPS	Renewable portfolio standard
RR_i	Ramping rate of the i^{th} unit (MW/min)
RTP	Real time pricing
RW	Real world customers
S	Salvage value
SL	Straight line depreciation method
SOYD	Sum-of-years digits depreciation method
SR	Short-range customers
T	Air temperature in (°K)
TGC	Tradable green certificate
$t_{i,down}$	Minimum down-time of the i^{th} unit
$t_{i,up}$	Minimum up-time of the i^{th} unit

TOU	Time of use
$TSMI$	Turbine-site matching index
U_i	Binary variable for the i^{th} unit status (1=online)
UMP	Uniform market price
$U_{off,it}$	Number of hours the i^{th} unit is ON during hour t
$U_{on,i(t-1)}$	Number of hours the i^{th} unit is ON during hour (t-1)
Usd_{it}	Binary variable for the i^{th} unit shut-down status(1= unit is shut-down)
Ust_{it}	Binary variable for the i^{th} unit start-up (1= units is started-up)
v	Wind speed in (m/s)
V_c	Turbine cut-in speed (m/s)
V_f	Turbine cut-out speed (m/s)
V_k	Voltage at bus k
V_r	Turbine nominal speed (m/s)
$WACC$	Average cost of capital
WT	Wind turbines
WWEA	World Wind Energy Association
X_{kj}	Line k-j reactance in p.u
Y_{kj}	Y-bus admittance matrix element
Z	Elevation above sea level in (m)
α	Ground friction coefficient
β_k	Marginal cost of generation at bus k
Γ	Complete Gamma function
γ	Lower incomplete Gamma function
δ_k	Power angle at bus k
θ_{kj}	angle associated with Y_{kj}
λ	Number of $\sigma_{ND,t}$ units corresponding to (1-a_λ)
ρ	Air density in (kg/m^3)
σ	Standard deviation
$\sigma_{PD,t}$	Standard deviation of $e_{PD,t}$
$\sigma_{wind,t}$	Standard deviation of $e_{wind,t}$
$\sigma_{ND,t}$	Standard deviation of $e_{ND,t}$
$\delta_{j,t}$	Power angle at bus j during hour t
1-a_λ	Predetermined confidence levels

Chapter 1
Introduction

1.1 Background

The growing interest in small scale electricity generation located near customers is driven primarily by the emerging new technologies, environmental regulations and concerns, electricity markets restructuring, and increased customer demand for quality and reliability of electrical supply. This type of generation is called Distributed Generation (DG), but the terms dispersed generation, imbedded generation, and decentralized generation are also used.

DG technologies can be divided into two main groups: renewable-based and fuel-based. Fuel-based DG units use fuels, mainly fossil fuel, as the primary energy resource to generate electricity, or in the process of producing alternative fuels. On the other hand, renewable-based DG technologies utilize available renewable energy resources to produce electricity. These technologies are becoming increasingly important due to fossil fuel resources' depletion and price associated risks, as well as emission and pollution concerns associated with other fuel-based power generation technologies. Renewable energy resources are sustainable and environmentally friendly.

1.2 Research Motivations and Objectives

One of the most important types of renewable-based DG technologies is the wind turbine, which utilizes locally available wind resources and converts part of the wind energy into electricity. Therefore, wind power can be used in many places to provide a viable solution to rising demand, energy security and independence, and climate change mitigation. Despite the benefits of wind power, investing in this sector faces many challenges. The focus of this thesis is on three of them:

1. Due to high upfront capital cost and relatively low Capacity Factor (CF)[1] of wind-based DG, investment in wind power has a cost disadvantage over conventional thermal-based power generators, especially when fuel prices are low. In addition, the intermittent nature of wind power imposes high risk on wind-based generators which participate in electricity markets. Therefore, to make the installation of wind energy more appealing, governmental long term support policies are required. One of the most effective tools to achieve this goal is the establishment of a Feed-in Tariff (FIT) scheme. Under this policy, wind power generators receive a higher price per unit of electricity

[1] Capacity factor is the normalized average output of any generator

injected in the grid than do conventional thermal generators for a guaranteed contract period. The FIT rate helps overcome the cost disadvantages of wind power, and helps reduce market and regulatory risks. In addition, due to the high capital cost of wind turbines, the role of Capital Cost Allowances (CCA) and other renewable energy incentives on the project's economic viability needs to be investigated.

2. Optimal selection of wind turbines can make wind power more economical. Since wind power generators considered in this thesis are paid a fixed price per unit of energy, the turbine selection is based on the average amount of captured wind energy. The Capacity Factor (CF) of a turbine is commonly used to estimate its average energy production. This amount is a function of both wind speed profile of the site under study and the turbine output characteristics. Therefore, accurate modeling of both local wind profile and candidate turbine characteristics is import in the optimal turbine-matching problem.
3. As wind penetration level increases in the system, technical and economical consequences and challenges are speculated. Due to the intermittent nature of wind power, reserve requirements on the system will increase as penetration level increases. Moreover, wind resources are location-dependent and therefore, network reinforcements might be necessary to securely accommodate wind power. At a high wind penetration level, new transmission lines will be needed to transport wind power output to other areas. New transmission lines and major network reinforcements are very expensive and will affect the real value of wind power to the system. Apart from environmental restrictions, this will lead to an increase in the cost of energy to electricity customers. Without enough network capacity, wind generation will need to be curtailed at a certain wind penetration level, leading to a decrease in the value of wind power. Careful analysis of wind power impacts is needed to maximize its benefit.

This research aims at broadly facilitating higher integration levels of wind-based DG without jeopardizing the system's economics, security or reliability. The main objectives of this thesis are:

- To study the role of taxation and incentive policies in the economic viability of wind-based DG power projects;
- To investigate the potential of wind power investment in a new city in Oman - for investments in this sector to get off the ground in Oman, a case study is presented;

- To develop a new CF model that can be used by wind power investors for turbine-site matching applications;
- To develop a new Turbine-Site Matching Index to assess the suitability of different turbines for local wind resources;
- To investigate the effect of different temporal wind profiles in scheduling costs of thermal-based generating units.

1.3 Outline of the Thesis

The remainder of this thesis is organized as follows:

Chapter 2 presents a literature survey on DG in general, and wind turbines in particular. In the first part of the survey, different definitions, technologies, potential benefits and issues of DG are discussed. The second part of the survey is devoted to wind turbines and their impacts on the system.

Chapter 3 presents a thorough techno-economic evaluation of wind-based DG projects to investigate the effect of taxes and incentives in the economic viability of investments in this sector, for the case of Ontario. This chapter considers the effects of provincial income taxes, capital cost allowance (CCA), property taxes, and wind power production federal incentives.

Chapter 4 proposes the use of wind power as a source of electricity in a new city being developed in the Duqm area of Oman. Recent wind speed measurements taken at the Duqm meteorological station are analyzed to obtain the annual and monthly wind profile models represented by Weibull parameters. A techno-economic evaluation of a wind power project is presented to illustrate the project's viability. A feed-in tariff and capital cost allowance policies are recommended to facilitate investments in this sector.

Chapter 5 presents a novel formulation for wind turbine capacity factor (CF) estimation using wind speed characteristics at any site and the power performance curve parameters of any pitch-regulated wind turbine. The proposed model is compared with the existing model for simplicity and accuracy. Illustrative case studies and parameter sensitivity analysis are presented to test the effectiveness of the model in turbine-site matching applications.

Chapter 6 presents a new formulation for the turbine-site matching problem. A new Turbine-Site Matching Index ($TSMI$) is derived based on a new CF model that includes the effect of turbine tower

height on captured energy. Additionally, the proposed $TSMI$ includes effects of tower heights and turbine rating on the initial capital cost.

Chapter 7 investigates the effects of wind power temporal profiles on the scheduling costs of thermal generation units. Two temporal profiles are considered: synoptic-dominated and diurnal-dominated variations of aggregated wind power. To simulate the wind profile impacts, a linear mixed integer unit commitment problem is formulated in a GAMS environment. The uncertainty associated with wind power is represented using a deterministic equivalent of a chance-constrained formulation.

Chapter 8 presents the thesis summary, contributions, and directions for future work.

Chapter 2

Background and Literature Review[2]

2.1 Introduction

In conventional vertically-integrated systems, electricity is generated in large central plants, such as nuclear, hydro, or coal-fired power stations, and transferred to load centers using high voltage transmission networks, as well as distribution networks operating at medium and low voltage levels. Although the first electricity systems were small size DC-based generators, operating at low voltage levels and located near load centers, vertically-integrated systems evolved due to technological improvements which enabled high voltage AC transmission systems. Further economies of scale promoted building larger generating stations [4].

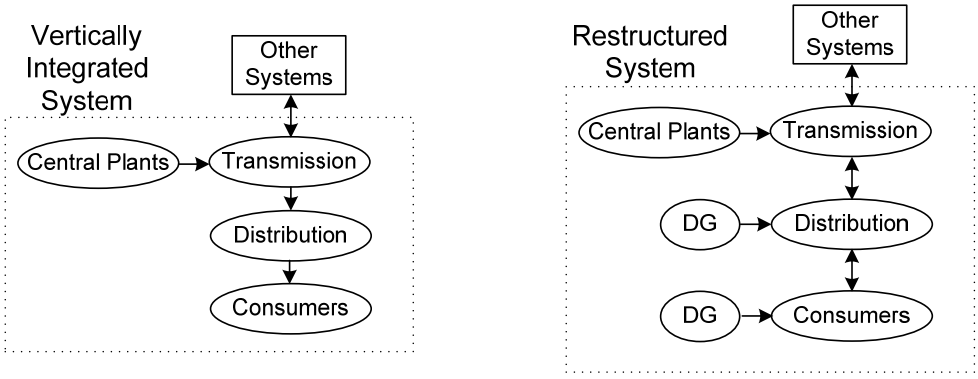

Figure 2-1: Vertically integrated power systems versus restructured systems

One of the main differences between conventional vertically integrated systems and restructured systems is the presence of DG units in the latter. Figure 2-1 presents a schematic for the two different systems.

[2] Some parts of this chapter have been published in:
[1] M. H. Albadi and E. F. El-Saadany, "The Role of Distributed Generation in Restructured Power Systems," in *IEEE PES 2008 North American Power Symposium (NAPS' 08)*, Calgary, AB, Canada, 2008, pp. 1-6.
[2] M. H. Albadi and E. F. El-Saadany, "Impacts of Wind Power Variability on Generation Costs- an Overview," *The Journal of Engineering Research (TJER),* vol. 7, to be published in June 2010.
Earlier version of [2] was published in:
[3] M. H. Albadi and E. F. El-Saadany, "Impacts of Wind Power Variability on Generation Costs: an Overview," in *International Conference on Computer Communication and Power (ICCCP' 09)*, Muscat, Oman, 2009, pp. 1-6.

2.2 Distributed Generation

2.2.1 Definitions

Although DG can be easily defined as a small scale generation located near or at load, there are many definitions for DG in the literature. Sometimes these definitions are not consistent. The International Conference on Electricity Distribution (CIRED) defined DG to be all generation units with a maximum capacity of 100MW, and which are usually connected to a distribution network. According to CIRED, these units are neither centrally planned nor dispatched [5]. Chambers [6] also defines distributed generation as relatively small generation units of 30MW or less. Ackermann et al. [7] and Pepermans et al. [4] agree in defining DG as an electric power generation source connected directly to the distribution network or on the customer side of the meter. Unlike previous definitions, these authors did not specify the size of the generation unit. The International Energy Agency (IEA) defines DG plants as those producing power on a customer's site or within local distribution utilities, and supplying power directly to the local distribution network [8]. The IEEE defines distributed generation as electric generation facilities connected to an area electric power system (local grid) through a point of common coupling [9]. As seen from the above definitions, the main differences between DG and the conventional central power stations include, but are not limited to the following:

- Location: DG units are located near loads and connected to distribution networks, unlike the central plants, which are far away and therefore connected to load centers via transmission networks;
- Capacity: The generation capacity of DG units is much smaller than that of the massive central plants;
- Ownership: DG units can be owned by utilities, customers or a third party;
- Technology: New cleaner technologies, including renewable energy sources, are used as DG units.

2.2.2 Technologies

DG can be divided into two main groups: renewable-based and fueled-based DG technologies. Most fueled-based DG technologies use fossil fuels as their primary energy resource to generate electricity, or as a means to produce alternative fuels. Fuel-based technologies include conventional steam and combustion turbines, internal combustion engine (ICE) generators, microturbines (MT), and fuel cells (FC). Renewable energy resources are becoming more important due to fossil fuel resource depletion,

price-associated risks, and environmental concerns. Moreover, renewable energy resources are sustainable and environmentally friendly. Renewable resource-based technologies include photovoltaic cells (PV), wind turbines (WT), and small-scale hydro-generation (Figure 2-2). Below is a brief description of each technology.

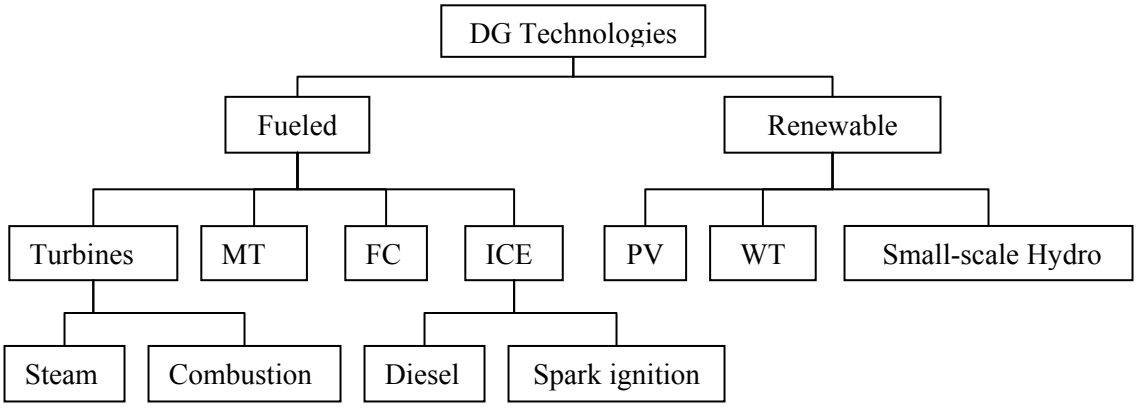

Figure 2-2: Classification of DG technologies

- Steam and Combustion Turbines

Conventional steam and combustion turbines are widely used because they are mature technologies. In a conventional steam turbine, the fuel is burned to boil water, creating pressurized steam, which drives a turbine-generator system to generate electricity. A combined-cycle system is one in which a steam turbine uses the heat waste from a combustion engine to fire the boiler. This combination results in overall efficiency improvement. In countries where natural gas is domestically available, large combined-cycle systems are used as base generation plants. In other places, the combined-cycle system is a viable DG resource, which could serve as peaking units or for combined-heat-power applications (CHP) [8].

- Internal Combustion Engine Generators

These engines include diesel cycle and spark ignition motors. They are the most widely used technologies for providing backup power. These generators are used to improve system reliability by minimizing the duration of supply interruption. Internal combustion DG units gained widespread acceptance due to their low installation cost per kW capacity, as well as other advantages. Diesel cycle engines can be fueled by diesel, heavy fuel oil and biodiesel. Spark ignition engines can run on natural gas, biogas and landfill gas [8]. Biogas is a methane-based fuel produced using biodigesters. Advantages of these generators include

reliability, efficiency and fast start-up capabilities. Disadvantages include emissions, noise and maintenance cost.

- Microturbines

Microturbines (MT) are small combustion-turbine generators based on turbocharger technology [10]. These units rotate at very high speeds: up to 120,000 rpm for the turbine and 40,000 for the generator [8]. Consequently, their output has a much higher frequency than the normal power frequency (50 or 60 Hz), and it therefore needs to be conditioned. The advantages of this new technology over conventional combustion turbines are lower noise and emissions, higher efficiency, smaller footprint requirements and lower cost.

- Fuel Cells

Similar to conventional batteries, fuel cells use an electrochemical process to produce electricity. The fuel cell has an anode and a cathode separated by an electrolyte. The fuel (hydrogen) is fed into the anode of the fuel cell while the oxygen or air enters the cell through the cathode. The hydrogen atoms split into protons and electrons with the help of a catalyst. The electrons flow through the anode to an external circuit creating a DC current, while protons pass to the cathode and then form water molecules, after combining with oxygen [10]. Although this technology was developed in the nineteenth century, the practical use started in the Sixties of the last century, when NASA used them to produce electricity in spacecraft. Although they are characterized as having relatively low efficiency in the range of 40%, relatively higher efficiency of energy conversion (up to 80%) can be achieved when combined heat and power takes place [8]. Different types and application of fuel cells are presented in [11].

- Photovoltaic Cells

Photovoltaic cells (PV) have the ability to convert energy received in the form of solar light into electricity. The semiconductor material in the PV cells absorbs solar radiation and releases electrons which form a DC current when flowing through a circuit. Because the output of a single PV cell is small, PV cells are connected in series and in parallel to form PV modules which are able to produce higher voltages and currents, respectively. PV modules are connected together to form PV panels and arrays. Since the output of a PV cells is DC, a power conditioner is needed to interface it with the grid or to produce AC voltage for local usage. Potential benefits of PV cells are limited to the availability of solar resources. In the standalone mode of operation, a hybrid system (e.g. PV-energy storage-fuel cell) should

be considered, to ensure continuity of supply when no solar resources are available. PV cells are suitable in remote areas for small power applications, such as telecommunications and space program applications [12]. PV systems have a high capital cost and low operating and maintenance costs.

- Small-scale Hydro-generation

The energy contained in small water streams can be captured by small-scale hydro-power DG and converted to electricity. Small-scale hydro-generation can be developed at existing dams without extensive civil engineering work [13]. Although this technology is efficient, there is considerable scope for research and development [13, 14]. The potential for small hydro-electric systems depends on the availability of water flow resources. Although this technology can provide cheap, clean, and reliable electricity, without significant storage facilities, variations in available water flow will cause power output fluctuation [14, 15]. This fluctuation is increased in a rocky and steep catchment area and short water streams and can result in a relatively small capacity factor [15].

2.2.3 Relevant Issues

The increased penetration level of DG in distribution systems brings up many issues and uncertainties. These are related mainly to economic efficiency, environmental concerns, energy security, and DG owner financial issues. A brief description of each of these issues is given below.

- Economic Efficiency

Economic efficiency means maximizing the net value of the benefits gained from the available resources [16]. In the DG context, it means efficient and optimum deployment of DG units. According to IEA, market structure, operation, and pricing determine whether DG units are integrated efficiently or not [8]. Market structure has a major influence on efficient DG penetration of the system. The liberalization of the wholesale market is not enough when the distribution level is still a monopoly. This monopoly could hinder the penetration of DG by imposing standby tariffs and high prices for ancillary services. To overcome this problem, the regulator should ensure non-discriminatory access of the DG to the grid once technical issues are resolved. For efficient market operation, liberalization of the retail market would give customers the option to locally generate their own electricity when electricity prices are high.

DG participation in electricity markets involves difficulties because the wholesale markets were originally designed for large central generation plants. Policy intervention is necessary to enable DG to actively participate in the market [8]. For example, DG owners must use the expensive spot market to cover for any discrepancy between expected needs and actual demand/generation, if the owner decides to participate in the market.

The liberalization of electricity markets evolved in price fluctuation. Higher prices of electricity during peak periods and lower prices during off-peak periods favor DG deployment during peak hours. In many places, electricity prices are not sensitive to location, and electricity markets have a uniform market price. In such a case, the true value of DG is underestimated. DG location plays an important role in reducing transmission and distribution losses, relieving distribution network congestion, deferring or avoiding transmission and distribution infrastructure upgrades and reinforcement, and providing ancillary services [8]. Restructuring of electricity prices is crucial for the true value of DG to be realized. Using Locational Marginal Prices (LMP), as in standard market design, will enable efficient DG investment decisions [17]. A case-study about the effect of DG on LMP is presented in [1].

- Environmental Concerns

DG technologies have a wide range of emission levels, from emission-free (PV & WT) to moderate (diesel). For fossil-fuel DG technologies, two areas of concern are identified: nitrogen oxide effects on local air quality, and the global greenhouse gas emission effects on climate change [8]. Although most DG technologies have lower nitrogen oxides (NO_x) emissions compared to coal-fired power stations, they have higher emissions than combined-cycle gas turbines with emission controls. This situation imposes a serious limitation on DG in areas where NO_x emissions are of concern. Similarly, except for CHP operation, DG greenhouse gas emission rates are generally lower than those of coal fired plants but higher than those of combined-cycle gas turbines with emission controls, for most fossil-fueled technologies. The authors in [8] recommend using economic measures to encourage DG owners to reduce emissions. As an example, carbon emission trading would give DG owners an incentive to minimize emissions.

- Energy Security

The large penetration of DG in the system can affect energy security. This effect can appear in two forms: primary fuel diversification and power system reliability. Although renewable technologies (e.g., PV and WT) help in diversifying the primary fuel of electrical energy, most other DG technologies use

natural gas, directly or indirectly, as a primary source of energy. Therefore, the overall effect on fuel diversity in the power system is expected to be limited [8]. The increased demand and dependency on one major primary fuel (natural gas) reduces energy security. An exception to this effect is the CHP, where higher fuel efficiency means lower fuel consumption, hence, enhanced energy security could be achieved.

DG could enhance power system reliability by integrating the available standby DG resources. It has been reported that the availability of standby generation helped in reducing blackout risks during California's 2001 electricity crises [8]. Moreover, DG can enhance system reliability by relieving distribution network congestion and reducing the demand flowing over transmission lines by using locally generated power. In addition, since DG units are much smaller than central power plants, lower capacity margin is needed to operate the system with the same reliability compared to a system with conventional large plants.

The main reliability concern for DG in this context is the fact that most DG units are nondispatchable due to natural or operational intermittency. In such cases, DG might not be able to respond to demand variations and this in turn reduces the system's ability to provide reserve power when needed [8].

- Owner Financial Issues

DG units have higher capital cost per kW of installed capacity when compared with conventional central power plants. In some cases (e.g. WT and PV), the capital cost of DG units is much higher compared with central plants' capital cost per installed MW capacity; thus, governmental incentives and subsidies are needed to facilitate the integration of some renewable-based DG technologies.

Utilities may require that the DG owner should pay for studies and sometimes system upgrades to ensure the reliability, safety and power quality of the system while the DG is part of it. When not regulated, distribution companies might impose high standby charges. According to the theory of economic efficiency, the power producer should pay for all the costs for upgrading the distribution system [8]. Therefore, the DG owner should pay for the cost incurred by the distribution system operator. These costs could be very high if the system needs to be reinforced. On the other hand, large central plants do not pay for transmission system upgrades and reinforcements. Having said that, a fair solution is for DG owners to pay a connection fee, and for the rest of the cost to be covered by customers as part of the operating cost [8].

2.2.4 Potential Benefits

In the new era of restructured electricity markets, DG has a wide range of applications. Utilities can benefit from using DG in their planning process. DG owners and customers can use DG to reduce their cost of energy. Additionally, the applications of DG can benefit all members of society.

2.2.4.1 Utility Applications

- Deferred or Avoided T&D Expansion

DG is becoming a viable choice in power delivery system planning [11]. Utilities can avoid expensive network expansion and other network reinforcements by installing DG in selected locations. DG has the potential to relieve transmission congestion and reduce power losses in both transmission and distribution networks. Since transmission and distribution system costs represent a considerable share of the total price of electricity, DG can save up to 30% of electricity costs on average [8]. Moreover, extending the network to remote areas is economically not practical. Utilities could gain substantial savings by using locally generated power [10]. The costs of network capacity expansion projects would otherwise be reflected in the price of electricity paid by consumers. Utility planning tools could be used to assess potential utility value to be gained by using DG instead of network expansion [18].

- Reduced System Losses

Power losses (I^2R) are proportional to the resistance, "R", of the power path and the loading, "I", of the line. Unlike central plants, DG is located near consumers; therefore, the resistance in the current path is much lower than that between central plants and electricity consumers. Moreover, DG will reduce the loading of transmission lines and relieve heavily loaded lines leading to more reduction in power loss. Quezada et al. demonstrated that loss reduction depends on DG penetration, technology, dispersion, location and reactive power control [18]. The value of this benefit can be substantial in some cases where system losses are high. Although loss reduction calculations can be done using power flow calculations, a lot of data is required and the results are valid only for certain loading profiles [19]. Nevertheless, it should be mentioned that with certain loading levels, especially with light loads, the DG might result in increasing the energy losses compared to situations for which DG is not used.

- Voltage Support to Electricity Grid

DG can be used to support the distribution system voltage profile through the injection of reactive power. This in turn improves power quality for nearby customers and reduces losses in distribution

systems. Losses are reduced when reactive power is locally provided; consequently, this minimizes the reactive component of the current flowing in the system. The benefit of this application is not substantial because there could be other cheaper means for voltage support, such as switched capacitors. Moreover, voltage support is characterized as a localized problem [20].

- Provision of Ancillary Services

Campbell et al. [21] presented different types of ancillary services that a DG unit can provide, including voltage control, regulation, load following, spinning reserve, supplemental reserve, backup supply, harmonic compensation, network stability, seamless transfer, and peak shaving. The value of these services varies depending on the services provided and the conditions of the contract. Spinning reserve, supplemental reserve, and network stability are of interest to the utility only. On the other hand, backup supply, peak shaving, load following and seamless transfer provide the DG owner with a direct financial value – avoiding the costs and inconvenience of interruptions in this case. Finally, voltage control, regulation, and harmonic compensation impact both the utility and the owner [21].

2.2.4.2 Customer Applications

- Lower Cost of Electricity

The transmission and distribution cost of electricity represents 30% of the total price in average [8]. Customers with onsite generation might find that the cost of installing and operating onsite generation is less than the cost of buying electricity from the grid. The difference between the two costs represents the value of this benefit to the customer. This value is case sensitive and depends on electricity price, load profile, DG unit capital cost, and operation and maintenance costs. It has been reported that the benefits of this application are the main driver for most customers considering DG deployment [20].

- Consumer Electricity Price Protection

DG can minimize the risks associated with electricity price volatility when price spikes appear due to congestion, generation shortage and market power [22, 23]. The DG owner can remove uncertainty from the energy cost by having a long-term fuel contract for a fixed price. Moreover, the owner will have the flexibility of switching between DG and utility generation if real-time pricing is used. The size of this benefit depends on price volatility and customer risk preferences [20].

- Enhanced Demand Response and Elasticity

Without DG, most customers do not have the means to react to changes in electricity price and its volatile fluctuations. Yet, onsite generation appeals to customers with its desirable flexibility. Customers with installed DG units in their facilities will certainly consider generating their own electricity instead of buying from the grid when electricity prices are higher than that for their own generation. This situation will appear as a demand response and elasticity in electricity markets, ultimately reducing electricity prices and price volatility for the benefit of all consumers [22]. The value of this benefit will increase as onsite generation penetration levels increase, up to a certain level - beyond which the value starts decreasing. Although this benefit is very difficult to quantify, it can be estimated using market simulation tools [20].

- Improved Reliability and Power Quality

For customers concerned with both the reliability and quality of main grid power, DG is an attractive solution. Reliability in this context can be expressed as the expected duration of an outage over a period of time, while the power quality is expressed by the frequency of occurrence and duration of voltage sags. The value of this application depends on the frequency, duration and timing of interruptions and voltage sags. Obviously, this differs from one class of customers to another, and sometimes even within the same class [19]. The value of higher reliability and power quality is the main, and sometimes the only, lure to installing onsite DG in places such as hospitals, high-rise buildings and process industries with sensitive loads. The value of this application is characterized by avoiding the costs incurred in case of interruption [20]. This value is customer-dependent and it can reach high levels - US$ 2 million per hour in the case of pharmaceuticals companies [24].

- Combined Heat and Power

Heat is generated as a byproduct when fuel is being burned to produce electricity. It has been reported that for the average power plant, two thirds of the energy content of the input fuel is converted to heat [25]. Unlike electricity, heat cannot be transmitted efficiently to customers over long distances. A combined heat and power (CHP) DG unit generates electricity and uses the generated heat energy locally. Combined heat and power, also called cogeneration, improves overall efficiency and fuel utilization and in turn lowers the overall energy cost for customers. The efficiency of a typical single-cycle power plant is between 30-33% and that of a combined-cycle plant is in the range of 55-60% [25]. Common DG CHP projects have been reported to have an overall fuel efficiency of 70-80%, and in

some systems, the values exceeded the 90% level [25]. CHP application has a substantial value for customers with heating or cooling requirements, as it reduces the overall fuel needed to meet electricity and heat requirements. The financial value of a CHP DG operation is perceived directly by customer as a direct saving in overall energy requirements. Another value is emission reduction, which is more difficult to quantify [20].

- Consumer Control

DG offers a useful alternative to customers seeking independence from utility power, generally individualistic consumers who want to be in charge of everything in their daily life, including supplying electricity requirements. Another group of candidates are consumers who want to get their electricity needs from a certain source, such as from environmentally friendly DG [20].

2.2.4.3 Other Benefits

- Improving Grid Security

Using DG to supply critical loads will reduce grid dependence on large central plants and the transmission system, which could be forced out of the system or become inoperative due to vandalism or natural events. This use will in turn reduce the impact of critical system component failures. Although this benefit is spread to the whole of society and could be substantial, it is very difficult to quantify [20]. As an example of this benefit, IEA reported that the availability of standby generation helped in reducing blackout risks during California's electricity crises of 2001 [8]. Furthermore, diversifying the fuel source is advantageous to system security.

- Effects on Land Use

Most DG technologies have smaller footprints; that is, they require less space compared to central plants. Moreover, DG does not need, or at least reduces, transmission and distribution infrastructure space requirements compared to central plants. It should also be obvious that a property located in an urban area is worth more than one that is remotely located away from the grid. With DG deployment, the price difference is decreased, and customers have more flexibility in deciding about the location of their projects. However, it is very difficult to estimate the value of DG land use effects [20].

- Reducing Opposition to Central Power Plants and Transmission Lines

Many individuals and groups oppose building new power plants and transmission line projects for a variety of reasons, including among others, environmental and property value concerns. They can exert a tremendous force to stop new central plants and transmission lines. It is expected that DG will not be faced with such strong opposition. The value of this benefit is complex and difficult to estimate. One method for estimating this value is to compare property value before and after the project [20].

- Reducing Emissions

Emissions, such as NO_x and CO_2, are byproducts of electricity generation. Renewable DG technologies do not produce emissions when converting renewable energy to electricity. Other technologies might have lower levels of emissions than those produced by displaced central plant generation. This benefit affects all of society, but is difficult to evaluate. However, clean DG technologies owners' receive incentives for reducing the health risks associated with emissions [20].

- Supporting Renewable Portfolio Standards (RPS) Goals

Renewable Portfolio Standards (RPSs) are legislations that mandate utilities to generate a minimum percentage of the electricity through use of renewable energy sources. As an example, Ontario RPS has a requirement that 5% of the province's power come from renewable sources by 2007 and 10% by 2010 [26]. Having renewable DG units in the system makes RPS standards achievable. The value of allowing a utility to meet RPS by having renewable DG is presented by renewable energy credits and incentives to DG owners [20].

2.2.5 Renewable-based DG Support Policies

As demonstrated by Huang and Wu in [27], long-term policies are required to help new renewable technologies, such as wind turbines, to gradually replace some of the conventional fossil fuels ones, such as gas turbines. In general, to stimulate investment in renewable energy, there exist two types of policy measures: direct and indirect [28]. A classification of these policies is given in Figure 2-3. The former instruments are used for the immediate stimulation of renewable energy technologies, while the latter are used to improve long term framework conditions. Support policy instruments can be further classified into two categories: investment-focused and generation-based. In the former scheme, renewable energy projects are subsidized based on installed capacity. In the later option, the support is given based on energy produced and sold.

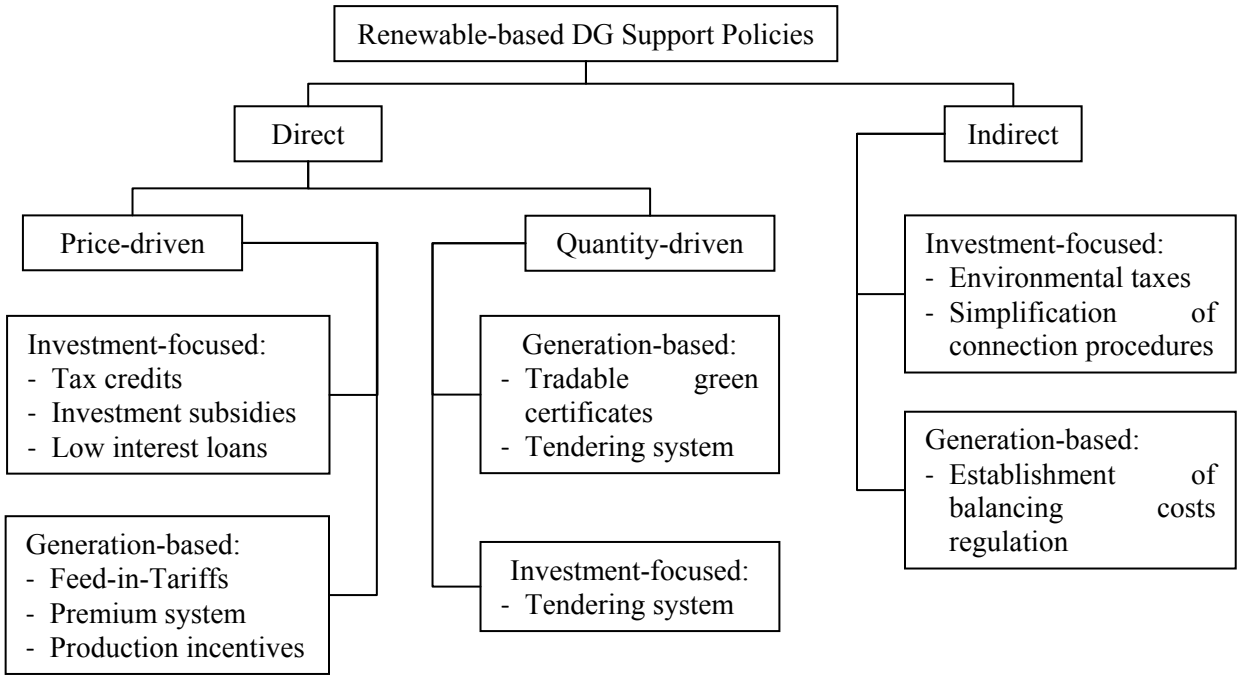

Figure 2-3: Classification of renewable energy support policies

Direct regulatory measures include price-driven and quantity-driven strategies. The price-driven mechanisms can be either generation-based or investment-focused systems. Feed-in-Tariff (FIT) and premium systems are examples of price-driven generation-based policy instruments. These two examples are long term agreements, according to which eligible renewable power producers are paid a regulated feed-in tariff, or a premium in addition to the electricity market price, for a guaranteed period of time [28]. Additionally, production incentives are used to support renewable generation. Price-driven investment-focused support mechanisms include tax credits, investment subsidies, and low interest loans.
In quantity-driven strategies, governments define a quota or a Renewable Portfolio Standard (RPS) by which a minimum percentage of the electricity is from renewable energy sources [28]. In investment-focused strategies, RPS goals can be achieved using two systems: Tradable Green Certificate (TGC) and tendering systems. In a TGC system, utilities are obliged to purchase a certain percentage of electricity from renewable energy sources. To demonstrate compliance, they have to submit the required number of certificates, which can be obtained from a renewable power generator or a broker. In tendering or Request For Proposal (RFP) systems, calls for tender are launched for a certain renewable capacity. The winners

will make contracts that offer an upfront investment grant per installed capacity. In generation-based tendering systems, winners will have contracts that offer a specific tariff for a guaranteed period of time.

There are other policy instruments that can indirectly support deployment of renewable energy resources in the long term. These indirect strategies can be in the form of environmental taxes, or of emission permits for electricity produced by non-renewable sources, as well as the removal of subsidies given to fossil fuel and nuclear generation [28]. Additionally, they could be in the form of simplification and standardization of renewable-based DG connection procedures, or avoiding unnecessary costs caused by inconsistency of interconnection requirements. Finally, the establishment of regulations that govern intermittency-related balancing costs can indirectly support deployment of renewable sources [28].

The authors in [28] concluded that FIT mechanisms are the most suitable policies for introducing renewable energy technologies to the market, and an investment grants tendering system is suitable for supporting immature technologies. Finally, a premium or a quota obligation, based on TGC, is best when technologies are sufficiently mature, the market is large and mature, and competition on the electricity market is guaranteed.

The FIT has proved to be the most effective policy in promoting investments in renewable energy, because it reduces regulatory and market risk [29]. In addition, Butler and Neuhoff in [30] concluded that the FIT policy generated sufficient competition among turbine producers and constructors. In [31], the authors presented an economically efficient feed-in tariff structure for renewable energy development.

2.3 Wind-based DG[3]

2.3.1 Wind Power around the World

According to the World Wind Energy Association (WWEA), 27.261 GW of wind power capacity were added in 2008. By the end of 2008, the global installed capacity had reached 121.188 GW [32]. Countries with 2GW or more installed wind capacity are show in Figure 2-4 [32]. West Denmark, the North of Germany, and Galicia in Spain are examples of areas that have relatively high wind penetration levels. In Denmark, more than 20% of the electricity supply is coming from wind power [33].

The strong growth in wind-installed generation capacity world-wide is attributable to three main reasons. The first one is growing public awareness and concern about emissions, climate change, and environmental issues related to other, competing, sources of energy. The second reason is awareness

[3] Some authors do not consider large wind farms that are connected to the transmission network as a DG. This is typically the case of off-shore wind farms.

about oil and gas reserve depletion and the predicted global peaking of oil production [34, 35]. According to a report published by the US Department of Energy, fuel prices and price volatility are expected to increase significantly as the peak of world oil production approaches [36]. It is generally believed that global peak oil production will occur during the second decade of the 21st century [34, 36]. This public awareness, and concerns related to fossil fuels, are encouraging governments in many parts of the world to promote renewable sources of energy, including wind power, in order to meet some part of their electricity requirements. Consequently, policies to support renewable energy source technologies have been implemented in many countries to help them reach approved national and local Renewable Portfolio Standards (RPSs). The third reason behind the strong growth of wind power is improvements in wind turbine technologies that have resulted in lower costs [28].

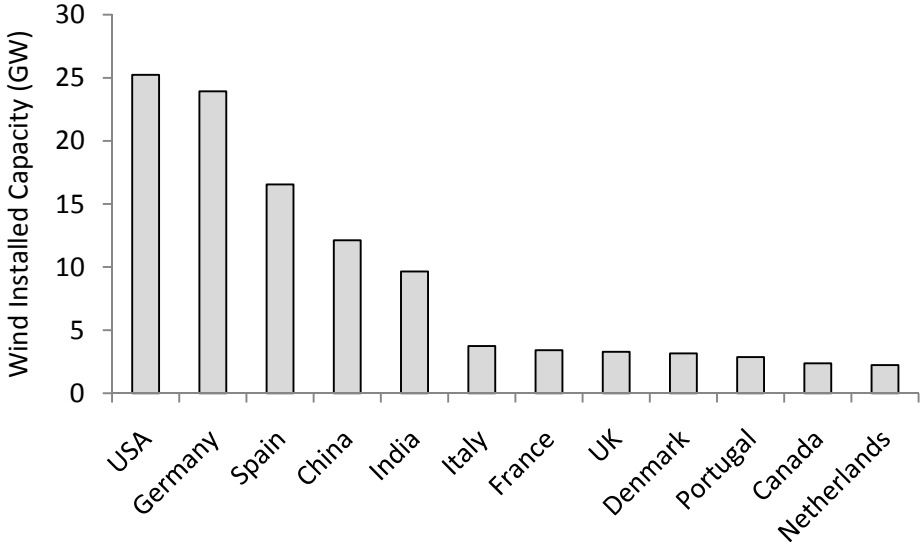

Figure 2-4: Countries having 2GW or more installed wind capacity by end of 2008

2.3.2 Wind Turbine Technologies

Modern wind turbine technologies are based on the ancient concept of a wind-driven rotor. Historical sources show that vertical-axis windmills were used in the Persian-Afghan border region of Seistan as early as the year 644 A.D [37]. The horizontal-axis (traditional) windmills were invented in Europe in the 12th century [37]. By the late 19th century, about 100,000 traditional Dutch windmills existed throughout Europe [28]. Preceding the electricity era, wind turbines were used for grinding grain and pumping water.

Modern wind turbines are required to generate electricity that is compatible with the grid supply. Wind turbines are a mature technology used by many utilities, customers and independent power producers to produce electricity from wind energy. Due to the space requirements of wind generators, they are more suitable for rural applications [38]. A hybrid system is needed to ensure continuity of supply in a standalone mode of operation.

2.3.2.1 Turbine Classifications

Similar to ancient windmills, there are two designs for modern wind turbines: horizontal axis and vertical axis. Although the horizontal axis design style is dominant, vertical axis turbines were considered with the expected advantage being omnidirectionality, and having gears and the generator at the tower base. However, due to the weight and cost of the transmission shaft, as well as low efficiency compared to a horizontal axis design, the vertical axis design disappeared from the mainstream commercial market. It is worth mentioning that there are currently some attempts to commercialize vertical axis design for building-rooftop applications [28].

Unlike multi-bladed old windmills, most modern wind turbines have three blades. In the 1980s and early 1990s, there were some attempts made to market one- and two-bladed wind turbine designs with expected advantage of reducing the turbine cost. However, these designs were eliminated mainly due to visual impact. It has been reported that "unsteady passage of the blade or blades through a cycle of rotation has often been found to be objectionable" [28].

The main components of a horizontal axis wind turbine, Figure 2-5, are listed below:

- The rotor: this consists of the blades and the hub. The hub connects the blades to the drive train.
- The nacelle: this contains the drive train (shafts, gearbox, coupling, a mechanical brake), the generator and the control system.
- The yaw system: this is located under the nacelle and is used to keep the rotor shaft properly aligned with the wind.
- The tower: this is used to raise the nacelle and the rotor so that winds with higher wind speeds are captured.
- The foundation: this holds the tower in place; its size and mass, therefore, are determined by the size of the wind turbine and by local ground conditions.
- Balance of electrical system: this consists of cables, switchgear, transformer, and power electronic converters.

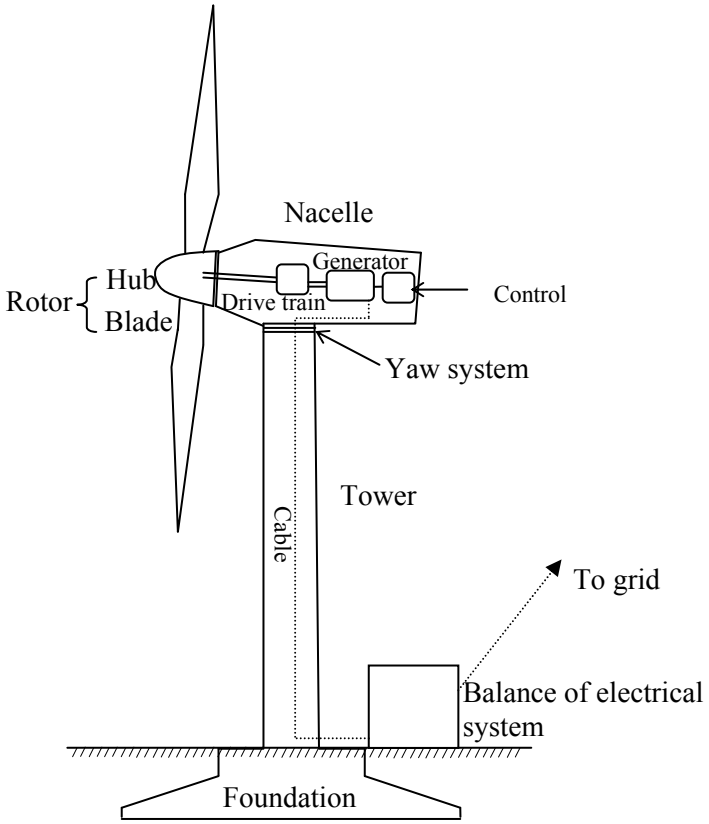

Figure 2-5: Main components of a horizontal axis wind turbine

2.3.2.2 Power Control

The power output of a wind turbine increases as wind speed increases. After a certain speed, called "rated" or "nominal" speed, the turbine reaches its maximum capacity. Beyond the rated speed, the output power needs to be controlled to limit the power output. To control the output power of a wind turbine, three types of control are used: stall, pitch, and active stall.

Stall control is the oldest scheme of controlling the power output. In this method, the rotor blades have a fixed angle. The geometry of the rotor blade profile is designed to ensure that when the wind speed is high, turbulences are created on the rear side of the blades; consequently this prevents lifting force of the blades from acting on the rotor. The advantage of stall control is avoiding moving parts in the rotor; while the disadvantage is the aerodynamic design complexity and the reduction of output power at high speeds [39]. Stall-regulated turbines were predominant until the introduction of MW-scale turbines in the mid 1990s.

The prevalence of pitch-regulated turbines over stall-regulated ones is mainly due to better output power quality. In pitch control, the blade pitch mechanism turns the blades out of the wind when the rated speed is exceeded, to limit the mechanical torque on the generator. When the wind speed decreases, the blade pitch mechanism turns the blades back into the wind [39]. By 2006, the number of pitch-regulated turbines installed was about four times that of stall-regulated ones [28]. Active stall control is a variant of pitch control. However, active stall control turns the rotor blades into the wind when the rated speed is exceeded. Consequently, this will force the blades to go into a deeper stall; spilling out excess wind energy. The exploitation of stall regulation characteristics achieves a smoother limited power than that obtained using pitch regulation.

2.3.2.3 Generator Speed

Generators used in wind turbines could be asynchronous or synchronous; working with fixed or variable speed. Initially, modern wind turbines operated at a fixed speed. Later, variable speed operation was introduced. Variable speed operation below rated power enables capturing more energy by allowing rotor speed and wind speed to be matched. Above rated power, variable speed operation can reduce pitch system loads and produce smoother output power [28].

Ackermann et al. classified the existing wind turbines into four types according to their speed control [40]. These are Type A, Type B, Type C, and Type D as discussed below.

- Type A: This configuration uses a fixed speed wind turbine with Squirrel Cage Induction Generator (SCIG) connected to the grid via a transformer. The asynchronous generator draws reactive power which means that reactive compensation is needed. In some cases, the generator is connected to the grid without reactive compensation and therefore, absorbs reactive power from the grid. In fixed speed wind turbines, fluctuations in wind speed are converted into electrical power fluctuations, and consequently into voltage fluctuations, if the grid is not stiff.
- Type B: This configuration provides a limited variable-speed wind turbine using a Wound Rotor Induction Generator (WRIG). The resistance of the wound rotor can be changed using an optically controlled converter mounted on the rotor shaft. Changing rotor resistance controls the slip, and therefore the power output. Using this method, the slip is typically controlled from 0 to -0.1 which means that the speed of the generator could be increased up to 10% of the synchronous speed.
- Type C: This configuration uses the so called Doubly Fed Induction Generator (DFIG) concept. Similar to type B, this configuration uses a WRIG. In addition, with DFIG, a frequency converter on

the wound-type rotor circuit is used to load the rotor with approximately 30% of nominal generator power. Using DFIG, the speed could vary from -40% to +30% of the synchronous speed.

- Type D: In this configuration, a full variable-speed wind turbine with asynchronous or synchronous generator, connected to the grid through a full load frequency converter, is used. The Asynchronous generator is a WRIG machine. On the other hand, the synchronous generator could be a Wound Rotor Synchronous Generator (WRSG) or a Permanent Magnet Synchronous Generator (PMSG).

All three power control types had been applied for type A, the old conventional fixed speed wind turbines. Variable speed turbines use pitch control only [40]. Table 2-2 summarizes wind turbine types and control methods. Most of today's MW-scale turbines are variable speed pitch-regulated turbines [40].

Table 2-1: Wind turbine types and control methods

Type	Speed Control	Power Control	Generator type*
A	Fixed	Pitch, Stall, Active Stall	SCIG
B	Variable	Pitch	WRIG
C	Variable	Pitch	DFIG
D	Variable	Pitch	WRIG, WRSG, PMSG

* SCIG: Squirrel Cage Induction Generator, WRIG: Wound Rotor Induction Generator, DFIG: Doubly Fed Induction Generator, WRSG: Wound Rotor Synchronous Generator, PMSG: Permanent Magnet Synchronous Generator

2.3.3 Wind Power Content

Any moving object, such as moving air, contains kinetic energy. The energy amount, in joules, depends on both the object mass in kilograms and its velocity in meters per second as shown in equation (2-1).

$$P_{wind} = \frac{1}{2}mv^2 \tag{2-1}$$

The power contained in a moving air mass, the wind, that flows at speed v through an area A_s is given in equation (2-2) [37].

$$P_{wind} = \frac{1}{2}\rho A_s v^3 \tag{2-2}$$

where P_{wind} is the power content of the wind in Watt; ρ is the air density in kilograms per cubic meter (kg/m^3); A_s is the swept rotor area in square meters (m^2), and v is the wind speed in meters per second (m/s).

The electrical power that can be extracted is much smaller than the value described by the above equation due to the fact that the air mass would be stopped completely in the intercepting rotor area for complete energy extraction. Theoretically, the maximum power that can be extracted from a wind turbine is 59.3%, the Betz limit, of the power contained in the wind [40]. In practice, this value is around 45% for large turbines. The power output of a wind turbine is given as follows [37]:

$$P_e = \frac{1}{2} C_p \rho A_s v^3 \tag{2-3}$$

where P_e is wind turbine output power and C_p is the turbine coefficient of performance. The coefficient value at each wind speed v_i can be found using the following formula [37]:

$$C_p(v_i) = \frac{P_e(v_i)}{P_{wind}(v_i)} \tag{2-4}$$

2.3.4 Turbine Power Performance Curve

The turbine power performance curve, simply called power curve, of a pitch-regulated turbine is characterized by three speeds; cut-in speed, nominal or rated speed, and cut-out speed. When the wind speed is below the cut-in speed, the output power is zero and the rotor cannot be loaded. After the cut-in speed, the power output increases as the speed increases. Variable-speed wind turbines have the capability of tracking the locus of maximum power, corresponding to the locus of maximum $\boldsymbol{C_p}$, as wind speed varies by adjusting the speed of the turbine [41, 42], see Figure 2-6.

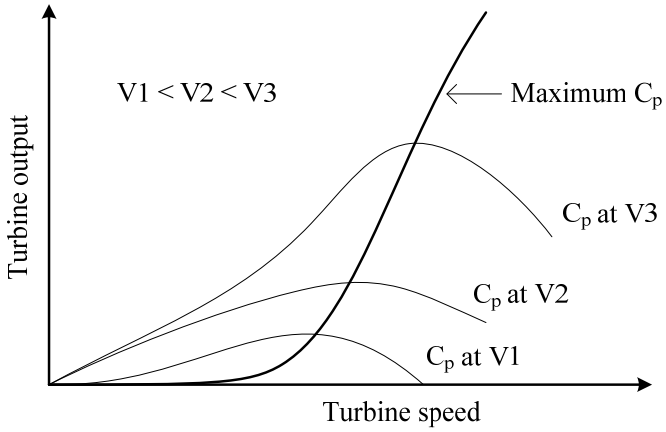

Figure 2-6: Maximum power tracking between cut-in and cut-out speeds [42]

At the nominal speed, the power output is at the rated value. The output power remains constant as wind speed increases by using power control mechanisms until the cut-out speed is reached, at which point, the turbine will be turned-off to prevent any damage to the mechanical structure. A typical simplified power curve is shown in Figure 2-7 for a Vestas V90-1.8MW wind turbine [43].

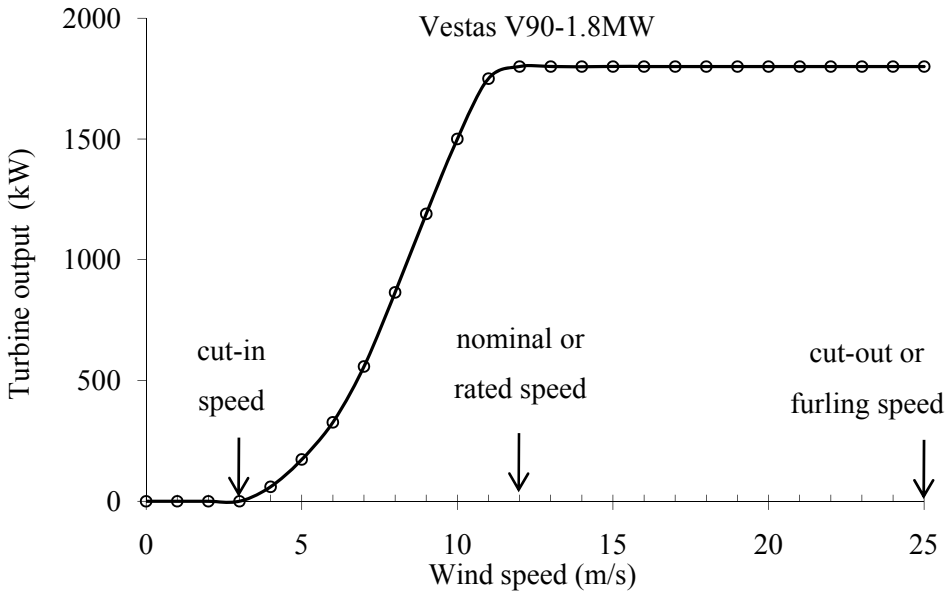

Figure 2-7: Power output curve for Vestas V90-1.8 MW wind turbine

2.3.5 Wind Speed Modeling

Wind speed variations are normally described using the Weibull probability density function (pdf) because it gives a good representation of the observed wind speed data, both at the surface and in the upper air [44]. The Weibull pdf is shown in the following formula:

$$f(v) = \frac{k}{c}\left(\frac{v}{c}\right)^{k-1} e^{-\left(\frac{v}{c}\right)^{k}} \tag{2-5}$$

where v is the wind speed in meters per second (m/s); k is a shape factor, and c is a scale factor. The Weibull parameters can be obtained using the mean ($\bar{v}$) and the standard deviation (σ) of wind speed at the chosen site. The Mean Wind Speed (MWS) can be calculated using the following formula.

$$\bar{v} = \int_0^{\infty} v \cdot f(v)\, dv \tag{2-6}$$

The above equation can be written as follows [44].

$$\bar{v} = c\Gamma\left(1 + \frac{1}{k}\right) \tag{2-7}$$

where Γ is the complete Gamma function given by

$$\Gamma(a) = \int_0^{\infty} x^{a-1} e^{-x} dx \tag{2-8}$$

The standard deviation of wind speed measurements is calculated using the following equation.

$$\sigma = \sqrt{\frac{\sum f(v_x)(v_x - \bar{v})^2}{\sum f(v_x)}} \tag{2-9}$$

The above formula can be written as follows:

$$\sigma = c\sqrt{\Gamma\left(1 + \frac{2}{k}\right) - \Gamma^2\left(1 + \frac{1}{k}\right)} \tag{2-10}$$

Knowing the mean and standard deviation of wind speed data at the potential site, one can estimate the two parameters of the Weibull function by solving (2.7) and (2.10) iteratively.

2.3.6 Impacts of Wind Power Variability

Although integrating a large amount of wind power is technically possible, higher integration costs might be incurred when wind penetration level increases. Examples of areas currently having relatively high wind power penetration levels are West Denmark, North of Germany and Galicia in Spain. In Denmark, more than 20% of the electricity supply is coming from wind power [33]. It is very important to accurately estimate the impacts and costs of wind power on system operation, when planning for high wind power penetration levels [45].

2.3.6.1 Variability Classification

Wind speed is characterized by its high variability, both spatially and temporally. On a global scale, spatial variability is attributed to the fact that there are different climate regions on the world affected by

the altitude and solar insulation. On a regional scale, wind speed varies according to the geographical location depending on the sizes of land and sea, and the presence of mountains and plain areas. In a local perspective, the type of vegetation and the local topography have a major role on wind speed [40].

At a given location, long-term temporal wind variability describes the fact that the amount of wind may vary annually. However, many studies estimated that the variation of mean wind power output from one 20-year period to the next has a maximum standard deviation of 10% [40]. Thus, the uncertainty of wind power production is not large for the lifetime of a wind turbine.

Seasonal variations are more predictable than annual ones. Wind speed synoptic variations associated with the passage of weather systems are not very predictable more than few days ahead. Wind variations with the time of day, which are called diurnal variations, are quite predictable.

Turbulences are variations of wind speed over minutes and seconds [40]. This type of variation can affect power quality, depending on both the network impedance at the point of common coupling, and the type of wind turbine. Variable-speed turbines have a smoother power output compared to fixed-speed ones.

Diurnal and synoptic variations can affect power balancing requirements [40].

2.3.6.2 Aggregation Effect on Variability

Aggregation of wind turbine outputs reduces the temporal volatility of wind power by two aspects: increased number of turbines within a wind farm and spatial distribution of wind generation resources [40]. On the one hand, as the number of turbines within a wind farm increases, turbulent wind effect is dampened because wind gusts do not hit individual turbines at the same time. In fact, a small number of turbines (n) are needed to achieve a significant smoothing effect, as the percentage variation of power output is reduced to $n^{-1/2}$, ideally. On the other hand, a wider geographical dispersion of wind farm reduces the impact of diurnal and synoptic variations. Spatial distribution of wind farms with certain aggregated capacity has a much lower up and down ramping rate requirements compared to a large single wind farm having the same capacity [40]. For Example, it has been reported that the combination of wind power outputs from 17 geographically dispersed sites in Ontario is estimated to reduce the variability of the aggregated wind power output about 60-70% compared to the output from one site, for 10-minute and 1-hour data [46]. Table 2-2 presents a summary of the sources of wind power temporal variation and relevant impacts on power system operation.

Table 2-2: Wind Speed Variability Summary

	Predictability	Aggregation effect	Impacts on power systems
Annual	Not predictable but small	NA	Reliability / Adequacy
Seasonal	Predictable	Limited	
Synoptic	Predictable few days ahead	Through wider geographical dispersion	Unit commitment / Reserves
Diurnal	Predictable		
Turbulences	Not predictable	Ideally $n^{-1/2}$ rule	Power quality

2.3.6.3 General Impacts of Wind Power

The impacts of wind power integration on any power system depend on two main factors: penetration level and system flexibility [40]. On the one hand, increased wind penetration will increase the impacts perceived by the system; on the other hand, systems that are inherently more flexible than others will be able to accommodate more wind power without perceiving unwanted impacts from wind generation facilities.

The first step to increase wind power penetration level is to understand and to quantify its impacts on utility systems. In addition, wind power plants' design and operation, power systems' design and operation, and market rules, all have great influence in accommodating wind power. Smith et al. reported that the existing case studies have explored high wind capacity penetrations, as a percentage of system peak, and have found that the primary considerations are economic, not physical [47]. This is summarized by how to deal with wind power uncertainty and variability. The main impacts of wind power on power systems are listed below.

- Generation Efficiency

  Fluctuating wind power affects other conventional dispatchable generation units. Intermittent performance of wind power leads to the fact that conventional units might operate in a suboptimal unit commitment. This problem can be reduced by accurate wind power forecasting and prediction. However, even with good forecasting and prediction tools, fluctuation of wind power causes less efficient operation of thermal units [40]. Consequently, reduced efficiency of conventional thermal units will reduce potential emission benefits of wind power. The costs of high wind penetration on thermal units have been studied in [47, 48]. The cost of reduced generation efficiency on the system depends on the initial unit commitment of conventional units, wind power uncertainties, and system flexibility.

- Reserves

  A system of reserves for regulation (1-minute), load following (5-minute), and operating reserve (10-minute), are needed to account for wind power fluctuations. The main factors that affect the amount of required reserves are initial load variations, the size of the balancing region, and the geographical dispersion of wind power resources. The Ontario case study [49] presents a good example of reserve requirements as a function of wind penetration. The study investigates the impacts of a wide range of wind penetration level scenarios (4%, 17%, 20%, 27% and 33%) on the operation of the Ontario bulk power system. According to the study, the 1-minute regulation requirement is not of concern, even with high wind penetration level, due to aggregation and spatial distribution of effect. The 5-minute load following requirement is found to be more substantial, and may exceed the capability of existing generators when wind penetration level exceeds 17% (5 GW). The study found that for the wind penetration scenarios of 20% (6 GW wind capacity) and higher, the 10-minute operating reserve requirement should be increased in order to accommodate extreme drops in wind generation.

- Curtailed Energy

  In some cases wind turbines' output needs to be curtailed to preserve balanced, stable and secured operation of the grid. In low load periods, system operator may consider wind power curtailment to ensure that enough dispatchable resources are online to guarantee enough reserves and ramping capabilities in order to accommodate demand's fluctuation [49]. In other cases, the operator will order wind power curtailment when wind power is high, local demand is low and transmission lines to other areas are approaching their thermal limits [40]. The need to curtail some wind power output depends not only on penetration level, but also on system flexibility. This flexibility can be enhanced by introducing more Demand Side Management (DSM) or Demand Response (DR) programs [22].

- Reliability

  Variable sources can be relied on in supplying peak demands if their patterns are correlated with demand pattern, an example would be solar power and air conditioning demand. Normally, wind power has no correlation with the load in many parts of the world. For example, Ontario, which is a summer peaking utility, has more wind power in winter than in summer [50]. Even with winter peaking utilities, there is no guarantee that wind power will be available when needed most (peak periods). Policy makers should be careful in estimating capacity value of wind power. Large wind power penetration could require large amounts of conventional plant to ensure supply adequacy and

security [51]. Additionally, the reliability of power systems that have a high wind power penetration levels is affected by original load demand, the geographical dispersion of wind power resources, the available transmission capacity, and by system flexibility.

- Transmission and Distribution Losses

  Wind power can increase or decrease network losses (transmission and distribution) depending on the wind power penetration level, the correlation between wind production and load profile, and the location of wind energy resources relative to load centers [18]. Moreover, high wind penetration levels may result in higher transmission capacity requirements; consequently, higher transmission losses. Transmission congestion can occur when wind generation is distant from loads [51].

- Voltage and Reactive Power

  Induction generators used in wind turbines inherently absorb reactive power from the grid. Fluctuations in power output results in voltage fluctuations when using fixed speed turbines. However, modern variable speed turbines, such as Doubly Fed Induction Generators (DFIGs), can provide reactive power support using appropriate interfacing [40].

2.3.6.4 Operational Impacts on Conventional Generation

The general approach of evaluating wind power impacts on the system is by evaluating the physical impacts of wind on the system and calculating the consequent costs. This process involves obtaining wind data that represent the actual performance of wind power plants. Each potential wind power plant location is represented by sets of virtual anemometers, which are used for power production calculations [52]. Most wind integration studies divide wind impacts into the four time frames corresponding to that of system operation: namely, regulation, load following, scheduling and unit commitment; Figure 2-8. The net load, which is the load minus wind production, should be served to maintain system balance for all time frames.

In regulation, short term reserve capacity is needed to maintain demand-generation balance, and usually performed by automatic generation control (AGC) of some designated generating units within seconds to few minutes. Regulation impacts of spatially distributed wind generation facilities are expected to be modest due to the smoothing effect of uncorrelated short term wind production. For example, it has been reported that the addition of 1500 MW (10% of peak demand) and 3300 MW (15% of peak demand) of wind in the US increased the regulation requirements by 8 MW [53] and 36 MW [54], respectively.

Load following is in the range of 10 minutes up to several hours, and includes morning ramp-up and evening ramp-down capabilities. The load-following impacts of wind are attributed to increased net load variability compared to original load variability. All wind integration impacts studies concluded that the distribution profile of the net load flattens and expands with large scale wind integration. This means an increase in ramping requirements for longer hours of the year.

In scheduling and unit-commitment, the operator objective is to ensure that sufficient generation is available for hours and days ahead, respectively, of real-time operation. The system operator should make sure that operating reserves are sufficient to maintain system balance according to local reliability standards e.g., North American Electric Reliability Council (NERC) standards [55]. As seen in Table 2-3 [48], the dominant balancing cost component is related to the unit commitment time frame in which decisions must be made about which units to start and stop, and when to do so to maintain system reliability at minimum cost [45]. Wind integration introduces uncertainty into the day-ahead unit-commitment process, which in turn results in an increase in the operating cost .This increase in cost varies depending on flexibility of generating units, fuel cost, market regulations, and both load and wind-generation resources characteristics.

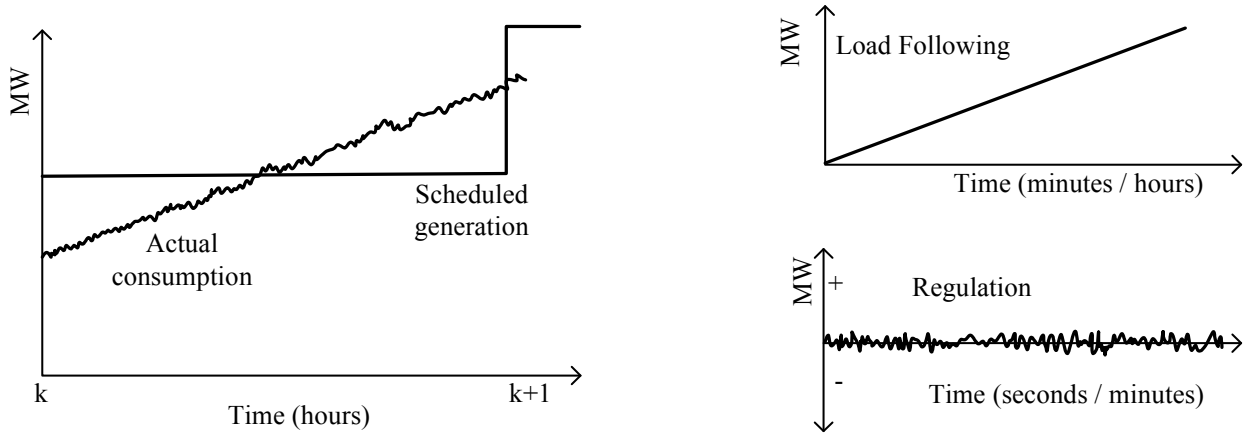

Figure 2-8: Operation time frames

Initially, it was thought that overall operational impacts of wind generation will cost utilities about US$ 15 to US$ 20 per MWh of wind energy. However, recent studies concluded that additional reserve capacity needed to integrate wind generation is at most 10% of the total wind plant nameplate capacity and in most cases, between 3% and 5% [56]. The results of many case studies developed in Europe and

North America estimated that the resulting operating costs related of wind power integration are between US$2 and US$4 per MWh for low wind power penetration levels, and increase up to US$ 6 per MWh for high penetration levels. These amounts, which represent the cost balancing operations, should be reflected in integration fees designed by utilities for wind projects.

Table 2-3: Break down of reserve costs attributed to wind power [48]

		US$/MWh			
Study	PL (%)	R	LF	UC	Total
UWIG/Xcel	3.5	0	0.41	1.44	1.85
PacificCorp	20	0	2.5	3.00	5.50
BPA	7	0.19	0.28	1.00-1.80	1.47 -2.27
We Energies II	29	1.02	0.15	1.75	2.92

PL: Penetration level, R: Regulation, LF: Load Following, UC: Unit Commitment

2.4 Summary

In this chapter, a literature survey on Distributed Generation (DG) in general, and wind-based DG in particular, is presented. In the first part of the survey, different DG definitions, technologies, potential benefits and possible issues are discussed. The second part of the survey focus on turbine technologies, wind power modeling, as well as possible impacts on the system. Despite the potential benefits of wind power, it is faced by two main challenges. The first one is related to the high capital cost requirements and the low CF values. The second is associated with several impacts of its intermittent nature. Hence, renewable energy support policies are required to facilitate investments in this sector.

Chapter 3

Role of Ontario Taxation and Incentive Policies in Wind-based DG Projects Viability[4]

3.1 Introduction

The Ontario electricity sector is facing the challenging problem of a projected supply deficit due to the increase in demand, and to the lack of investment in electricity capacity during the past decade. Demand growth and generation retirement will create a gap of 24,000 MW by 2025. This is equivalent to almost 80% of system capacity [60]. In 2005, the Ontario Power Authority (OPA) submitted its supply mix recommendation to the Ministry of Energy, highlighting the best way to meet electricity needs over the long term. According to this advice, the capacity of renewable resources would be increased to 37% of the total installed capacity in 2025. This capacity is expected to provide Ontarians with 47% of their electricity needs. Wind power is expected to be a significant part of Ontario's supply mix, representing 15% of the total installed capacity by 2025 [60]. A comparison between the 2005 and the proposed 2025 supply mix is presented in Figure 3-1.

The installed capacity of wind generation in Canada had an average annual growth rate of 45% between 2000 and 2008. In 2008, 526 MW of new capacity was installed, and it is expected that, in 2009, wind-installed capacity will grow by a minimum of 650 MW. Figure 3-2 shows the increase in wind generation installed capacity in Canada [61]. In 2008, Canada became one of 12 countries around the word that have 2GW or more of installed wind-power capacity. The total installed wind capacity in Canada as of July 2009 was 2854MW, out of which, 1161.5MW is in the province of Ontario [61]. Because of the proposed changes in Ontario's power mix and the anticipated increase of wind share, OPA and Ontario's Independent Energy System Operator (IESO) commissioned studies about Ontario's future wind power and its integration in the system [46, 50].

---

[4] Some parts of this chapter have been published in:

[57] M. H. Albadi and E. F. El-Saadany, "The role of taxation policy and incentives in wind-based distributed generation projects viability: Ontario case study," *Renewable Energy,* vol. 34, pp. 2224-2233, 2009.

Earlier results appeared in:

[58] M. H. Albadi and E. F. El-Saadany, "The Role of Taxation policy and Incentives in Wind-based Distributed Generation Projects Viability: Ontario SOP Case Study," in *IEEE PES 2008 North American Power Symposium (NAPS' 08)*, Calgary, AB, Canada, 2008, pp. 1-6.

[59] M. H. Albadi and E. F. El-Saadany, "Wind Power in Ontario: An Economical Valuation," in *IEEE Canada 2007 Annual Electrical Power Conference (EPC' 07)*, Montréal, QC, Canada, 2007, pp. 496-501.

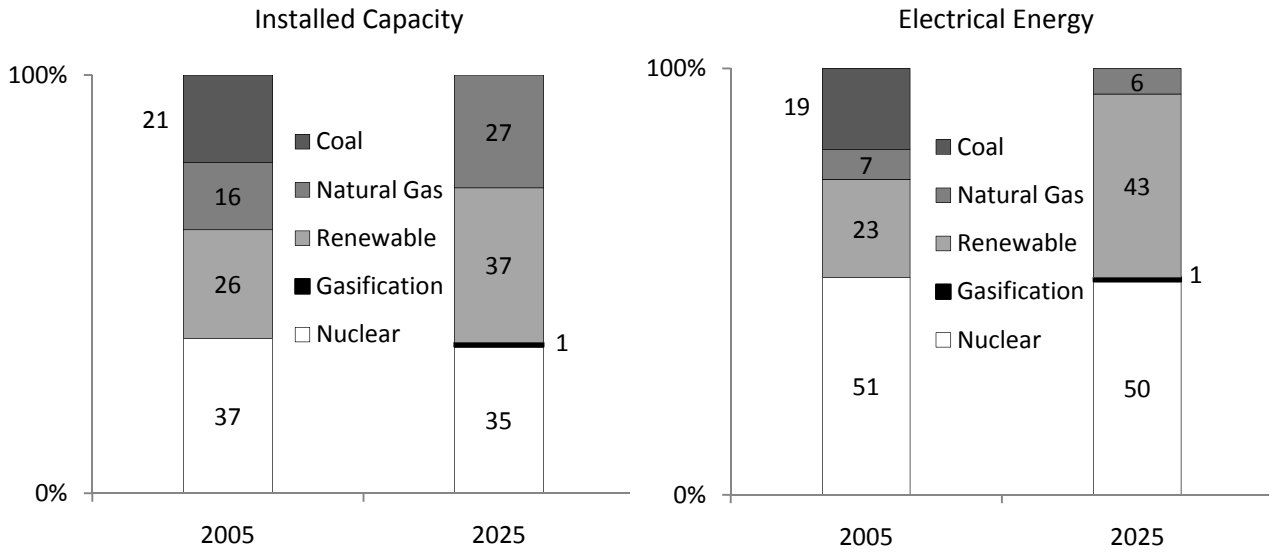

Figure 3-1: Ontario supply mix according to OPA advice

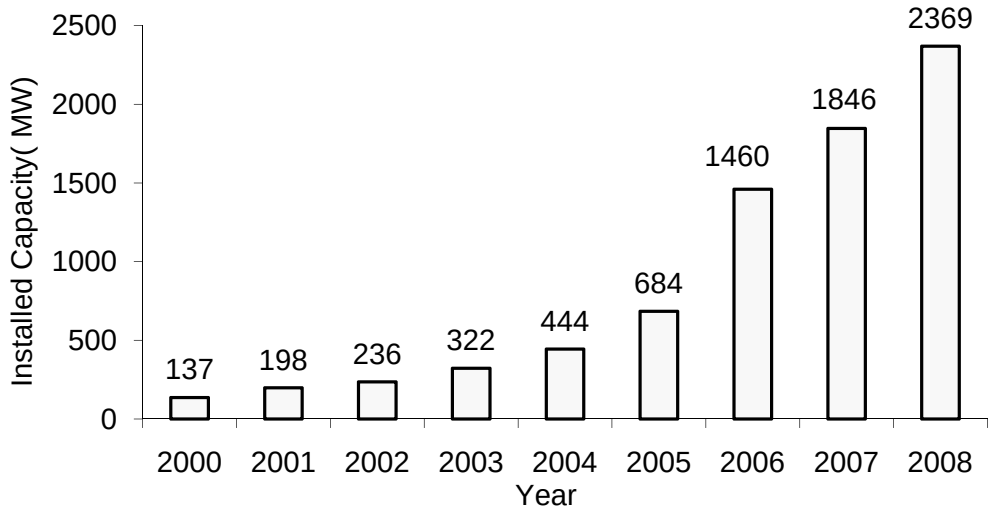

Figure 3-2: Wind generation installed capacity in Canada

In March, 2006, the OPA introduced the Standard Offer Program (SOP) to encourage the owners of small renewable (wind and PV) energy generating facilities to contribute to Ontario's electricity supply, by providing power to their Local Distribution Company (LDC) and receiving payments for the power they provide [62]. According to this program, wind generation is credited C$0.11/kWh with contracts up to 20 years. To take the inflation rate into consideration, 20% of the base rate will be indexed annually. Monetary policy in Canada is guided by an inflation-control target. Currently, the target range is 1 to 3%,

within which the Bank of Canada aims at the 2% target midpoint [63]. Therefore, in this study, the annual percentage increase for wind energy is assumed to be 0.4% of the base tariff.

After this introduction, this chapter presents a review of wind power modeling and economic evaluation methods. A thorough cost-benefit analysis for wind projects that are enrolled in the SOP, from an investor's perspective, is presented in Section 3.3. This will be followed by a discussion of the Canadian taxation and incentive policies related to wind power projects. Different scenarios using wind speed and turbine data are presented and considered in the results section. Moreover, the effects of taxes - including income taxes, capital cost allowance, and property taxes - as well as wind power production incentives are included. Further, the sensitivity analysis section highlights the effects of variations in the capital cost, mean wind speed, discount rate, the annual operation and maintenance cost, and the SOP base rate. Cost of electricity at different mean wind speed and discount rate scenarios are calculated. Finally, conclusions are presented.

3.2 Annual Energy Calculation

3.2.1 Wind Speed

The Canadian Wind Energy Atlas (CWEA) uses k=2 for wind modeling [64]. When k=2, the Weibull pdf, described by equation (2-5) is called Rayleigh pdf and is demonstrated in equation (3-1) [44]. A plot for the Rayleigh pdf with a mean wind speed of 6m/s is presented in Figure 3-3.

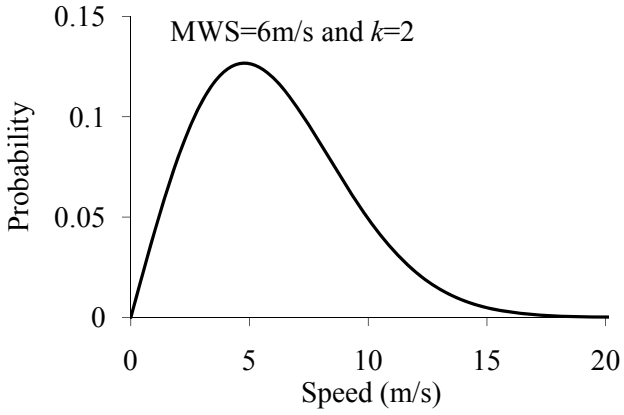

Figure 3-3: Rayleigh pdf for an MWS of 6m/s

$$f(v) = \frac{2v}{c^2} e^{-\left(\frac{v}{c}\right)^2} \tag{3-1}$$

In this case, the scale factor c can be found using the mean wind speed as follows:

$$\bar{v} = \int_0^\infty v \cdot f(v)\, dv = \frac{\sqrt{\pi}}{2} c \tag{3-2}$$

3.2.2 Capacity Factor

Capacity Factor (CF) in general is defined as the ratio of the average output power to the rated output power over a certain period of time. For example, the monthly CF is the average output of a wind turbine over a period of one month.

$$CF = \frac{P_{ave}}{P_{rated}} \tag{3-3}$$

The annual CF is given by equation (3-4) below.

$$CF = \frac{E_a}{P_{rated} \times 8760} \tag{3-4}$$

where E_a is the annual energy produced by the wind turbine, and 8760 is the number of hours in a year.

The annual energy is calculated by multiplying the hourly power output of the turbine at a certain speed by the probability of having that speed in a year as shown in equation (3-5) [41, 42]:

$$E_a = 8760 \times \sum_{v_x = v_1}^{v_2} f(v_x)\, P_e(v_x) \tag{3-5}$$

where v_1 and v_2 are the cut-in and cut-out speeds, respectively; $P_e(v_x)$ is the hourly power output at speed v_x, and $f(v_x)$ is the probability of the wind speed being within $v_x \pm \frac{\Delta v}{2}$, where Δv is the step size.

Figure 3-4 illustrates how to calculate the annual energy yield, given the turbine power curve and the wind speed probability distribution function. It is worth mentioning that the capacity factor calculated above normally results in an overestimation of the annual energy yield of wind turbines. To reach a more realistic value of the annual factor, energy yield should be corrected by multiplying the gross energy yield

by an adjustment loss factor, as described in Figure 3-5 below. Different components of the loss factor are discussed in the next subsection.

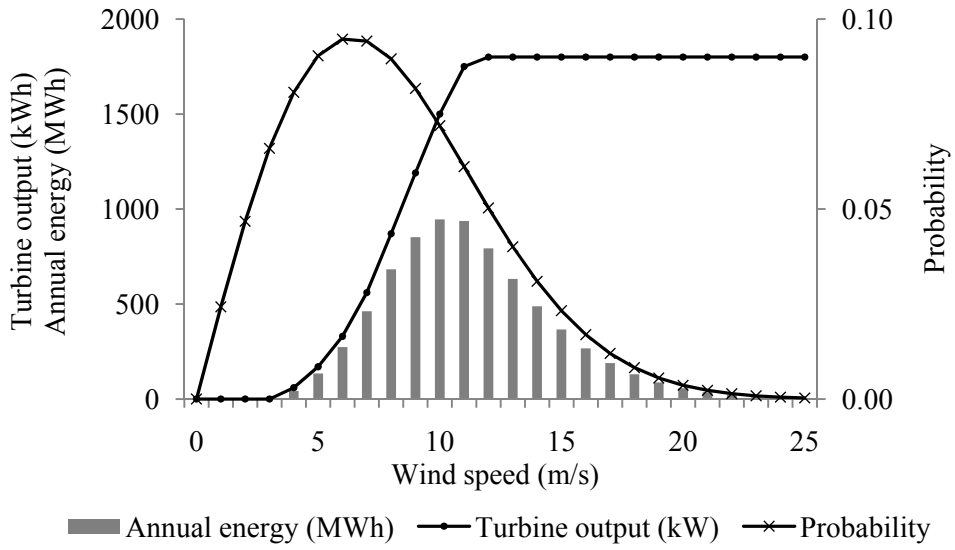

Figure 3-4: Gross *CF* calculation

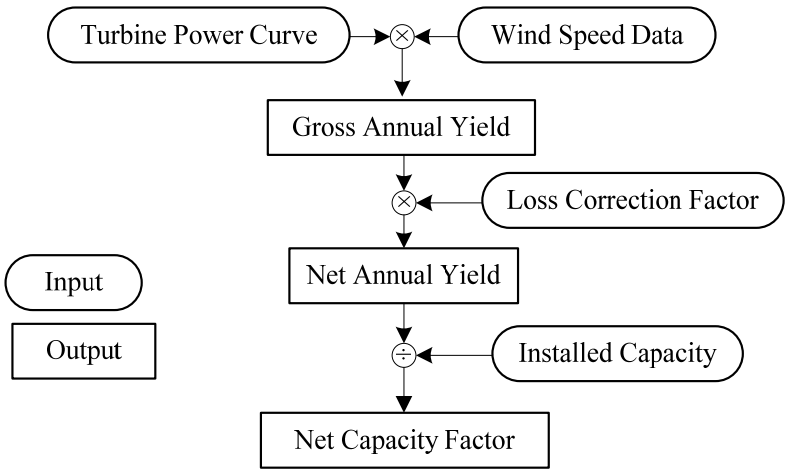

Figure 3-5: Annual net energy calculation

3.2.3 Adjustment Loss Factor

A wind energy adjustment loss factor is used to calculate the net energy yield [28]. Components of this factor include the following:

- Wake loss, which occurs because the wind is disturbed, and its speed decreases, while passing from the first turbine to the next in a wind farm. Part of the wind energy content is being used by the first turbine to generate electricity, resulting in a reduced performance of downwind turbines compared to turbines located in the first row of a wind farm array. Moreover, the wake effect can result in premature damage of downstream turbine structure due to turbulence caused by upstream turbines [65];
- Air density, which occurs due to the difference between the standard sea level air density (1.225 kg/m^3), for which the wind turbine's power curve is constructed, and the actual air density at the site;
- Blade soiling, which will reduce the rotor's efficiency over time. Similarly, accumulation of ice on the blades reduces rotor efficiency in converting wind power to electricity;
- Electrical losses, which occur because not all turbines' generated electricity is transmitted to the grid. A small fraction is lost in transmitting the electricity to the grid via feeders or in the interfacing converters due to switching and other losses;
- Availability, because in practice, wind turbines are not always available, thus, cannot convert the available wind resources into electricity. Wind turbine availability varies as wind turbines need regular servicing and inspection to ensure safe operation. Additionally, turbine component failures and accidents decrease turbine availability. A minor factor of wind turbine availability is grid availability.

Table 3-1 summarizes the magnitude of each component, used in four different studies. In this study, a small number of wind turbines are considered; therefore, the wake effect is expected to be small compared to that of big wind farms. A loss factor of 0.9 is used in the analysis.

Table 3-1: Adjustment factor considered by different Studies

<table>
<tr><th>Components</th><th>Helimax [50]</th><th>GE [49]</th><th>KEMA [66]</th><th>TrueWind [46]</th></tr>
<tr><td>Wake loss</td><td>6%</td><td rowspan="2">6 - 10%</td><td>3-4%</td><td rowspan="3">5%</td></tr>
<tr><td>Blade soiling and/or Icing effect</td><td rowspan="3">10%</td><td>-</td></tr>
<tr><td>Availability</td><td rowspan="2">4%</td><td>3%</td></tr>
<tr><td>Electrical losses</td><td>2-3%</td><td>2%</td></tr>
<tr><td>Air density</td><td>-</td><td>-</td><td>-</td><td>3-5%</td></tr>
<tr><td>Adjustment Factor
(1-Σ Components)</td><td>0.84</td><td>0.84 – 0.88</td><td>0.88 – 0.90</td><td>0.90 – 0.92</td></tr>
</table>

3.3 Economic Evaluation Methods

In this section, project evaluation methods are briefly discussed. These methods include Net Present Value (NPV), Internal Rate of Return (IRR) and Payback Period (PP). In addition, due to the high capital cost of wind power projects, depreciation methods are discussed as well.

3.3.1 Net Present Value

The Net Present Value (NPV) approach uses the time value of money to convert future cash flow into a present value at a certain discount rate. Therefore, this approach is also called Discounted Cash Flow (DCF). Due to the time value of money, a hundred dollars today are more valuable than a hundred dollars in the future, see Figure 3-6. Mathematically, the present value of future cash flow is defined by the following formula [67]:

$$PV = \frac{FV}{(1+dr)^N} \tag{3-6}$$

where PV and FV are the Present and the Future Values, respectively; dr is discount rate, and N is number of years in the future.

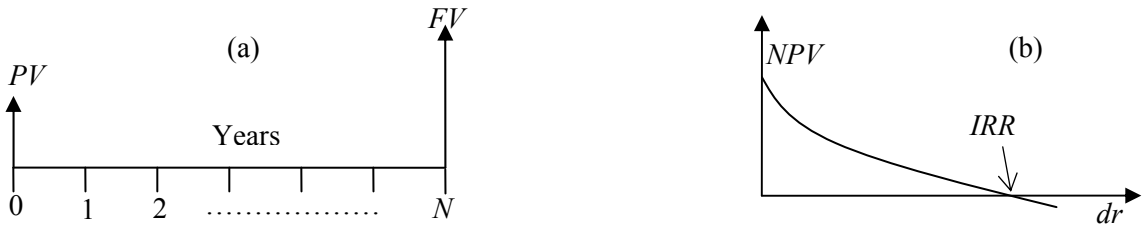

Figure 3-6: Present value (a) and IRR (b) mathematical definitions

For a recurring constant annual income, the present value can be found using the following formula [67]:

$$PV_A = A\frac{(1+dr)^N - 1}{dr(1+dr)^N} \tag{3-7}$$

where PV_A is the Present Value of the recurring annuity A. The NPV of a project is the difference between revenues and costs in today's money. In any comparison of investing options, the project with the maximum NPV is the winning one.

3.3.2 Internal Rate of Return

Mathematically, Internal Rate of Return (IRR) is defined as the discount rate that gives a NPV of zero, see Figure 3-6. IRR is the effective annual return of investment over the life of the project. Therefore, the project will have value for investors if its IRR is greater than the discount rate or the Weighted Average Cost of Capital ($WACC$). When using IRR for project ranking, the project with the highest IRR is the winner.

3.3.3 Payback Period

Payback Period (PP) is defined as the length of time required to recover the initial investment in a project. The shorter the length, the more economically attractive to investors the project is. Although simple PP is easy to understand, it does not account for the time value of money; therefore, it has serious limitations. Using discounted cumulative cash flow, better results can be achieved. Renewable energy investments have intensive capital costs, therefore, relatively long payback periods.

3.3.4 Depreciation

Depreciation is an accounting process in which the cost of the initial investment in a physical asset (e.g., wind turbines) is distributed over the expected lifetime of the asset. Methods used for depreciation calculations include the Straight Line (SL) method, Sum-of-years Digits ($SOYD$) method, and Declining Balance (DB) method.

The SL method assumes a constant depreciation value each year. The annual depreciation (AD) is calculated using the price of the asset (Pr) and its salvage value (S) after (N) years, as described in equation (3-9).

$$AD = \frac{Pr - S}{N} \tag{3-8}$$

In contrast, using the SOYD method allows more depreciation to occur earlier in the asset's life. The annual depreciation (AD) of the nth year is described by equation (3-9) below.

$$AD = \frac{N + 1 - n}{SOYD} Pr - S \tag{3-9}$$

For example, for a 5-year project, $SOYD$ =1+2+3+4+5=15.

Similarly, more depreciation can occur earlier in the asset's life when the DB method is used. This method assumes a constant depreciation rate per year. In a single DB, the annual depreciation is $(1/N)\%$ of the previous year's asset value. In Accelerated Declining Balance (ADB), more annual depreciation than in $(1/N)\%$ is allowed. For example, double DB allows $(2/N)\%$ depreciation rate.

Figure 3-10 compares the asset's annual depreciation by applying different depreciation methods for a project with these assumptions: Pr = C$19.8M, S = C$0.99M, N = 20. A 50% depreciation rate, $(10/N)\%$, is considered for the ADB method example.

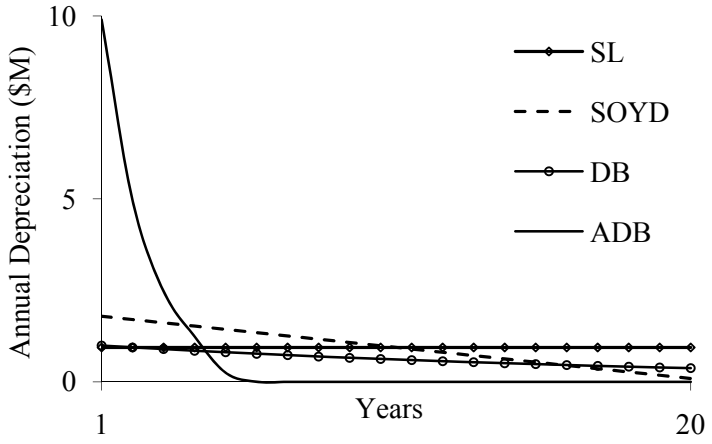

Figure 3-7: Annual asset's depreciation for different depreciation methods

It is clear that ADB is the best method as it allows the highest annual depreciation during the earlier years of the asset's life. This quality is important for investors because the amount of allowable depreciation is deducted from taxable income. Using ADB reduces or delays tax payment early in the project's lifetime, and time value of money makes this important as it delays future tax payment. Consequently, this deferral of taxes has a positive impact on the project's NPV, IRR and PP.

3.4 Wind Speed and Turbine Data

3.4.1 Wind Speed Data

In capacity factor calculations, six scenarios of mean wind speed were considered. In the first five, Rayleigh pdf is considered for wind speed profile representation. In the sixth, actual measurements of

wind speed are obtained from the Canadian Wind Energy Atlas (CWEA) where 80m altitude is considered [64]. This site is located at latitude 42.342 and longitude -82.115. The mean wind speeds of different scenarios are presented in Table 3-2.

Table 3-2: Wind speed at different Scenarios

Scenario #	1	2	3	4	5	6
MWS (m/s)	6	6.5	7	7.49	8	7.49

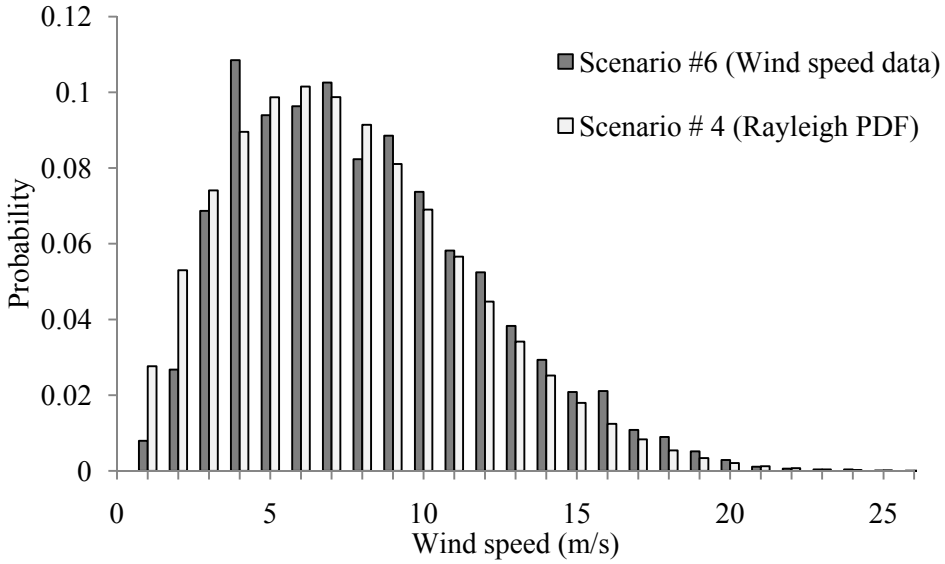

Figure 3-8: Comparison between measured site data and Rayleigh pdf model

A comparison between wind speed of scenario #6 (measured data) and scenario #4 (Rayleigh representation) is given in Figure 3-8. Note that the MWS in both scenarios is 7.49 m/s. It is clear that although Rayleigh pdf is a good representation for wind speed, there are some discrepancies especially at low wind speeds. Therefore, investors should consider measured data (when available) for more accurate analysis.

3.4.2 Turbine Power Curve Data

Six wind turbines were considered in this study [43]. The power output data of each of them is presented in Table 3-3 below.

Table 3-3: Wind turbines data

Turbine	Rating	Cut-in speed (m/s)	Nominal speed (m/s)	Cut-out speed (m/s)
T1	0.85kW	4	16	25
T2	1.8 MW	4	15	25
T3	2.0 MW	5	15	25
T4	1.8 MW	3.5	12	25
T5	2.0 MW	3.5	13	25
T6	3.0 MW	4	15	25

3.4.3 Turbines Cost

Different types of wind turbines under study are considered to have the same cost components. The cost of wind turbines can be classified into two components: capital cost and operation and maintenance (O&M) costs. Factors affecting capital cost includes turbine's type and manufacturer, location and transportation, grid connection, and other installation-related costs. According to OPA, the capital cost of wind-based distributed generation projects is estimated to be between C$2,000 and C$2,750 per kW of installed capacity [62]. This range is attributed mainly to the size of the turbine. Smaller size turbines tend to be more expensive than larger ones. The OPA website presented an example of a 1.8MW single turbine project with a capital cost of C$2000 per kW installed capacity.

O&M costs of wind-based distributed generation are estimated to be 1.5-2% of initial investment per year [68]. This fixed amount may include the following cost components:

- *Turbine service, maintenance and insurance*
- *Property taxes*
- *Annual connection fees*
- *Land lease*
- *Daily management*
- *Own electricity consumption*

3.5 Results

3.5.1 Capacity Factor

The capacity factor for each turbine in different scenarios is presented in Figure 3-9. It is clear that capacity factor increases as mean wind speed increases. Moreover, it is worth mentioning that the turbine T4 yields the maximum CF at all wind speed scenarios. This is attributed to the fact that the cut-in speed is low and the nominal speed of this turbine is the lowest; see Table 3-3. At a mean wind speed of 7 m/s, the turbine T4 yields 39.5% and 9.4% more energy than turbines T6 and T5, respectively. Therefore, the turbine T4 has been chosen for further analysis.

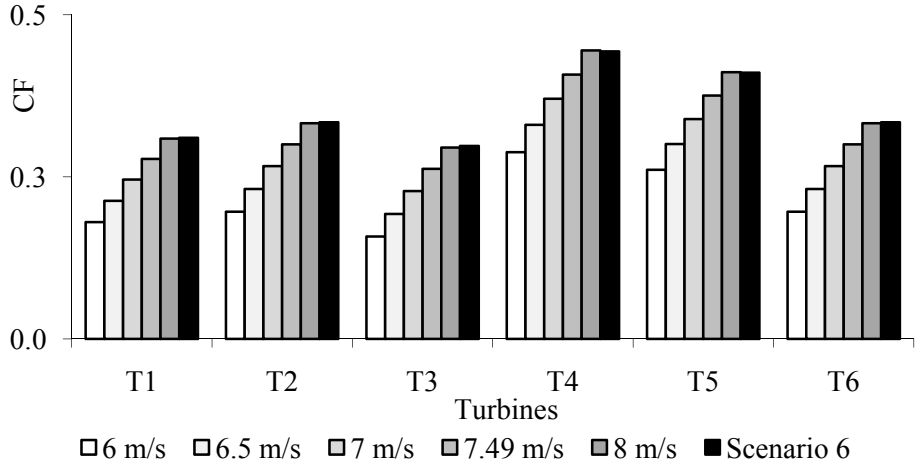

Figure 3-9: Capacity factor for each turbine at different MWS scenarios

3.5.2 Pretax Analysis

In this part, five units of T4 were considered having a total capacity of 9MW. This capacity is used to observe the 10MW capacity limit of the SOP. The base-case assumptions are listed below:

- *Mean wind speed at hub height: 7 m/s*
- *Lifetime: 20 Years*
- *Wind capacity capital cost: C$2200/kW*
- *Annual O&M cost: 1.5% of capital cost*
- *Cost of debt: 8%*

- *Cost of equity: 15%*
- *Debt ratio: 0.75*
- *Salvage value: 5% of capital cost*
- *Energy price: 0.11 C$/kWh base rate +20% indexed annually for inflation.*

The *dr* of the project according to the base-case assumptions is 9.75%, which represents the WACC (0.75*8% + 0.25*15%).

Figure 3-10 demonstrates the project's cash flow, excluding incentives and income taxation. The annual cash flow (ACF) starts with a high capital cost, C$19.8 Million (C$2200 /kW * 9MW), at year zero. Starting from year 1, a positive net cash flow occurs annually as a result of earnings from energy sales according to the SOP program, and O&M costs. At year 20, a higher cash flow occurs because of the project salvage value (5% * C$19.8 M). The simple payback period is six years, as shown by the cumulative cash flow (CCF). Using discounted cumulative cash flow (DCCF), an 11-year payback period is obtained, which represents a more realistic figure. The value of the discounted cumulative cash flow at year 20 represents the NPV of the project (C$6.36M).

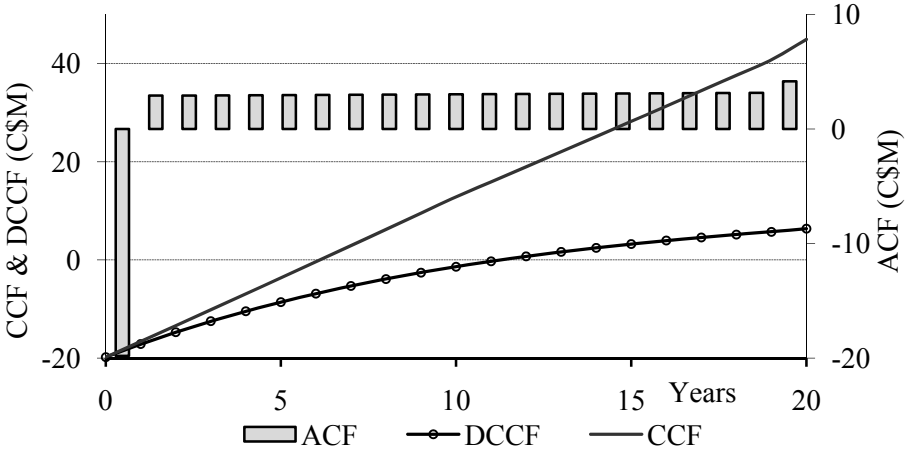

Figure 3-10: Pre-tax cash flow for base-case assumptions

3.5.3 Incentives and Taxation

In addition to Ontario's long-term power purchase agreement, SOP, wind power projects are promoted through incentive and tax write-off programs. Below is a brief discussion of these programs.

3.5.3.1 Capital Cost Allowance

According to Class 43.1 in Schedule II of the Canadian Income Tax Act, taxpayers are allowed an accelerated write-off of certain equipment designed to produce energy in a more efficient way or to produce energy from alternative renewable resources[69]. Taxpayers are allowed to deduct the cost of eligible equipment at up to 30 percent per year, on a declining balance basis. Moreover, half this value is to be used in the first year of the project lifetime. In the 2005 Budget, Class 43.2 was created, which further accelerated the capital depreciation rate for certain Class 43.1 assets (including wind projects) to 50 percent per year[69]. This modification came into effect on June 1, 2006.

Fully deductible expenditures associated with the start-up of renewable energy and energy conservation projects are described in the Canadian Renewable and Conservation Expenses (CRCE) section. Wind energy electrical generation system projects are eligible for this accelerated Capital Cost Allowance (CCA). The eligible expenses are [69]

- *Machinery and equipments;*
- *Related soft costs for design, engineering, and commissioning;*
- *Other services required to make the system operational.*

Other intangible costs eligible for the accelerated CCA are

- *Costs of pre-feasibility and feasibility studies;*
- *Costs related to determining the extent, location, and quality of energy resources;*
- *Costs related to negotiations and site approval;*
- *Certain site preparation costs, and*
- *Service connection costs.*

Figure 3-11 shows the base-case depreciation calculations. As presented by the figure, the ADB depreciation method allows investors to claim the CCA in the first five years of the project lifetime.

3.5.3.2 Property Taxes

Generally, local municipalities collect property taxes to raise additional revenues to cover the costs of local government services. The amount of property tax is based on the assessed value of property owned.

Therefore, both property value assessment and local tax rate are of great importance in the calculation of property taxes payable by the owner of a property. Both the wind power industry and local governments and municipalities across Canada agree that wind power facilities should pay property taxes. However, the appropriate methods and level of taxation is debatable. Normally, property tax is based on the market value assessment of the land and the building, not on the equipment housed. A wind turbine consists of four main parts: a foundation, a tower, a nacelle, and blades. Therefore, it is debatable when it comes to which part of wind turbines is subject to property tax. On the one hand, it is clear that the foundation would be taxable whereas the nacelle would not. On the other hand, the tower can be argued that it is to hold the main equipment contained in the nacelle; therefore, it is not taxable. Moreover, for a fully erected turbine it is difficult to value the price paid for the different parts separately.

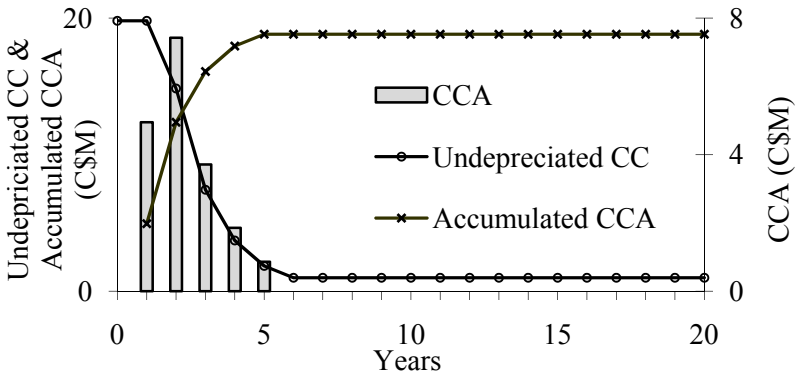

Figure 3-11: Base-case depreciation calculations

In Canada, there is a wide range of interpretation of what is considered taxable property and what is considered as machinery and equipment [70]. In Ontario, there are three components of wind power facilities property tax: a turbine property or structure component, a land component, and the value of the site building. A fixed rate of property/structure includes the tower and foundation only. This rate is currently C$40,000 per installed MW capacity regardless of the number of turbines. For the land component, the Municipal Property Assessment Corporation (MPAC) considers an acre of industrial land for each turbine [70]. Below is the property tax calculation for the 9MW wind project considered in this study.

- *Land value: C$10,000 per acre (ranges from C$4816 to C$17000)*

- *Site Buildings: C$50,000*
- *Assessed value: C$450,000 (structure: 40,000*9, Buildings: 50,000, Land: 4*10,000)*
- *Tax rate: 0.05 (ranges from 0.05527644 to 0.0389325)*
- *Annual property taxes: C$ 22,500*
- *Annual property taxes per MW installed capacity:C$2,500*

It can be concluded that property taxes do not have a major impact on the viability of a wind project compared to other factors, according to the current policy. Property taxes represent about 7.5% of the base-case O&M costs.

3.5.3.3 Federal Incentives

The Federal Government of Canada is promoting renewable energy resources in general, and wind power in particular, through incentive programs. One of the most important vehicles for promoting wind power in Canada was the Wind Power Production Incentive (WPPI) program. According to this program, eligible wind farms are entitled to receive financial incentives as follows [71]:

- *¢1.2 /kWh of eligible production if the project was commissioned after March 31, 2002, and on or before March 31, 2003.*
- *¢1 /kWh of eligible production if the project was commissioned after March 31, 2003, and on or before March 31, 2006.*
- *¢0.8 /kWh of eligible production if the project was commissioned after March 31, 2006, and on or before March 31, 2007.*

Another program was introduced after the WPPI program concluded on March 31, 2007. The new federal program is called ecoENERGY, and it targets projects to be constructed over the next four years, from April 1, 2007 to March 31, 2011. According to Natural Resources Canada (NRCan) [71], the ecoENERGY incentive program for renewable power will invest C$1.48 billion to increase Canada's supply of clean electricity from renewable sources such as wind, biomass, low-impact hydro, geothermal, solar photovoltaic, and ocean energy. The program is expected to encourage the production of 14.3 TWh from renewable energy sources. According to this program, eligible renewable electricity projects will

receive an incentive of ¢1 /kWh for up to 10 years [71]. In this analysis, an incentive of ¢1 /kWh for the first 10 years of the project is considered.

3.5.3.4 Income Taxes

Corporations operating in Ontario are generally taxed at a rate of 36.12 %. However, wind power companies, being classified as manufacturing and processing industries, are subject to a lower rate of 34.12 % (12 % Provincial tax rate and 22.12 % Federal Manufacturing and Processing (M&P) rate) [72].

Taxable income (TI) is defined by Equation 15 as follows:

$$TI = R - O\&M - CCA - I \tag{3-10}$$

where R is project's annual revenues; $O\&M$ are the annual Operation & Maintenance costs; CCA is the annual capital cost allowance, and I is the annual interest paid for debt. Figure 3-12 shows the cost of debt calculations. In spite of the constant annuities paid to lending agencies, the amount of interest paid is proportional to the debt remaining. This reduces taxes paid early in the project lifetime.

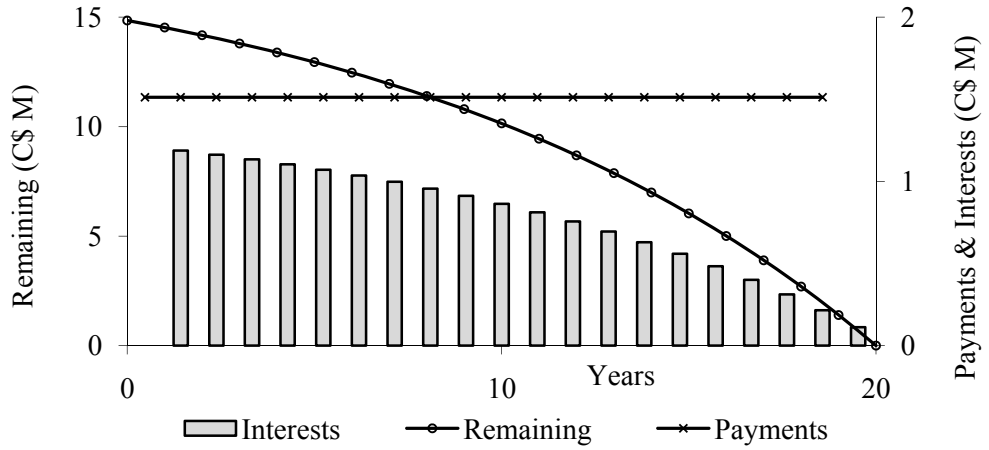

Figure 3-12: Cost of debt calculations

Figure 3-13 demonstrates income tax calculations when the incentives are taxable and when they are not. It is clear that taxes are higher in case of taxable incentives. Additionally, the figure demonstrates that using the ADB depreciation method for the CCA calculation delays tax payment compared to using the SL method.

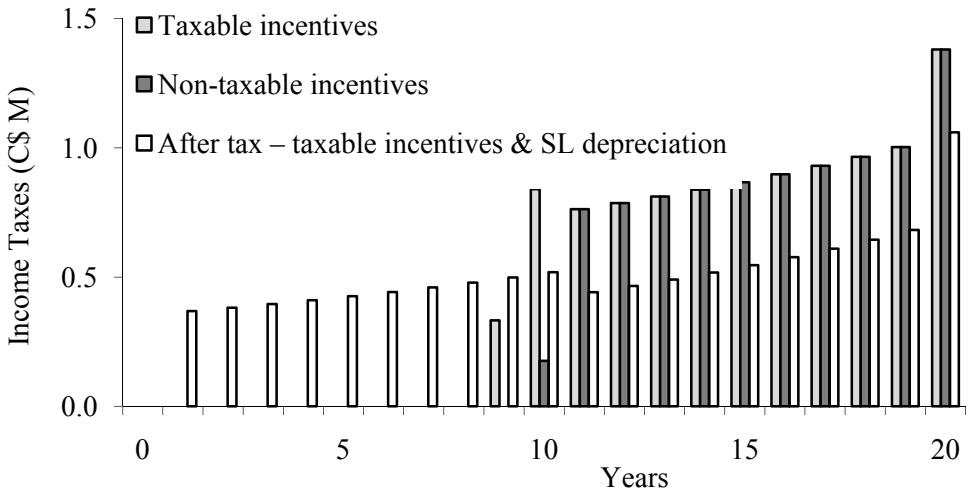

Figure 3-13: Income tax calculations

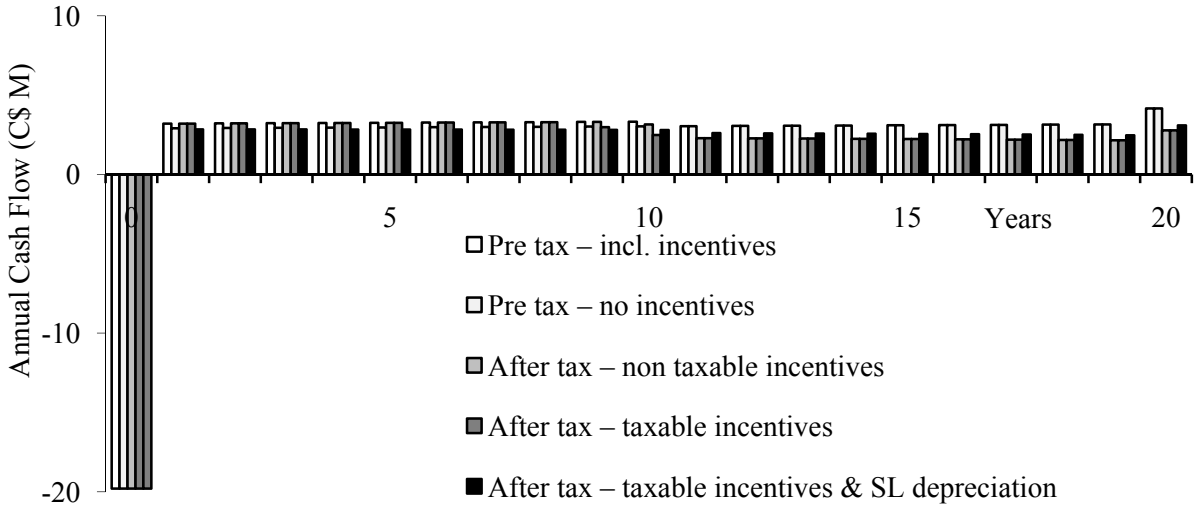

Figure 3-14: Annual cash flow

Figure 3-14 and Figure 3-15 present the annual cash flow and the discounted cumulative cash flow, respectively, including taxation and incentive effects. It is clear that incentives will improve the economical viability of wind projects when taxes are neglected. However, this in practice is not the case. In fact, taxation reduces the NPV of the project from C$6.36 million to C$5.521 million with taxable incentives, a reduction of 13%. Having non-taxable incentives improves the NPV to C$5.927 million. Additionally, the figure illustrates the effect of using the SL method instead of ADB for the CCA

calculation. Using the SL method would cause NPV to drop to C$4.139 million, compared with C$5.521 when using the ADB method - a drop of 25%.

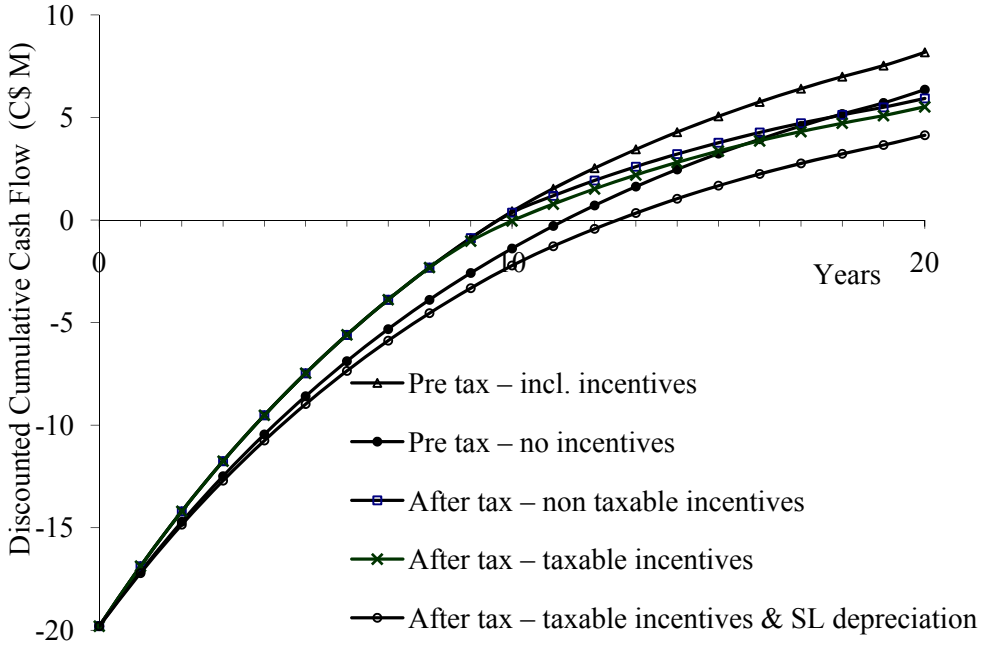

Figure 3-15: Discounted cumulative cash flow

3.5.4 Sensitivity Analysis

In this analysis, the effect of mean wind speed, capital cost, discount rate, O&M, and SOP base rate are highlighted. The NPV is shown in Figure 3-16 for different mean wind speed scenarios. As the figure demonstrates, NPV is very sensitive to mean wind speed. Theoretically, a 25% increase in speed would result in a 95% increase in the wind power content, according to equation 2-2. At low mean wind speed, such as 6m/s, the project is not viable because very low or negative NPV is expected.

The effect of discount rate and capital cost is illustrated in Figure 3-17. It is clear that the NPV is highly affected by the value of the discount rate. The NPV decreases as the discount rate increases and becomes zero at the *IRR* of the project. Beyond this discount rate, the project is economically not viable. Since the discount rate is the weighted average cost of capital, it is strongly affected by the cost of debt and its ratio, as well as by the cost of equity. Similarly, capital cost is very crucial in renewable energy projects because such projects require intensive capital investments and have relatively low O&M costs. Although wind power projects are eligible for CCA, increasing capital cost reduces the project's NPV dramatically.

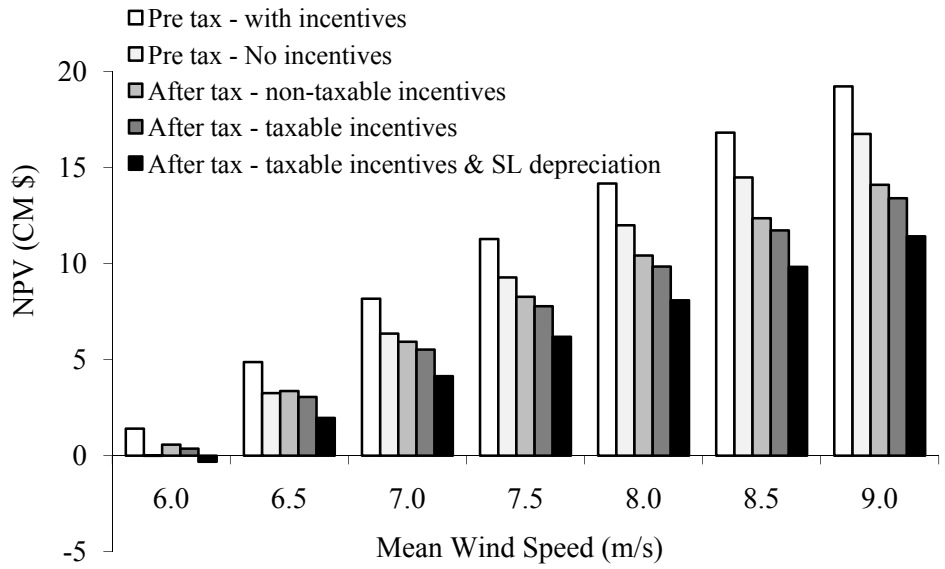

Figure 3-16: Effect of MWS on NPV

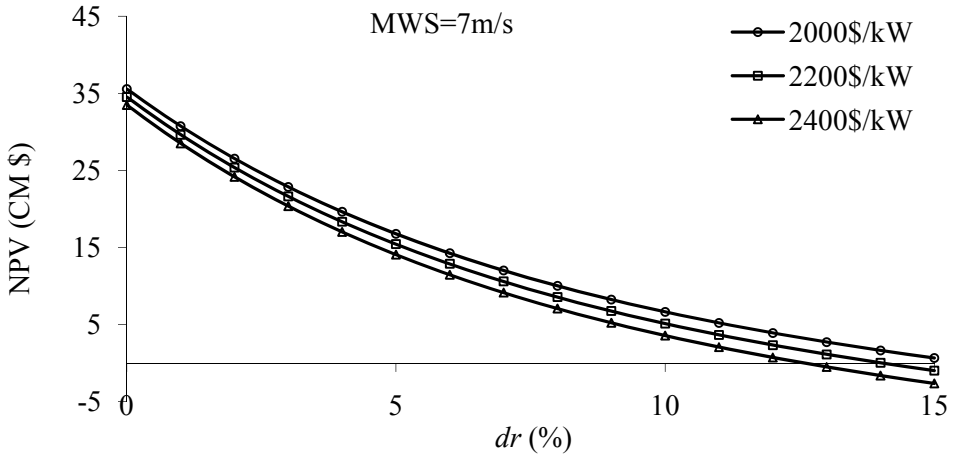

Figure 3-17: Effect of discount rate and capital cost

The effect of a tremendous increase on the O&M cost, which could be caused by very high property taxes, is presented in Figure 3-18. Increasing the O&M from 1.5% of the capital cost to 2.5% reduces the project's viability. Therefore, using the cost approach in calculating property taxes could be very costly, depending on what is considered to be taxable.

Figure 3-19 highlights the effect of changing the SOP base rate on both *IRR* and NPV of the project. For the base-case parameters, increasing the rate by 27% would cause the *IRR* to double.

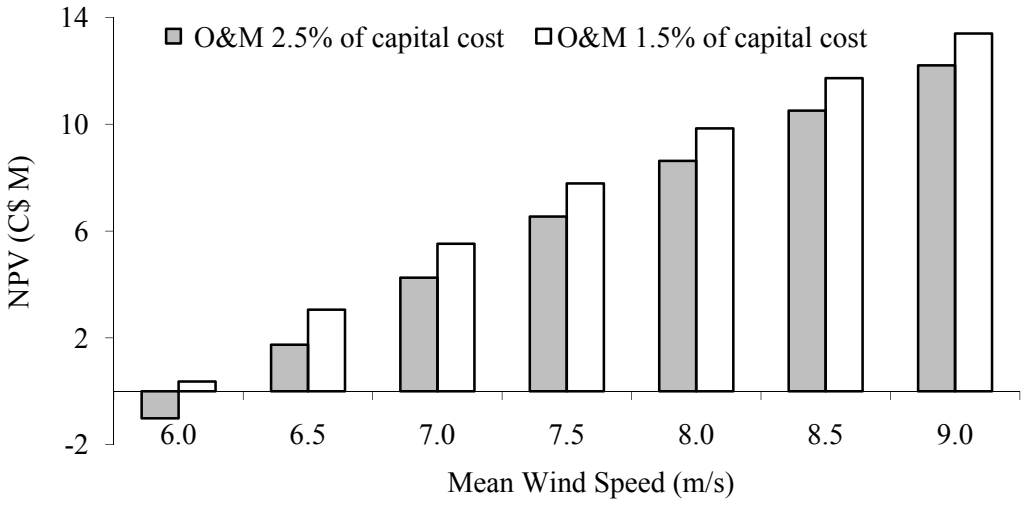

Figure 3-18: Effect of O&M costs for different MWS scenarios

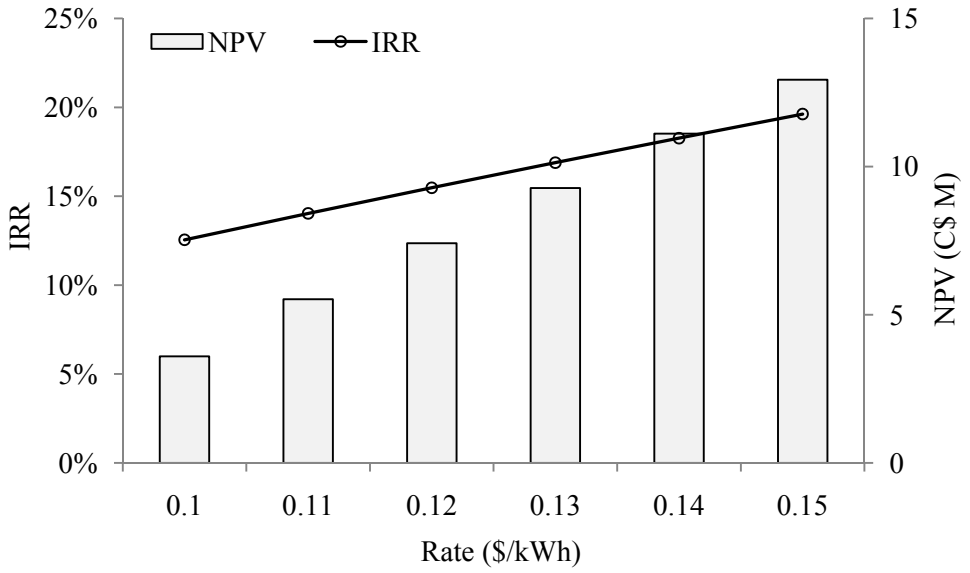

Figure 3-19: Effect of SOP base rate on NPV and IRR for the base-case parameters

The Cost of Electricity (COE) in C$/kWh at the base-case parameters for different mean wind speed and discount rate scenarios is shown in Figure 3-20. The cost of electricity is obtained by dividing the projected annual energy yield by the annualized cost of the project.

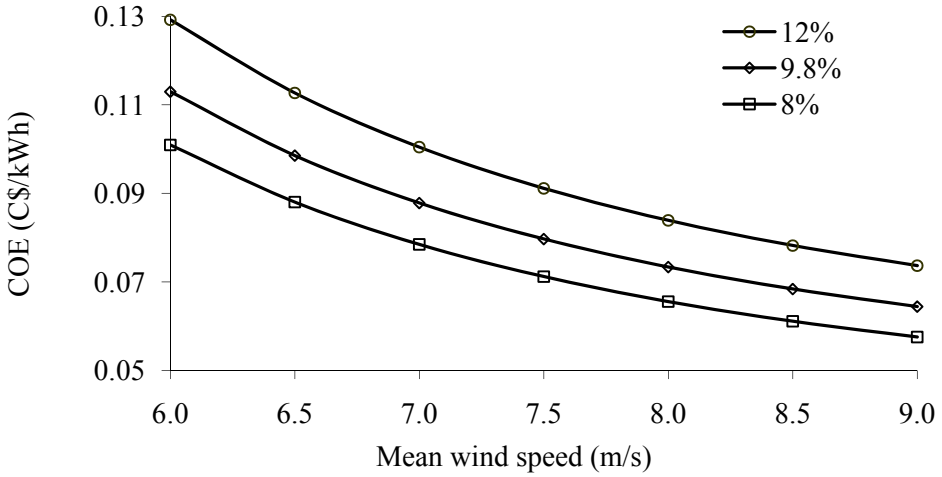

Figure 3-20: Cost of electricity at different MWS and discount rate scenarios

3.6 Summary

A thorough techno-economic evaluation of wind-based DG projects was presented to demonstrate the role of Ontario's taxation and incentive policies in the economical viability of investments under Ontario's SOP. The case study presented in this chapter considered different wind turbines, and various mean wind speed scenarios. The net capacity factor of each turbine for different wind speed scenarios was calculated. A comparison between actual wind speed measurements and wind speed representation using Rayleigh pdf illustrates that actual wind speed measurements are necessary for accurate economic assessment.

It can be concluded that property taxes in Ontario do not have a major impact on the viability of wind projects compared to other factors according to the current policy. However, income taxes result in a 13% decrease of the project' NPV, for the base-case parameters. The project's economic viability can be improved considering non-taxable incentives. Additionally, using the ADB depreciation method for the *CCA* calculation delays tax payment compared to using the SL method, and improves the project's viability tremendously. The sensitivity analysis demonstrated the effect of changing the capital cost (C$/kW), O&M cost (%of capital cost), discount rate, and the SOP base rate (C$/kWh) on the project's economic viability. According to the base-case parameters, increasing the rate by 27% would cause the IRR to double.

Chapter 4

Wind to Power a New City in Oman[5]

4.1 Introduction

The Sultanate of Oman is located in southwest Asia on the extreme southeastern corner of the Arabian Peninsula, covering an area of 309,500 km^2. It shares borders with the United Arab Emirates to the northwest, the Kingdom of Saudi Arabia to the north and west, and the Republic of Yemen to the southwest. The Sultanate's coastline extends 3,165 km from the Strait of Hormuz in the north, to Ras Darbat Ali at the borders of the Republic of Yemen in the south, Figure 4-1 [75]. Oman shares its coast with three seas: the Persian Gulf, the Gulf of Oman and the Arabian Sea [76]. The Sultanate has a population of about 3 million people and its economy is heavily dependent on the oil and gas sectors. In 2007, revenues from these two sectors accounted for 75.8% of total government revenue, 82.8% of total exports, and 45.2% of the gross domestic product (GDP) [77].

As identified in [78], to implement a sustainable energy development strategy, three major technological changes are required: demand-side management, generation-side efficiency improvements, and the utilization of renewable energy sources. Unlike fossil fuels, renewable resources in general and wind in particular are sustainable local sources of energy. Harvesting wind power is, in fact, in line with a long-term development strategy, the Oman 2020 Vision, which is aiming for sustainable development [79]. Yet there are no utility-scale wind turbines connected to the grid, despite that some publications have suggested a strong potential for wind power at some sites [80, 81]. Dorvlo and Ampratwum in [80] identified four potential sites for wind power projects: Thumrait, Sur, Masirah, and Marmul. Moreover, the diesel fuel saving benefits of using wind power in rural areas were demonstrated [81]. None of the previous articles identifies the Duqm area as a potential site for wind power projects, or proposed the use of wind power as a source of electricity in the new city being built there.

After this introduction, this chapter proceeds to investigate wind resources in the Duqm area. Section 4.3 presents a techno-economic evaluation of wind power projects in the area. Finally, a results summary and recommendations are presented.

---

[5] Some parts of this chapter have been published in:

[73] M. H. Albadi, E. F. El-Saadany, and H. A. Albadi, "Wind to power a new city in Oman," *Energy,* vol. 34, pp. 1579-1586, October 2009.

An earlier version appeared in:

[74] M. H. Albadi, E. F. El-Saadany, and H. A. Albadi, "Wind to Power a New City in Oman," in *International Conference on Computer Communication and Power (ICCCP' 09)* Muscat, Oman, 2009, pp. 1-6.

Figure 4-1: Map of Oman [75]

4.2 Wind Power in Duqm

4.2.1 Why Duqm?

The vision for Oman's economy, Oman 2020, adopted in 1996, aims for achieving sustainability and fiscal balance and introduces substantial changes in the national economy's structure intended to diversify the production base, expand the role of the private sector, and develop human resources [77]. Among its efforts to create the necessary infrastructure favorable to future diversification programs, the government is investing in the area of Duqm, 600km south of Muscat. Although Duqm used to be considered a remote location in Oman, there is a plan being implemented to turn it into an industrial centre through the investment of billions of dollars in the infrastructure. In the past few years, the tender board has awarded infrastructure projects and contracts worth more than US$2 billion [82]. These projects include a master plan to develop a free trade zone and industrial area, construction of a port and dry dock complex, a desalination station, a power station, hotels, regional roads, and schools and houses for local people [82]. More infrastructure projects, such as Duqm International Airport, are being tendered [82].

Oman is currently using fossil fuel, mainly the domestically available natural gas, to generate electricity. Duqm's location on the southeastern coastline of Oman presents a good opportunity for legislators and policy makers to initiate utility scale wind projects, thus achieving sustainable development in this sector. Additionally, as is demonstrated in this chapter, there exists an excellent opportunity for investment in wind power in the Duqm area.

4.2.2 Wind Speed Data

Oman is affected by two main wind systems: the summer and the winter monsoons. These systems exhibit a clear seasonal reversal in direction. In the winter monsoon, wind blows mainly off the continent, keeping it dry. In the summer monsoon, the flow is predominantly off the Indian Ocean, keeping the continent wet.

Data on average hourly wind speeds were obtained from the Meteorology Department at Muscat International Airport for the period September 2003 to December 2007. A significant part of the data for the years 2003 and 2005 are missing; therefore, these years were filtered out. Although the effects of both monsoon systems are clearly evident in the wind speed profile, the summer monsoon system is more important, as demonstrated in Figure 4-2.

Although the average wind speed for Oman is moderate, with an annual speed of 3.36 m/s [80], wind resources Duqm are quite promising, with an annual average speed of 5.33 m/s. Moreover, since Oman is a summer peaking utility, wind power can replace some dispatchable generators and therefore improve system reliability. The capacity credit of wind power is enhanced by the high seasonal correlation between the demand of the Main Interconnected System (MIS) [83] and Duqm wind speed profiles. This high correlation could be utilized to reduce the level of peak demand as in [84].

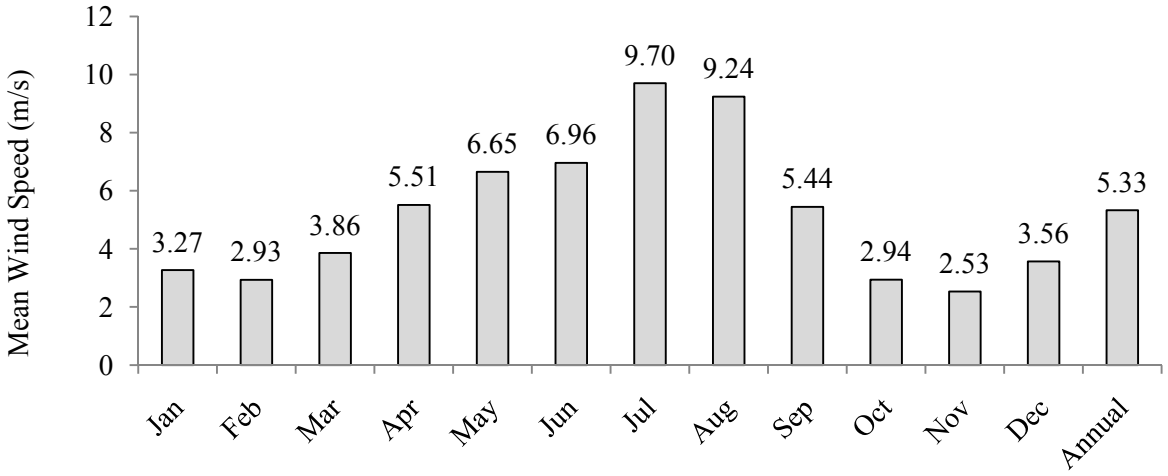

Figure 4-2: MWS at Duqm meteorological station (measured 10m above ground)

4.2.3 Wind Speed Model for Duqm

The cumulative distribution function $C(v)$, which gives the probability of the wind speed having values less than or equal to v, is given by the following equation [85]:

$$C(v) = 1 - e^{-\left(\frac{v}{c}\right)^k} \tag{4-1}$$

To obtain the values of c and k of the Weibull function, this equation can be linearized as follows [85]:

$$ln(-\ln[1 - C(v)]) = k\ln(v) - k\ln(c) \tag{4-2}$$

where $\ln(v)$ is the natural logarithm of v. The Weibull parameters can be obtained by plotting the right hand side of (4-2) as a function of $\ln(v)$, k is the slope of the straight line, and - $k\ln(c)$ is the intercept. The values of k and c for the Weibull representation of the annual wind speed in Duqm are 1.47 and 6.94, respectively. A comparison between the measured wind speed and the modeled one is given in Figure 4-3.

The small discrepancies between the annual wind profile model and measured data could be attributed to limited measured data and high seasonal wind speed variations.

Similarly, the parameters of the monthly wind speed Weibull distribution are calculated and presented in Table 4-1 and Figure 4-4. The results show that the monthly scale factor is proportional to the monthly mean wind speed. In addition, the shape factor of the monthly Weibull representation exhibits a clear seasonal variation. On the one hand, during the period from October to March, low k values illustrate the high irregularity in wind speed. On the other hand, the other six months, April to September, have higher k values due to the continuous summer monsoon wind that peaks in July and August.

Normally, the heights of the meteorological masts are much lower than that of the turbine's hub; therefore, wind speed measurements should be adjusted for height. Wind shear at ground level causes wind speed to increase, with the height h, depending on the ground friction coefficient α.

$$v_2 = v_1 \left(\frac{h_2}{h_1}\right)^{\alpha} \tag{4-3}$$

where v_2 is wind speed at hub height; v_1 is the measured wind speed; h_1 is the meteorological mast height, and h_2 is the turbine's hub height. According to [44], the friction coefficient ranges between 0.1 for smooth terrain and 0.4 for rough ones. The commonly known $1/7^{th}$ exponent rule is assigned to this coefficient, similar to that of [81, 86]. This value is commonly used for flat and open terrain [87].

Table 4-1: Wind Characteristics in Duqm

	Weibull parameters		Mean Wind Speed (m/s)	
	k	c	at 10 m	at 80 m
Jan	1.44	4.39	3.27	4.40
Feb	1.35	3.90	2.93	3.95
Mar	1.47	5.15	3.86	5.20
Apr	2.09	7.36	5.51	7.42
May	2.12	9.00	6.65	8.96
Jun	2.07	9.76	6.96	9.37
Jul	2.71	13.62	9.70	13.06
Aug	3.33	13.32	9.24	12.44
Sep	1.78	8.03	5.44	7.33
Oct	1.40	4.28	2.94	3.96
Nov	1.42	3.47	2.53	3.41
Dec	1.52	4.84	3.56	4.80
Annual	1.47	6.94	5.33	7.17

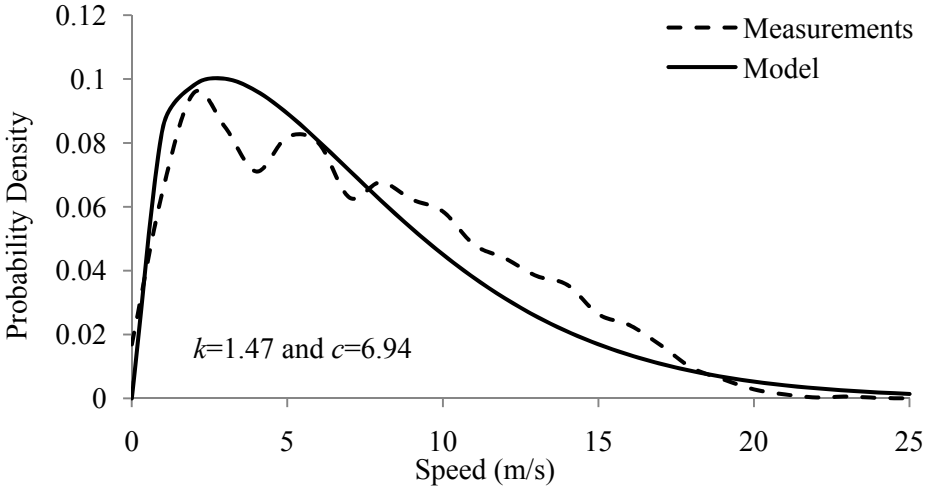

Figure 4-3: Annual wind speed distribution

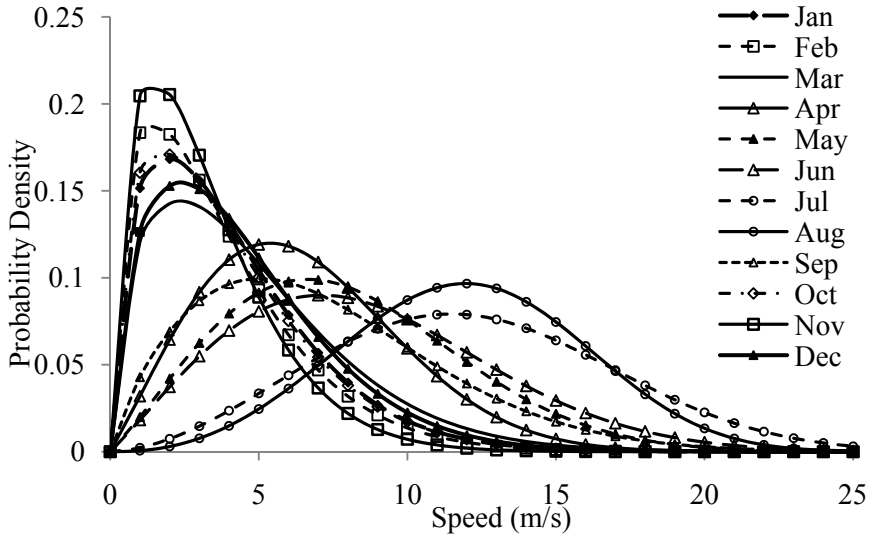

Figure 4-4: Monthly wind speed distribution

4.3 Techno-economic Evaluation Case Study

4.3.1 Base-case Assumptions

Actual measured wind speeds and manufacturer data of Vestas V90-1.8 [43] wind turbine characteristics are used in this study. The other base-case assumptions are presented in Table 4-2. These assumptions are slightly more conservative than those presented in [88].

Table 4-2: Base-case assumptions

Wind Project	Lifetime	20 years
	Number of turbines	5
	Wind capacity capital cost	US$1900/kW
	Annual O&M cost	1.5% of capital cost
	Cost of debt	7%
	Cost of equity	15%
	Debt ratio	0.75
	Discount Rate	9%
	Salvage value	5% of capital cost
Wind Turbine Vestas V90-1.8	Rated power (P_{rated})	1.8 MW
	Cut-in speed (V_c)	3.5 m/s
	Nominal speed (V_r)	12 m/s
	Cut-out speed (V_f)	25 m/s
	Hub height (h)	80 m
Feed-in Tariff (FIT)	US$0.10 per kWh for 20 years	

4.3.2 Annual Energy Yield

The annual energy of a wind turbine can be calculated by multiplying the power output of the turbine at a certain speed by the probability of having that speed in a year, as previously described in equation (3-5). As mentioned in chapter 3, the energy yield should be corrected by multiplying it by an adjustment loss factor, to account for turbulence and wake-effect losses, air density deviation, electrical losses, and turbine/grid availability [57].

The turbine power performance curve, $P(v_i)$, is given for standard conditions of 15°C air temperature, 101,325 Pa air pressure, 1.225 kg/m^3 air density. The air density can be adjusted for elevation using the following equation [40].

$$\rho(z) = \frac{P_0}{rT} e^{-\frac{gz}{rT}} \tag{4-4}$$

where P_0 is the standard sea level atmospheric pressure (101,325 Pa), r is the specific gas constant for air (287 J/kg.K), T is the air temperature in degrees Kelvin (°K), g is the gravitational constant (9.81 m/s²), and z is the elevation above sea level in meters. Substituting the values of the above parameters in (4-4), the air density in kilograms per cubic meter at any altitude is given by the following equation.

$$\rho(z) = \frac{353.05}{T} e^{-0.034\frac{z}{T}} \quad (4\text{-}5)$$

Based on the measured average annual measured temperature of 26.7°C and a turbine tower height of 80 m, the value of the air density is 1.170 kg/m^3. This value is 4.46% lower than that used in the power curve calculation. However, for pitch-regulated turbines, which is the case here, losses due to air density occur only in the ascending segment of the power curve [37]. For this case study, about 40% of the captured energy is from the ascending segment. Therefore, the losses due to air density are about 1.8%.

Electrical losses are considered to be 3%, according to [66, 89]. Due to the small number of turbines in the project, losses due to turbulence and wake-effect are also, coincidentally, considered to be 3% [66]. The reduced efficiency due to delay in the yaw system is assumed to be 2.5% [37]. The industry standard of 97% availability is considered for the overall turbine system [90]. Based on the above considerations, the overall loss adjustment factor of about 0.87 is used for further economic analysis. The net CF of the wind project is presented in Figure 4-5.

The annual CF of this specific wind turbine is 0.36, which represents about 3153 hours of full load operation. Figure 4-5 illustrates that monthly CFs are above the annual level during summer months, from April to September, with peak levels in July and August. This profile coincides with the Main Interconnect System (MIS) load profile [91].

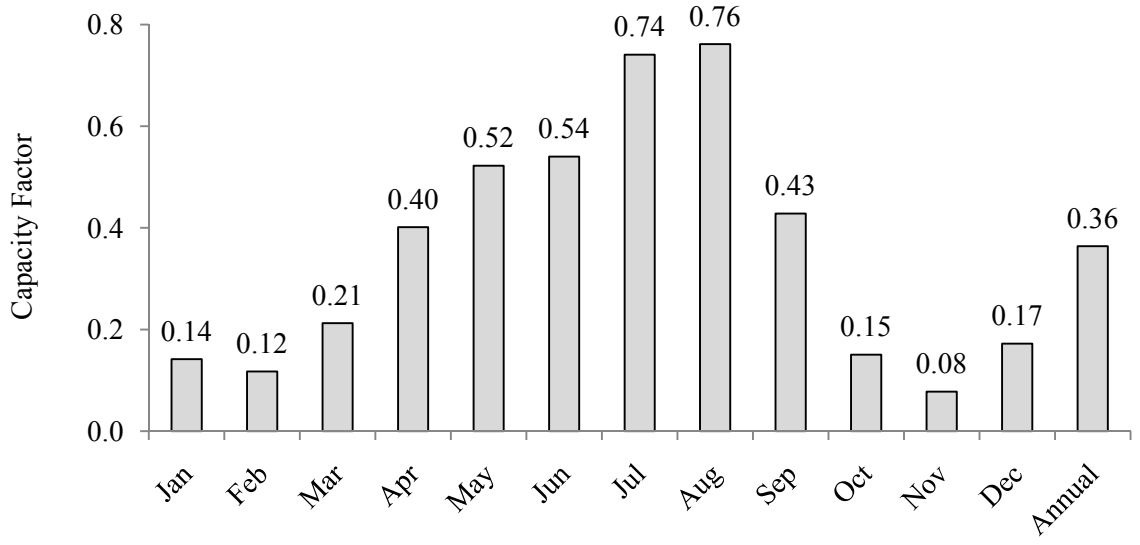

Figure 4-5: Capacity factor of wind power in Duqm

4.3.3 Cost of Electricity

Cost of Electricity (COE), in US$/kWh, for different capital cost and discount rate scenarios is shown in Figure 4-6. This figure illustrates that, for the base-case assumptions, the cost of electricity is about US$0.056 (OMR[6]0.021) and US$0.088 (OMR0.034) per kWh for discount rates of 5% and 10%, respectively.

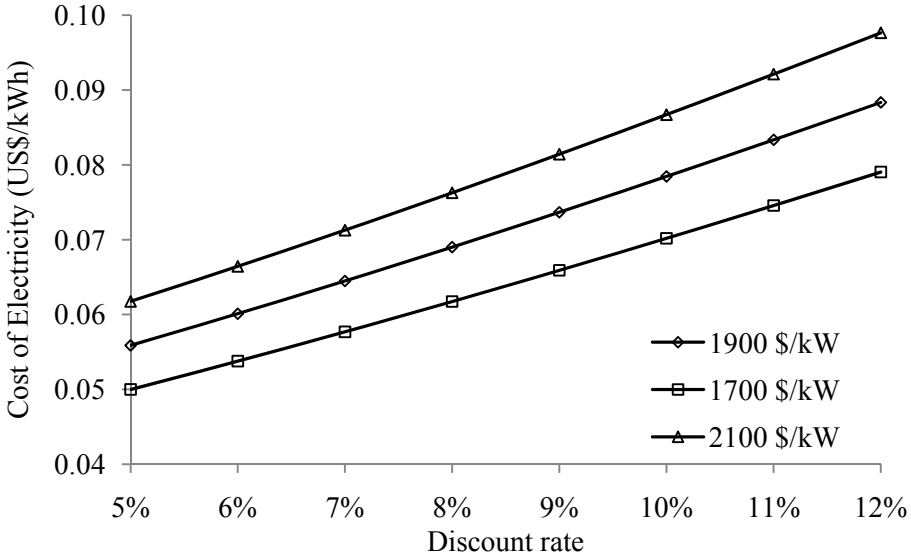

Figure 4-6: Cost of electricity from the wind project

4.4 Towards Investing in Wind Power

The average cost of electricity in the MIS is a function of the natural gas price, as shown in Figure 4-7 [91]. Based on the price of domestically available natural gas of US$1.5 per MMBtu, the average COE is OMR 0.0094 per kWh, which is equal to US$0.024 per kWh (1OMR=2.59 US$). However, international prices for natural gas are much more expensive than domestic ones. For example, in the United States, according to the Energy Information Administration (EIA), the average Henry Hub spot price is expected to be about US$11.53 per MMBtu in 2008 and US$11.29 per MMBtu in 2009 [92]. Assuming a fuel price of US$10 per MMBtu, the cost of electricity is US$0.111 or OMR0.043 per kWh. As illustrated in the previous section, this cost is higher than that of wind power. From Figures 4-6 and 4-7, one can conclude that wind power becomes economically competitive with natural gas-based generation system at a price

[6] The Omani Riyal (OMR) is pigged to US Dollar at 1 OMR =2.6 US$.

about US$6/MMBtu, for the base-case assumptions. Any saving on domestically consumed natural gas can be exported or used in other industrial activities.

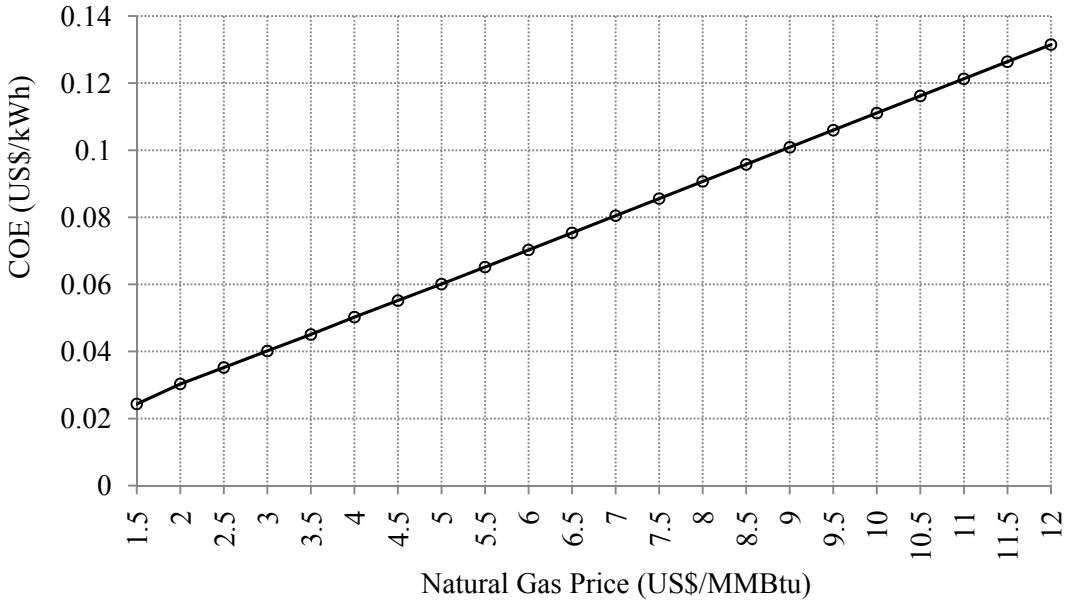

Figure 4-7: Cost of electricity from the existing natural gas-based system

According to Oman 2020, which aims at economic diversification away from the oil sector, the natural gas sector's contribution to the GDP is expected to increase to 10% to compensate for the expected decrease in the oil sector [79]. Although Oman passed its peak for conventional oil production in 2000, its production of natural gas increased from 176.2 Billion Cubic Feet (BCF) in 1997 to 851.1 BCF in 2007 [93]. Despite the huge expansion of natural gas-based industries such as petrochemicals, power generation, and Liquefied Natural Gas (LNG), Oman's proven natural gas reserves in 2007 stood at 30 trillion cubic feet, the same as the proven reserves in 1997 [93]. According to the EIA, there are speculations that, natural gas supplies in Oman may be overcommitted due to its long-term LNG export obligations [93].

Therefore, given the high international natural gas prices, the country's long-term LNG export obligations, and the expansion of natural gas-based industries, investing in wind power can be economically justified. Renewable energy support policies are required to support investing in wind power. In this work, FIT and CCA are considered.

4.5 Investor's Cost Benefit Analysis

In this work, a US$0.10 per kWh FIT rate is proposed to reduce regulatory and market risk associated with investments in wind power. Assuming a 20-year FIT contract, the Annual Cash Flow (ACF) and the Discounted Cumulative Cash Flow (DCCF) for a 5-turbine wind project are presented in Figures 4-8 and 4-9, respectively.

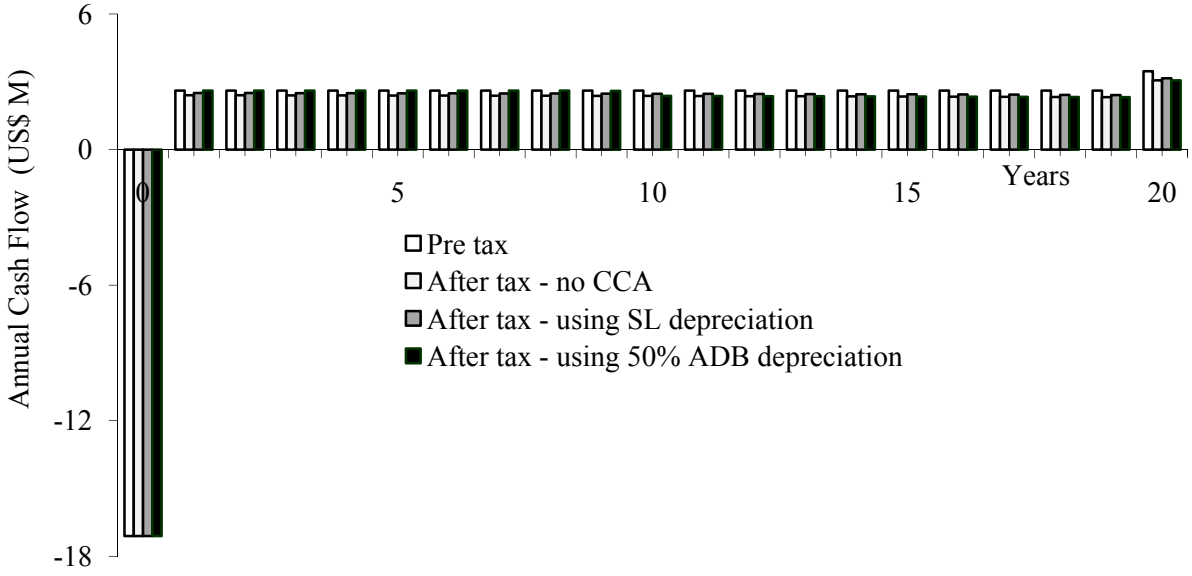

Figure 4-8: Annual cash flow of the base-case scenario

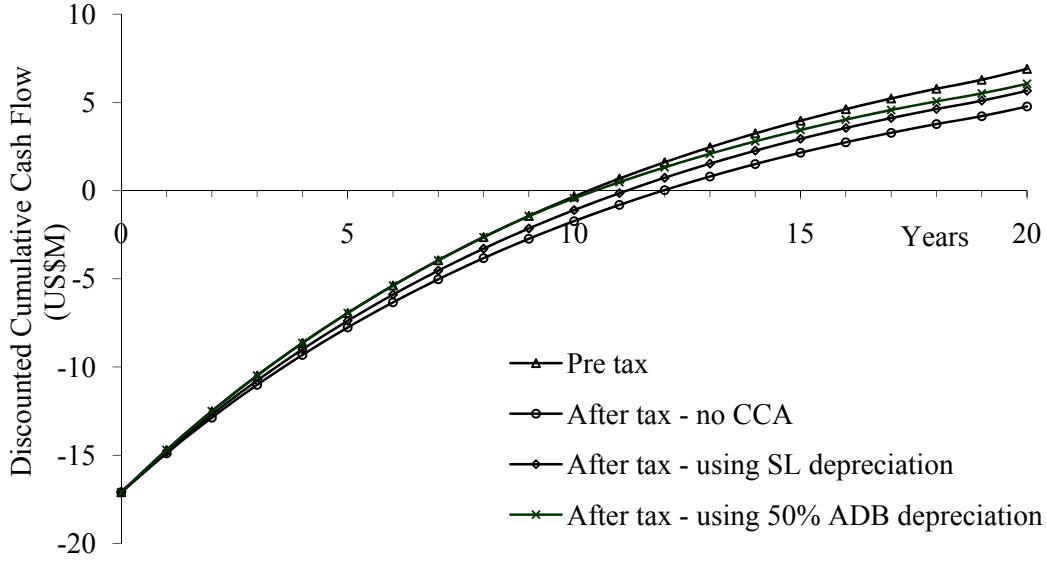

Figure 4-9: Discounted cumulative cash flow the base-case scenario

4.5.1 Pretax Analysis

The ACF starts with a high capital cost, US$17.1 Million (US$1900 /kW * 9000 kW), at year zero. Starting from year 1, a positive net cash flow occurs annually as a result of earnings from energy sales. At year 20, a higher cash flow occurs because of the project salvage value (5% * US$17.1 M). The payback period is the time at which the DCCF crosses the zero line, 11 years according to pretax calculations. The value of the DCCF at year 20 represents the NPV of the project (US$6.9M).

4.5.2 Effect of Taxation

The Ministry of National Economy of Oman is working on new income tax legislation to replace the current law, which was originally issued in 1981 by royal decree 47/1981. According to current legislation, the highest corporate tax rate is 12 percent [79]. Although this rate is quite generous, any wind power project investors will pay a total amount of US$5.0 Million as income taxes, with an NPV of US$2.1 Million. This amount would reduce the NPV of the project to US$4.8 Million, a reduction of about 30% compared with pretax calculations.

4.5.3 Capital Cost Allowance

Renewable energy projects are characterized by high capital cost requirements. Normally, these projects are promoted through tax write-off programs, such as Capital Cost Allowance (CCA) programs. In these programs, taxpayers are allowed to deduct the cost of eligible equipment (e.g., wind turbines) at a certain rate depending on depreciation method [57]. In this analysis, the effects of two depreciation methods on taxes are highlighted: the Straight Line (SL) method and the Accelerated Declining Balance (ADB) one. In this analysis, a declining balance rate of 50% is considered.

Figure 4-10 illustrates that the CCA policy reduce taxes substantially, from US$5.0 to US$3.1 Million, for both depreciation methods. However, using the ADB depreciation method delays tax payment, and the time value of money makes this quality important. The NPV of taxes incurred when using the ADB method is US$0.8 Million compared with US$1.2 Million incurred when using the SL depreciation method. Interestingly, considering the ADB method, the payback period of the project is almost the same as that obtained from pretax calculations, as presented in Figure 4-9.

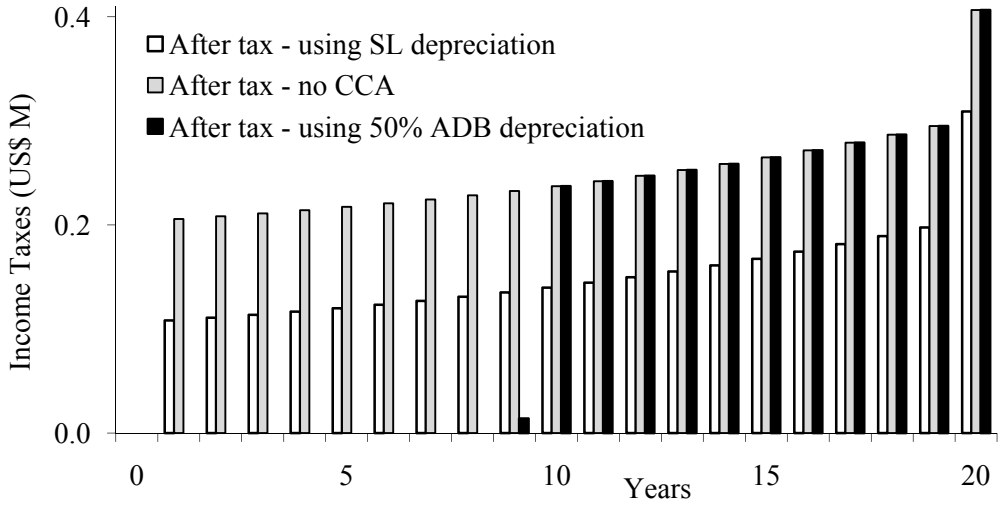

Figure 4-10: Income taxes with/without CCA

4.5.4 Sensitivity Analysis

The effect of discount rate and the FIT rate on the project's viability are illustrated in Figures 4-11 and 4-12, respectively. Both factors are crucial to any wind power investment. The high initial cost and the long lifetime of wind projects make the NPV very sensitive to discount rates, as illustrated in Figure 4-11. In addition, the figure shows that the IRR of the project, for the base-case assumptions, decreases from 14.3% in pretax calculations to 13.8% and 13.4% with the ADB and SL depreciation methods, respectively.

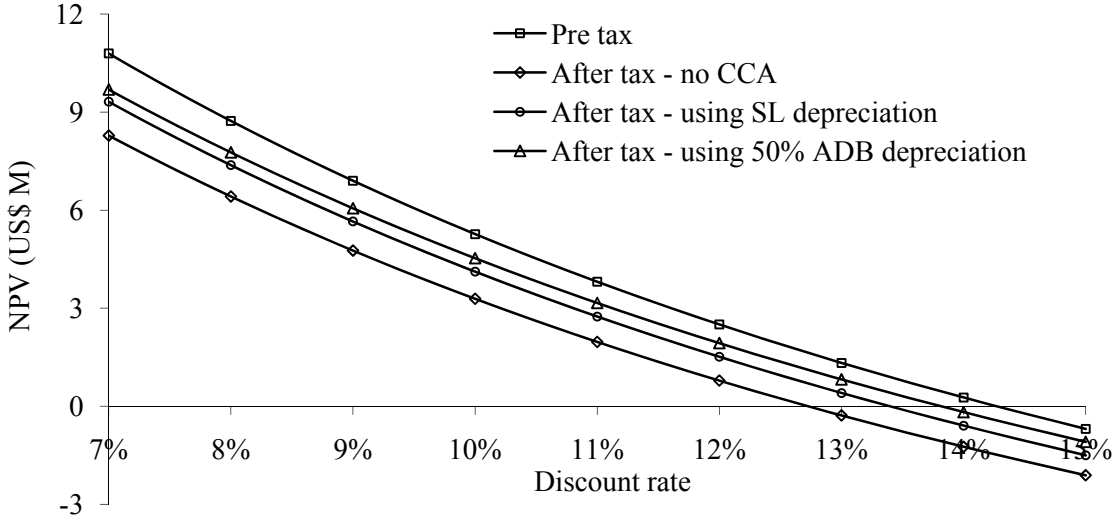

Figure 4-11: Effect of discount rate on the project's viability (FIT =US$0.10/kWh)

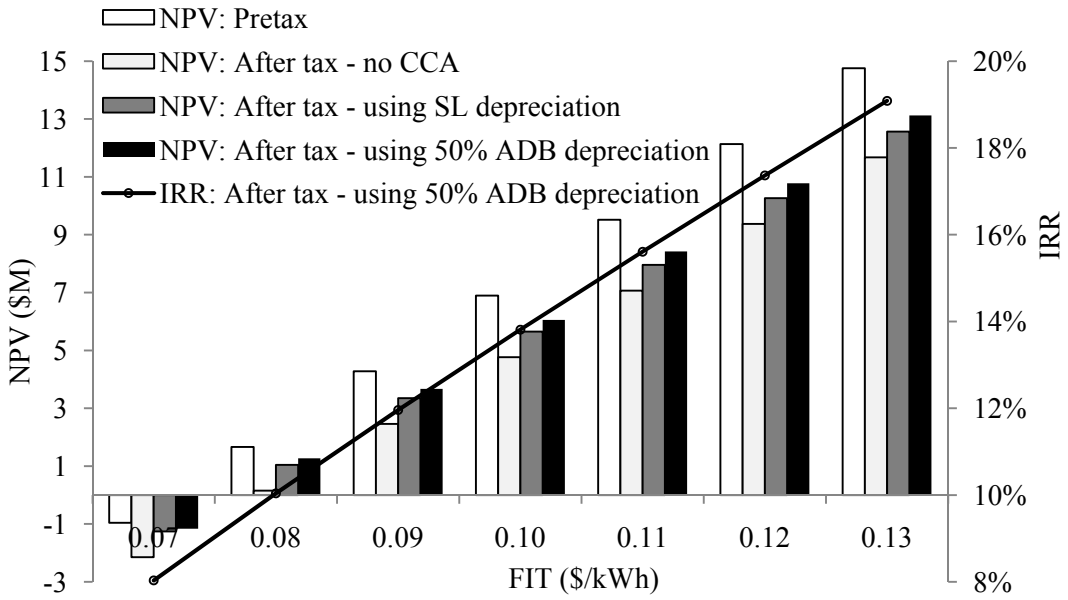

Figure 4-12: Effect of FIT on the project's viability (dr=9%)

The implication of the varying FIT rate on the project's NPV and IRR is presented in Figure 4-12. For example, a rate of US$0.12 per kWh would result in an IRR of about 17.4%. Any discount rate that is lower than the IRR would yield a positive NPV. The project is not viable, i.e. the NPV is negative, when the rate is US$0.07 per kWh because the IRR in this case is lower than the *dr*.

4.6 Summary

The utilization of wind power to generate electricity is in line with Oman's long-term development strategy, which aims for sustainable development. However, in spite of publications promoting potential sites for wind power projects, no utility-scale wind turbines have been connected to the grid. This chapter highlights a new potential site for wind power projects, in a new city in the Duqm area, which is currently the focus of huge investments in infrastructure. Duqm wind speed data, measured over the past few years, were analyzed to obtain the annual and monthly wind probability distribution profiles represented by Weibull pdf parameters. Due to the summer monsoon wind system, excellent capacity factors are expected during the period from April to September. Interestingly, there is a high correlation between the anticipated monthly wind power production and the load profile in the Main Interconnected System (MIS).

The 5-turbine project case study shows that the COE is US$0.056 and US$0.088 per kWh for discount rates of 5% and 10%, respectively. This price is more than the average COE of the MIS (about US$0.024 per kWh) because of the low prices of domestically available natural gas (US$1.5 per MMBtu). However, when the actual high prices of natural gas in international markets (US$10 per MMBtu) are used to calculate the COE, wind power is cheaper. It can be concluded that wind power becomes economically competitive with natural gas-based generation system at a price about US$6/MMBtu. A Feed-in Tariff (FIT) of US$0.10 per kWh is assumed to investigate the project's viability from an investor's perspective. The pretax analysis shows that the project's payback period is 11 years. Despite the generous corporate tax rate in Oman, taxes reduce the NPV from US$6.9 to US$4.8 Millions, a 30% reduction. Due to the high initial capital cost required to start a wind power project, a Capital Cost Allowance (CCA) policy is proposed to reduce and delay tax payment. Two depreciation methods are used to test the effectiveness of CCA on the project's viability: the Straight Line (SL) depreciation method and the 50% depreciation rate for the Accelerated Declining Balance (ADB) method. The project's NPV, when CCA was considered, increased to US$5.7 and US$6.1 Million using the SL and the ADB methods, respectively. In addition, this work presented parameter sensitivity analysis to demonstrate the significance of the discount rate (the average cost of capital) and the FIT rate in the viability of the project. Finally, it is recommended that the Public Authority for Electricity and Water (PAEW) in Oman adopt FIT and CCA policies for wind power to facilitate private investment and achieve a sustainable development in this sector.

Chapter 5

New Method for Estimating CF of Pitch-regulated Turbines[7]

5.1 Introduction

The output power of a wind turbine is variable and is not always at its rated value, due to wind speed variability and the characteristics of wind turbines. Therefore, the Capacity Factor (CF) of a turbine is commonly used to estimate its average energy production, which in turn can be used for economic appraisal of wind power projects at potential sites. Moreover, CF models can be used by manufacturers and wind power project developers for optimum turbine-site matching, and for the ranking of potential sites [96-101].

The amount of energy produced by a turbine depends on the characteristics of both wind speed at the site under investigation, and the turbine's power performance curve. Wind speed at any site is commonly modeled by the Weibull probability density function (pdf), which is characterized by two parameters: the scale factor, c, and the shape factor, k. The turbine's power performance curve can be described by three parameters: the cut-in, nominal, and cut-out speeds. This chapter presents a new model to estimate the CF of modern pitch-regulated wind turbines, based on the turbine's power performance curve and the Weibull parameters of wind speed at the site under investigation.

After this introduction, this chapter continues with a literature survey devoted to wind power output modeling, which includes wind speed modeling, power curve generic models, and the existing CF estimation model. A new generic CF model is then proposed in Section 5.3. Verification of this proposed model's accuracy is presented in Section 5.4 and its effectiveness is illustrated by four case studies in Section 5.5. Finally, a summary and conclusions are presented.

5.2 Wind Power Output Modeling

5.2.1 Turbine Power Curve Modeling

The power performance curve of pitch-regulated turbines can be represented by the following formula:

---

[7] Some parts of this chapter have been published in:

[94] M. H. Albadi and E. F. El-Saadany, "Wind Turbines Capacity Factor Modeling - A Novel Approach," *IEEE Transactions on Power Systems,* vol. 24, pp. 1637-1638, 2009.

Some parts of this chapter have been reported in:

[95] M. H. Albadi and E. F. El-Saadany, "New Method for Estimating the CF of Pitch-regulated Wind Turbines " submitted to *Electric Power Systems Research*.

$$P_e(v) = P_{rated} \times \begin{cases} 0 & v < V_c \text{ or } v > V_f \\ P_{asc} & V_c \leq v \leq V_r \\ 1 & V_r \leq v \leq V_f \end{cases} \quad (5\text{-}1)$$

where P_{asc} is wind turbine output (as a percentage of rated power) throughout the ascending segment of the power curve.

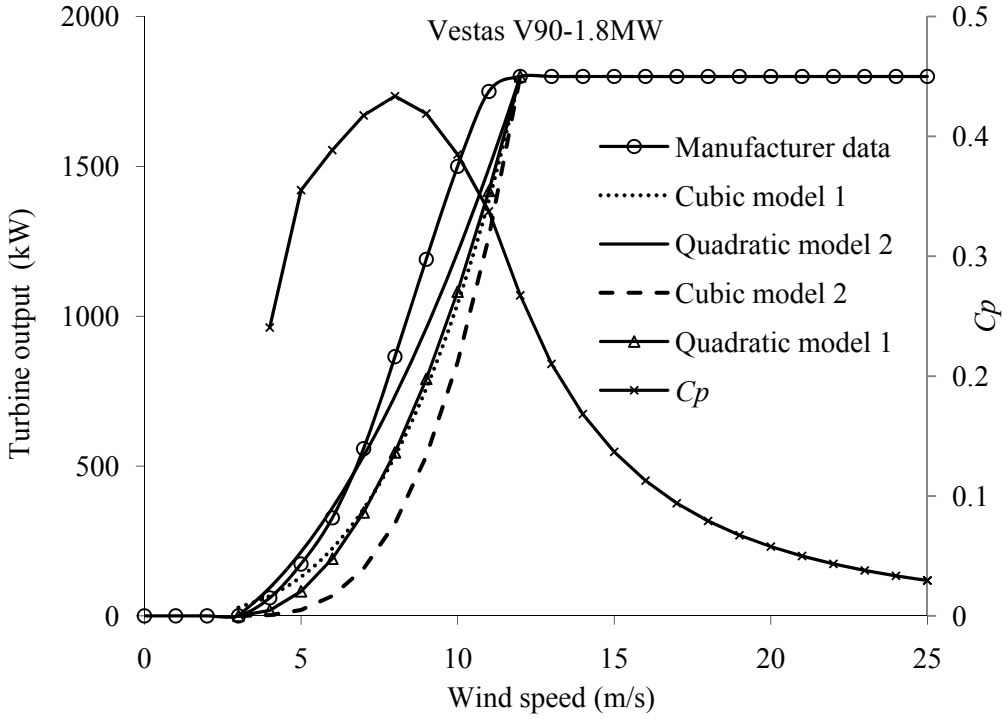

Figure 5-1: Graphical comparison of the quadratic and cubic models

From Figure 5-1, it can be observed that the increase in turbine output between V_c and V_r, is not monotonic. The manufacturer data show a point of inflection in the ascending segment of the power curve; this point indicates that the turbine efficiency experience a change. Despite the single point of inflection in the ascending power curve segment, C_p is not constant for most of the speed range. Although C_p is unique for each turbine and difficult to be generalized, there have been attempts to represent the ascending segment of the power curve by a generic model. By generic, it is meant that a turbine output, as a percentage of rated power, is described using the cut-in and nominal speeds only, without the knowledge of turbine output throughout the ascending segment. Generic models available in open literature include linear, quadratic, and cubic models [102]. Below is a brief description of each model.

1. The linear model assumes a linear increase in the turbine output between the cut-in and the nominal speeds. This model, generally, overestimates wind potential. The linear model is given by the following equation:

$$P_{asc}(v) = \frac{v - V_c}{V_r - V_c} \tag{5-2}$$

2. Cubic model 1, considered by the authors in [97, 101], implicitly assumes a constant overall efficiency of the turbine throughout the ascending segment of the power curve. Cubic model 1 is given by the following equation:

$$P_{asc}(v) = \frac{v^3}{{V_r}^3} \tag{5-3}$$

3. Cubic model 2 is very similar to Cubic model 1. The only difference is the presence of V_c in the former. This model is given by the following formula [102]:

$$P_{asc}(v) = \frac{(v - V_c)^3}{(V_r - V_c)^3} \tag{5-4}$$

4. Quadratic model 1 is originally proposed in [103], and coefficients are calculated in [104]. These coefficients are determined based on the assumption that the output of the turbine increases according to the cubic rule, equation (5-3), between $(V_c + V_r)/2$ and V_r [103].

$$P_{asc}(v) = a_0 + a_1 v + a_2 v^2 \tag{5-5}$$

5. Quadratic model 2, presented in [105], does not have a linear term ($a_1 v$) as the previous model does.

$$P_{asc}(v) = \frac{v^2 - {V_c}^2}{{V_r}^2 - {V_c}^2} \tag{5-6}$$

As demonstrated in Figure 5-1 and Table 5-1, the quadratic model presented in [105] gives the most accurate generic model to represent manufacturer data throughout the ascending segment of the power curve.

A better representation of manufacturer data can be achieved by using a higher order polynomial function described by the following equation [106].

$$P_{asc}(v) = \sum_{i=0}^{n} a_i v^i \tag{5-7}$$

where n is the order of the polynomial function. However, due to the unique and nonlinear behavior of C_p, the model coefficients, a_i, are turbine specific and difficult to be generalized. The authors in [107, 108] use a third order polynomial function to represent the turbine output in the ascending power curve segment, and regression is used to find the coefficients (a_i).

Table 5-1: Comparison of different models for V90-1.8MW

Wind speed	pdf*	Turbine output (kW)					
		Data [43]	Eq.(5-2)	Eq. (5-3)	Eq. (5-4)	Eq. (5-5)	Eq. (5-6)
≤ 3	0.234521	0	0	28	0	0	0
4	0.122592	60	200	67	2	17	93
5	0.126011	173	400	130	20	80	213
6	0.119054	327	600	225	67	188	360
7	0.104705	558	800	357	158	342	533
8	0.086368	865	1000	533	309	541	733
9	0.067145	1190	1200	759	533	786	960
10	0.049363	1500	1400	1042	847	1076	1213
11	0.034399	1750	1600	1386	1264	1411	1493
12-25	0.05584	1800	1800	1800	1800	1800	1800
Annual energy yield (MWh)		4519	5446	3434	2414	3278	4175
Error (MWh)			+927	-1085	-2105	-1241	-344
% Error in CF			+20.5%	-24.0%	-46.6%	-27.5%	-7.6

* Based on MWS=6 m/s and k=2.

5.2.2 Capacity Factor Modeling

The average power produced by a wind turbine can be calculated by integrating the power curve multiplied by the Weibull function, represented by (2.5).

$$P_{ave} = \int_0^{\infty} P_e(v) f(v) dv \tag{5-8}$$

The CF is the ratio between the average and the rated power of the turbine. Authors in [97, 101] used cubic model 1, represented by equation (5-3), to derive the existing model for estimating the CF.

$$CF = \frac{P_{ave}}{P_{rated}} = \frac{1}{{V_r}^3} \int_{V_c}^{V_r} v^3 f(v) dv + \int_{V_r}^{V_f} f(v) dv \tag{5-9}$$

The authors of [101] compared the values of the CF obtained from (5-9) to the measured ones, and found that the model significantly underestimated wind potential at the site under study, as illustrated in Table 5-1. To compensate for the mismatch between the modeled and the measured CF values, [101] investigated the effect of using the Root Mean Square Wind Speed ($RMSWS$) and the Cubic Mean Wind Speed ($CMWS$) to estimate the Weibull function parameters of the wind profile. The authors of [101] found that using the $CMWS$ resulted in a better estimation of the CF, at the site under study, than using the original (arithmetic) MWS or the $RMSWS$. The $RMSWS$ and $CMWS$ are defined by the following formulas:

$$RMSWS = \sqrt[2]{\frac{\sum_x f(v_x)\, {v_x}^2}{\sum_x f(v_x)}} \tag{5-10}$$

$$CMWS = \sqrt[3]{\frac{\sum_x f(v_x)\, {v_x}^3}{\sum_x f(v_x)}} \tag{5-11}$$

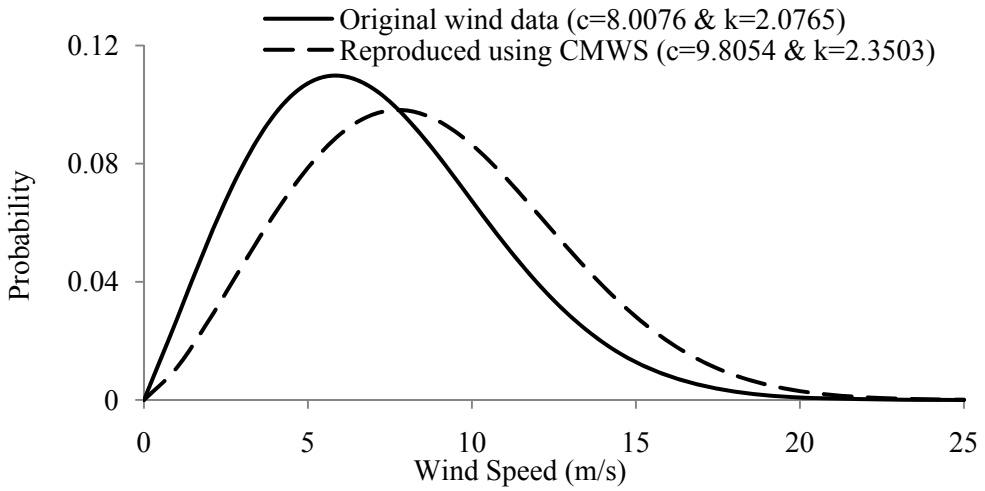

Figure 5-2: Effect of using the *CMWS* to obtain *c* and *k* (data are from [101]).

However, when one compares the original wind profile, obtained using the arithmetic mean wind speed (MWS), with that obtained using the $RMSWS$ or the $CMWS$, a significant difference in the profile is observed. In fact, using the $RMSWS$ or the $CMWS$ shifts the original wind speed data towards higher values, as illustrated in Figure 5-2. A comparison is presented in Table 5-2 [101], between the original wind speed characteristics for the site under study and those obtained using the $CMWS$.

The authors of [98, 99] solved the integral presented in [97, 101] and devised a CF model as a function of the main turbine curve parameters, V_c, V_r, and V_f, and the two parameters of Weibull function, c and k, that are obtained based on the $CMWS$.

$$CF = \left(\frac{V_c}{V_r}\right)^3 e^{-\left(\frac{V_c}{c}\right)^k} - e^{-\left(\frac{V_f}{c}\right)^k} + \frac{3\Gamma\left(\frac{3}{k}\right)}{k\left(\frac{V_r}{c}\right)^3}\left[\gamma\left(\left(\frac{V_r}{c}\right)^k, \frac{3}{k}\right) - \gamma\left(\left(\frac{V_c}{c}\right)^k, \frac{3}{k}\right)\right] \tag{5-12}$$

where γ is the lower incomplete Gamma function given by

$$\gamma(u, a) = \frac{1}{\Gamma(a)}\int_0^u x^{a-1}e^{-x}dx \tag{5-13}$$

$\Gamma(a)$ is described in chapter 2, equation (2-8).

5.3 Generic CF Model

For an "*n*" order polynomial model for the ascending segment of the power curve of pitch-regulated wind turbines, the new CF model is given by the following equation.

$$CF = \frac{P_{ave}}{P_{rated}} = \int_{V_c}^{V_r}\left(\sum_{i=0}^{n} a_i v^i\right) f(v)dv + \int_{V_r}^{V_f} f(v)dv \tag{5-14}$$

where $f(v)$ is the Weibull pdf, given in equation (2-5), and its parameters are based on the MWS not the $CMWS$.

Using integration by substitution and by parts [109], the new CF model is derived as follows. Assume $x = \left(\frac{v}{c}\right)^k$, $dx = \frac{k}{c}\left(\frac{v}{c}\right)^{k-1}$, and $v = cx^{1/k}$, equation (5-14) can be written as a summation of three integrals:

$$CF = I_1 + I_2 + I_3 \tag{5-15}$$

where $I_1 = a_0 \int_{V_c}^{V_r} e^{-x}dx$, $I_2 = \int_{V_c}^{V_r}\left(\sum_{i=1}^{n} a_i\, c^i x^{i/k}\right) e^{-x}\, dx$, and $I_3 = \int_{V_r}^{V_f} e^{-x}dx$

I_1 and I_3 are easily calculated as follows:

$$I_1 = -a_0 e^{-x}|_{x(V_c)}^{x(V_r)} = a_0\left(e^{-\left(\frac{V_c}{c}\right)^k} - e^{-\left(\frac{V_r}{c}\right)^k}\right) \tag{5-16}$$

$$I_3 = -e^{-x}|_{x(V_r)}^{x(V_f)} = e^{-\left(\frac{V_r}{c}\right)^k} - e^{-\left(\frac{V_f}{c}\right)^k} \tag{5-17}$$

I_2 can be solved using integration by parts [109], where

$$\int_{x_1}^{x_2} udv = uv|_{x_1}^{x_2} - \int_{x_1}^{x_2} vdu \tag{5-18}$$

where $x_1 = \left(\frac{V_c}{c}\right)^k$ and $x_2 = \left(\frac{V_r}{c}\right)^k$

Let $u = a_i c^i x^{i/k}$ and $dv = e^{-x}dx$,

then, $du = a_i \frac{ic^i}{k} x^{(i/k)-1} dx$ and $v = -e^{-x}$, and I_2 can be written as follows:

The second part of (5-18) can be written as

$$\begin{aligned} &\int_{x_1}^{x_2} a_i \frac{ic^i}{k} x^{(i/k)-1} e^{-x} dx \\ &\qquad = \int_0^{x_2} a_i \frac{ic^i}{k} x^{(i/k)-1} e^{-x} dx - \int_0^{x_1} a_i \frac{ic^i}{k} x^{(i/k)-1} e^{-x} dx \end{aligned} \tag{5-19}$$

Equation (5-19) can be represented using the complete Gamma function (Γ), described by equation (2-8), and the lower incomplete Gamma function (γ) as follows:

$$\int_0^u x^{a-1} e^{-x} dx = \Gamma(a)\gamma(u,a) \tag{5-20}$$

Using equations (5-19) and (5-20), equation (5-18) can be written so:

$$\begin{aligned} I_2 = \sum_{i=1}^{n} a_i c^i &\left(\left(\frac{V_c}{c}\right)^i e^{\left(\frac{V_c}{c}\right)^k} - \left(\frac{V_r}{c}\right)^i e^{\left(\frac{V_r}{c}\right)^k} \right) \\ &+ a_i \frac{ic^i}{k} \Gamma\left(\frac{i}{k}\right) \left[\gamma\left(\left(\frac{V_r}{c}\right)^k, \frac{i}{k} \right) - \gamma\left(\left(\frac{V_c}{c}\right)^k, \frac{i}{k} \right) \right] \end{aligned} \tag{5-21}$$

Combining equations (5-16), (5-17), and (5-21), the *CF* model can be written in this way:

$$CF = e^{-\left(\frac{V_r}{c}\right)^k} - e^{-\left(\frac{V_f}{c}\right)^k} + a_0\left(e^{-\left(\frac{V_c}{c}\right)^k} - e^{-\left(\frac{V_r}{c}\right)^k}\right) + \sum_{i=1}^{n}\left[a_i c^i\left(\left(\frac{V_c}{c}\right)^i e^{-\left(\frac{V_c}{c}\right)^k} - \left(\frac{V_r}{c}\right)^i e^{-\left(\frac{V_r}{c}\right)^k}\right) + a_i\frac{ic^i}{k}\Gamma\left(\frac{i}{k}\right)\left[\gamma\left(\left(\frac{V_r}{c}\right)^k, \frac{i}{k}\right) - \gamma\left(\left(\frac{V_c}{c}\right)^k, \frac{i}{k}\right)\right]\right] \quad (5\text{-}22)$$

Equation (5-22) can thus be simplified:

$$CF = e^{-\left(\frac{V_c}{c}\right)^k}\left(\sum_{i=0}^{n} a_i {V_c}^i\right) + \left(1 - \sum_{i=0}^{n} a_i {V_r}^i\right)e^{-\left(\frac{V_r}{c}\right)^k} - e^{-\left(\frac{V_f}{c}\right)^k} + \sum_{i=1}^{n} a_i\frac{ic^i}{k}\Gamma\left(\frac{i}{k}\right)\left[\gamma\left(\left(\frac{V_r}{c}\right)^k, \frac{i}{k}\right) - \gamma\left(\left(\frac{V_c}{c}\right)^k, \frac{i}{k}\right)\right] \quad (5\text{-}23)$$

Since $\sum_{i=0}^{n} a_i {V_c}^i = P_e(V_c) = 0$ and $\sum_{i=0}^{n} a_i {V_r}^i = P_e(V_r) = 1$,

the first two terms in equation (5-23) vanish; therefore, the model could be further simplified as follows:

$$CF = -e^{-\left(\frac{V_f}{c}\right)^k} + \sum_{i=1}^{n} a_i\frac{ic^i}{k}\Gamma\left(\frac{i}{k}\right)\left[\gamma\left(\left(\frac{V_r}{c}\right)^k, \frac{i}{k}\right) - \gamma\left(\left(\frac{V_c}{c}\right)^k, \frac{i}{k}\right)\right] \quad (5\text{-}24)$$

The above equation is independent of a_0 and can be used for any "n" order polynomial representation of the power curve.

Similarly, the CF model based on quadratic model 2 can be calculated by substituting $a_1 = a_3 = a_4 = 0$, and $a_2 = 1/{V_r}^2 - {V_c}^2$ in equation (5-24)

$$CF = -e^{-\left(\frac{V_f}{c}\right)^k} + \frac{1}{{V_r}^2 - {V_c}^2}\frac{2c^2}{k}\Gamma\left(\frac{2}{k}\right)\left[\gamma\left(\left(\frac{V_r}{c}\right)^k, \frac{2}{k}\right) - \gamma\left(\left(\frac{V_c}{c}\right)^k, \frac{2}{k}\right)\right] \quad (5\text{-}25)$$

For sites at which wind distribution can be represented by the Rayleigh distribution ($k = 2\ and\ c = 1.128\bar{v}$), the above formula can be further simplified to the following equation:

$$CF = -e^{-\left(\frac{V_f}{c}\right)^k} + \frac{1.273\bar{v}^2}{{V_r}^2 - {V_c}^2}\left[\gamma\left(\frac{{V_r}^2}{1.273\bar{v}^2}, 1\right) - \gamma\left(\frac{{V_c}^2}{1.273\bar{v}^2}, 1\right)\right] \quad (5\text{-}26)$$

5.4 Model Verification

To verify the accuracy of the proposed model represented by equation (5-25), wind speed data and the measured CF at Kappadagudda wind power station [101] are used. Wind speed data at the site are summarized in Table 5-2. A comparison of the calculated CF, including both the existing model and the proposed one as well as the measured values, are presented in Table 5-3 and Figure 5-3. The power performance curve parameters of Turbine 1, presented in Table 5-4, are used in the CF calculation as in [101].

For the annual CF values, the results show that the proposed model gives more accurate CF estimations. The mismatch between the annual CF calculated using the proposed model and the measured value is less than 6%. Although the existing model is based on a model of the turbine performance curve that underestimates wind production during the ascending segment of the power curve significantly, it overestimates the annual CF by 34 % at this specific site. This phenomenon can be attributed to the use of the $CMWS$ instead of the MWS in estimating the Weibull parameter; therefore, the original wind profile is shifted toward higher speeds.

For the monthly CF, the results show that the proposed model estimates are, in general, more accurate than that of the existing model. However, it should be mentioned that monthly CF might not give a clear conclusion, mainly due to wind profile modeling error caused by the limited wind speed data and the irregularity of monthly wind profiles as demonstrated in [101].The inaccuracy in Weibull pdf models of monthly wind profiles results in the proposed model slightly underestimating the CF in the months of March, September, and July. For the same reason, both the existing and proposed models underestimate the CF in October, and overestimate it in May. In November, the estimated CF using both the existing and proposed model estimates is much higher than the measured CF. This difference is attributed to energy losses due to load shedding and disturbances in the 33 kV system to which the wind power station is connected [101].

It is worth mentioning that with an accurate turbine power curve model, and an accurate probability distribution model of wind speed data at a given site, calculated CF values are expected to be higher than measured. This phenomenon is attributable to energy losses that occur for many reasons, such as wake effect, reduced blade efficiency due to soiling, electrical losses between the turbine and the grid, and availability of both the turbines and the grid. In addition, turbine power curves are obtained at certain conditions, such as air density, which might differ from that at sites at which turbines are installed [57].

Table 5-2: Wind speed data of Kappadagudda wind power station [101]

	Original Data				Using $CMWS$			
	MWS	SD	c	k	$CMWS$	SD	c	k
Jan	5.14	1.93	5.77	2.90	5.80	2.04	6.48	3.11
Feb	5.27	2.56	5.95	2.19	6.36	2.78	7.17	2.45
Mar	4.78	2.62	5.38	1.92	6.05	2.92	6.83	2.21
Apr	2.60	3.44	6.99	1.90	7.83	3.81	8.85	2.19
May	9.47	4.04	10.67	2.52	10.90	4.28	12.25	2.76
Jun	9.67	3.05	10.74	3.49	10.48	3.16	11.62	3.67
Jul	10.55	3.73	11.79	3.09	11.76	3.92	13.11	3.30
Aug	9.45	3.29	10.56	3.14	10.41	3.43	11.60	3.34
Sep	7.19	3.13	8.11	2.47	8.28	3.32	9.31	2.70
Oct	4.55	2.41	5.13	1.99	5.65	2.65	6.38	2.27
Nov	6.85	2.21	7.62	3.42	7.50	2.30	8.32	3.60
Dec	5.82	2.33	6.54	2.08	6.64	2.47	7.44	2.93
Annual	7.09	3.62	8.01	2.08	8.69	3.96	9.81	2.35

Table 5-3: Comparison between measured and calculated *CF*

	Existing model [98, 99]	Measured values [101]	Proposed model
Jan	0.121	0.107	0.121
Feb	0.182	0.151	0.150
Mar	0.168	0.153	0.125
Apr	0.318	0.171	0.237
May	0.571	0.371	0.507
Jun	0.558	0.515	0.539
Jul	0.655	0.610	0.608
Aug	0.547	0.493	0.515
Sep	0.346	0.315	0.307
Oct	0.136	0.293	0.106
Nov	0.245	0.114	0.254
Dec	0.187	0.186	0.197
Monthly RMSE*	34%	-	28%
Annual	**0.388**	**0.290**	**0.307**
Error	**34%**	**-**	**6%**
* Root Mean Square Error			

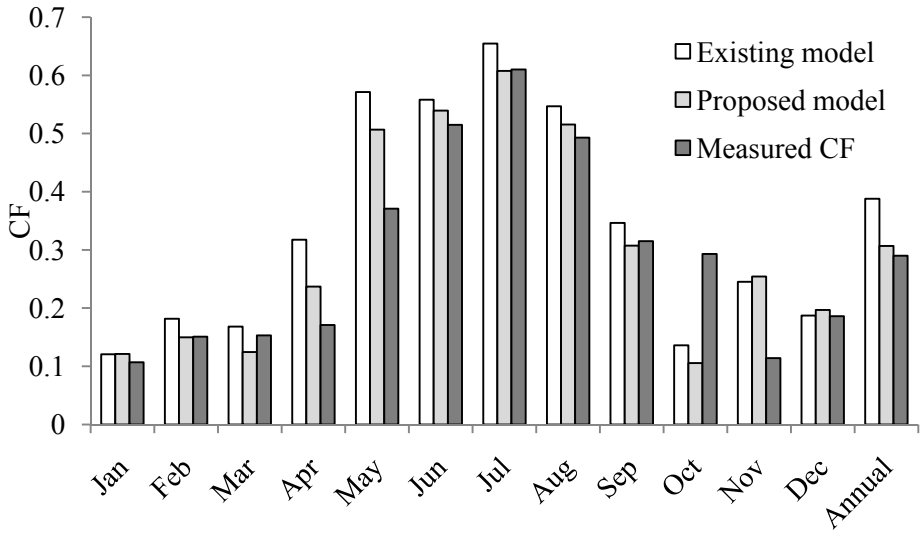

Figure 5-3: Comparison between measured and calculated *CF*

5.5 Illustrative Case Studies

5.5.1 Turbine-Site Matching

In a turbine-site matching problem, the turbine that yields the highest CF at a specific site is the best match for that site. The annual wind speed data at Kappadagudda wind power station [101], presented in Table 5-3, is used to calculate the CF for different turbines, using both the existing and the proposed models. The power curve parameters, V_c, V_r, and V_f, of 12 turbines are presented in Table 5-4 [101]. In the aforementioned table, the turbines are ranked according to the highest annual CF calculated using the proposed CF model. Figure 5-4 presents a comparison between the two models. The results reveal that the existing model overestimates the captured wind energy for all turbines.

From a wind energy capture perspective, for either model, Turbine 12 is by far the best match for this site, because this turbine has the lowest nominal speed, V_r. Both models yield similar results for the second- and third-best matches due to the relatively low V_r of Turbines 9 and 10. However, for the fourth-best match and beyond, there is a significant difference in turbine ranking. For example, while Turbine 7 is the fourth-best match according to the proposed model, it is the sixth-best option when using the existing model.

Table 5-4: Turbine-site matching for Kappadagudda

Turbine parameters				CF	
Sl. No.	V_c	V_r	V_f	Existing Model	Proposed model
12	4.3	7.7	17.9	0.7104	0.5557
9	3	10	25	0.5787	0.4667
10	4	10	25	0.5763	0.4362
7	3	13	25	0.3882	0.318
6	3.5	13	20	0.3831	0.3056
8	4	13	25	0.3871	0.2945
5	5.5	12	24	0.4386	0.2896
1	3.5	13.5	25	0.3604	0.2875
2	3.5	13.8	25	0.3446	0.2765
4	5	12.9	24	0.3895	0.2705
3	5	13	25	0.3841	0.2668
11	4	14	28	0.3339	0.2581

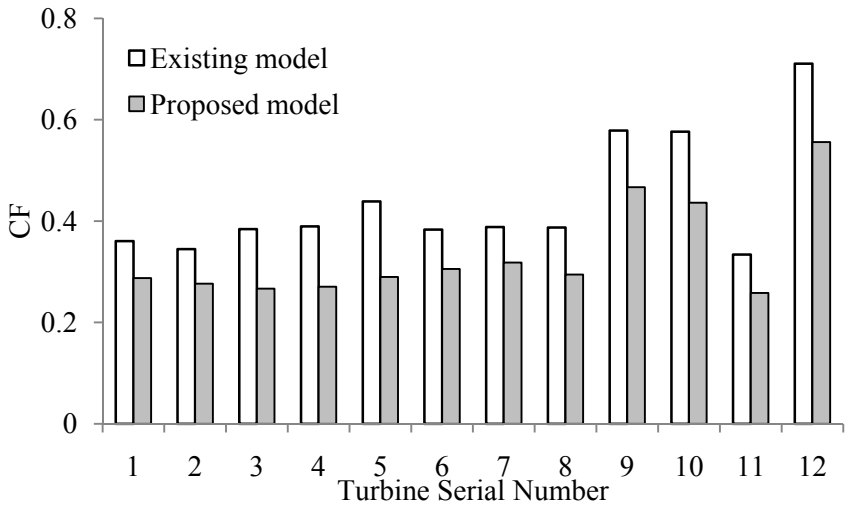

Figure 5-4: *CF* for Kappadagudda wind power station

5.5.2 Effect of MWS on Turbine-Site Matching

The previous subsection investigated the turbine-site matching for a given site with specific wind parameters. In this subsection the effect of the MWS, which determines the Weibull function scale factor, c, is studied. Seven MWS scenarios are considered: 6m/s to 12 m/s. For the sake of comparison, the shape factor, k, is assumed to be 2.

The existing CF model uses the Weibull parameters, c and k, based on the $CMWS$ calculated by equation (5-11). To calculate these parameters from the original data, equation (2-9) is used to obtain

σ_{CMWS}. Then, equation (5-27) is iteratively solved for k. Finally, equation (2-7) is used to find c by using the calculated $CMWS$ instead of $\bar{v}$. A summary of wind speed data is presented in Table 5-5.

$$\left(\frac{\bar{v}_{CMWS}}{\sigma_{CMWS}}\right)^2 = \frac{\Gamma^2\left(1+\frac{1}{k}\right)}{\Gamma\left(1+\frac{2}{k}\right)-\Gamma^2\left(1+\frac{1}{k}\right)} \tag{5-27}$$

Table 5-5: Wind speed characteristics using *MWS* and *CMWS*

Original Data			Reproduced Data		
MWS	c	k	$CMWS$	c	k
6	6.770	2	7.444	8.402	2.307
7	7.899	2	8.682	9.800	2.301
8	9.027	2	9.903	11.178	2.297
9	10.155	2	11.064	12.490	2.292
10	11.284	2	12.114	13.675	2.284
11	12.412	2	13.012	14.690	2.267
12	13.541	2	13.742	15.516	2.237

Figures 5-5 through 5-8 present the CF values calculated using both the existing and proposed models for the 6, 8, 10 and 12 m/s MWS scenarios. The ranking of the turbines for all wind speed scenarios, based on the CF estimated using the proposed (*CF1*) and existing models (*CF2*), is presented in Table 5-6.

For 6, 7, 8, and 9 m/s MWS scenarios, Turbine 12 yields the highest CF when using either model. This result is attributed to the fact that this turbine has the lowest V_r. However, for the higher MWS scenarios, 10, 11, and 12 m/s, using the existing model results in a lower ranking of this turbine compared to that obtained using the proposed model. For the 12 m/s MWS scenario, Turbine 12 is ranked the third-best option using the proposed model, compared to its being the seventh-best option using the existing model. This phenomenon is attributable to the fact that using the $CMWS$ to estimate the Weibull function parameters shifts the original wind speed data towards higher values, as illustrated in Figure 5-2. Consequently, due to its low V_f, the existing model results in estimating more non-captured wind energy, due to too-high wind speeds, than actually happens. This phenomenon causes the value of the CF estimated using the existing model to peak at 8 m/s compared to 10 m/s with the proposed model (see Figure 5-9). Interestingly, at an MWS scenario of 12 m/s, using the proposed model yields a higher CF compared to that obtained using the existing model for reasons described above and illustrated in Figure 5-9.

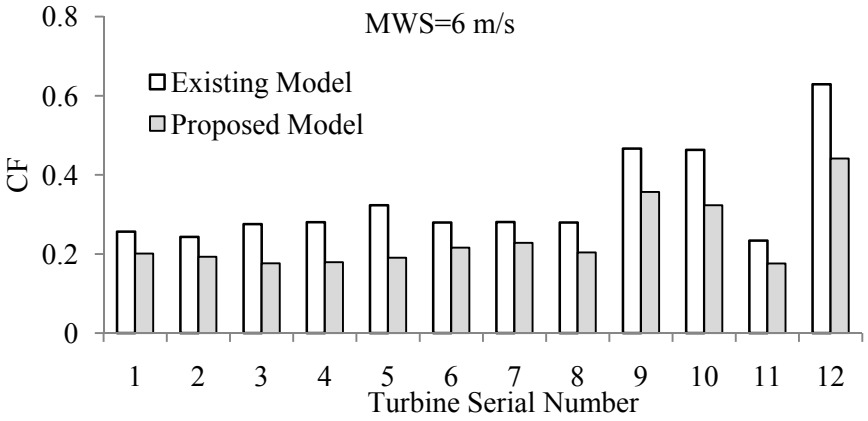

Figure 5-5: Comparison of the existing and the proposed model for an MWS of 6m/s

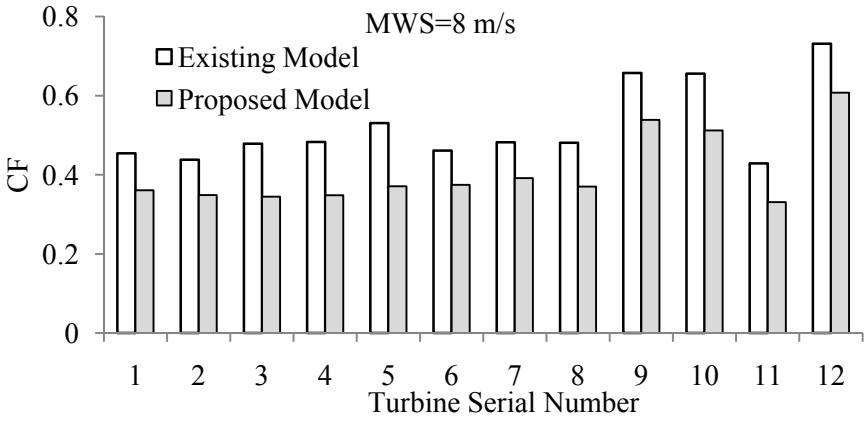

Figure 5-6: Comparison of the existing and the proposed model for an MWS of 8m/s

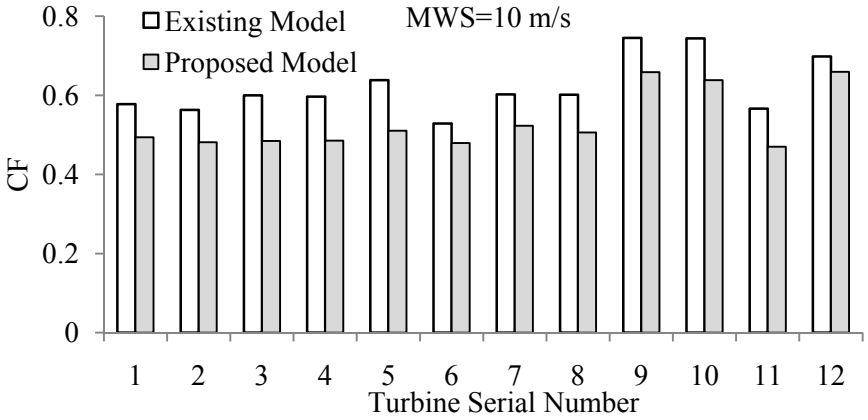

Figure 5-7: Comparison of the existing and the proposed model for an MWS of 10m/s

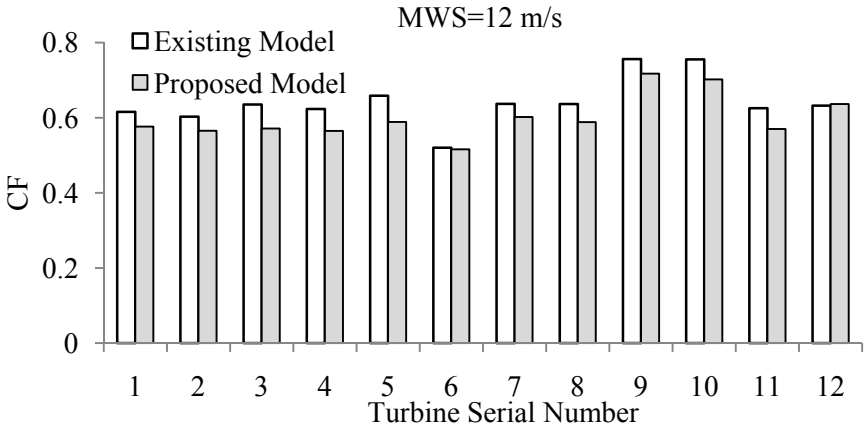

Figure 5-8: Comparison of the existing and the proposed model for an MWS of 12m/s

Table 5-6: Summary of turbine-site ranking for different MWS scenarios

	6 m/s		7 m/s		8 m/s		9 m/s	
Ranking	$CF1$*	$CF2$+	$CF1$	$CF2$	$CF1$	$CF2$	$CF1$	$CF2$
1st	12	12	12	12	12	12	12	12
2nd	9	9	9	9	9	9	9	9
3rd	10	10	10	10	10	10	10	10
4th	7	5	7	5	7	5	7	5
5th	6	7	6	4	6	4	5	7
6th	8	4	8	7	5	7	8	8
7th	1	6	5	8	8	8	6	4
8th	2	8	1	3	1	3	1	3
9th	5	3	2	6	2	6	4	1
10th	4	1	4	1	4	1	3	2
11th	3	2	3	2	3	2	2	6
12th	11	11	11	11	11	11	11	11

	10 m/s		11 m/s		12 m/s	
Ranking	$CF1$	$CF2$	$CF1$	$CF2$	$CF1$	$CF2$
1st	12	9	9	9	9	9
2nd	9	10	10	10	10	10
3rd	10	12	12	12	12	5
4th	7	5	7	5	7	7
5th	5	7	5	7	5	8
6th	8	8	8	8	8	3
7th	1	3	1	3	1	12
8th	4	4	3	4	3	11
9th	3	1	4	1	11	4
10th	2	11	2	11	2	1
11th	6	2	11	2	4	2
12th	11	6	6	6	6	6

* Turbine serial number when the ranking is based on the proposed CF model.
+ Turbine serial number when the ranking is based on the existing CF model.

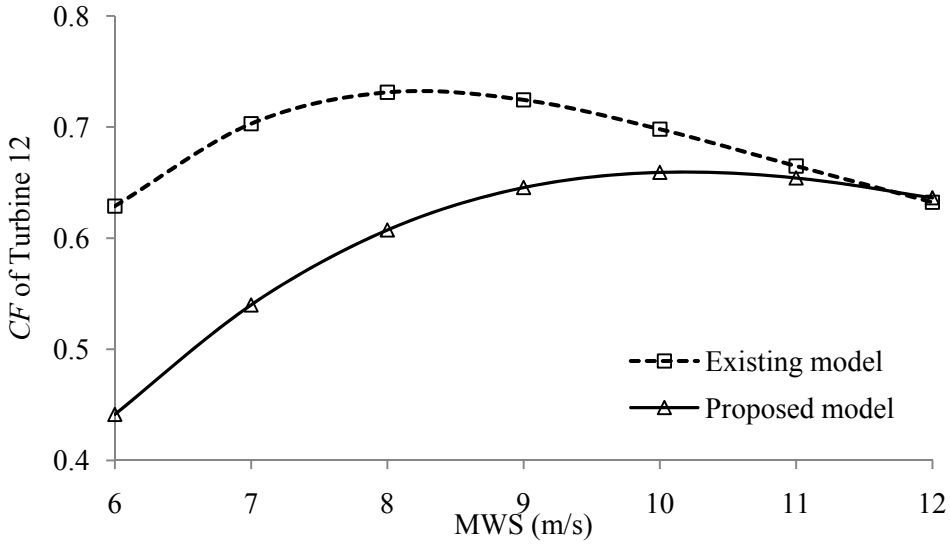

Figure 5-9: *CF* of Turbine 12 as a function of the site's *MWS*

5.5.3 Turbine Nominal Speed Design

The proposed model can be used to design the optimum turbine nominal speed, V_r, for a specific site as described in [99]. In Figure 5-10, the values of the CF calculated using both models are plotted against the normalized nominal turbine speed (V_r/c), where c is based on the MWS for Kappadagudda wind power station. The turbine power curve parameters are as in [99].

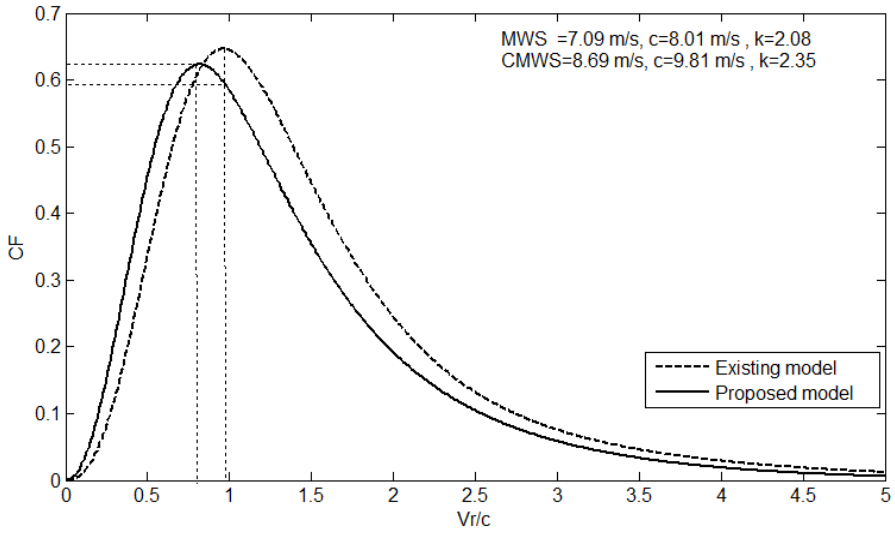

Figure 5-10: *CF* as a function of the normalized nominal speed (V_r/c)

As demonstrated by the figure, there exists an optimum value for the normalized nominal speed at which the maximum wind energy capture occurs. The results demonstrate that if the existing model is used, the optimum design value is shifted to the right. This phenomenon is attributed to the use of $CMWS$ in obtaining the Weibull parameters. The results show that the proposed model yields a lower optimum (V_r/c) design ratio compared to that obtained using the existing model. Consequently, the optimum ratio obtained from the proposed model would yield about 5% more energy from the same turbine.

5.5.4 Sensitivity Analysis

In this subsection, CF sensitivity analysis is presented to demonstrate the effectiveness of the proposed model. Figure 5-11 illustrates the effect of the Weibull pdf shape factor, k, on the optimum design of the normalized nominal speed for a typical turbine with $V_c/V_r = 0.275$ and $V_f/V_r = 1.85$ [99]. The (V_r/c) design ratio decreases slightly from 0.71 to 0.84 as k increases from 1.5 to 3.

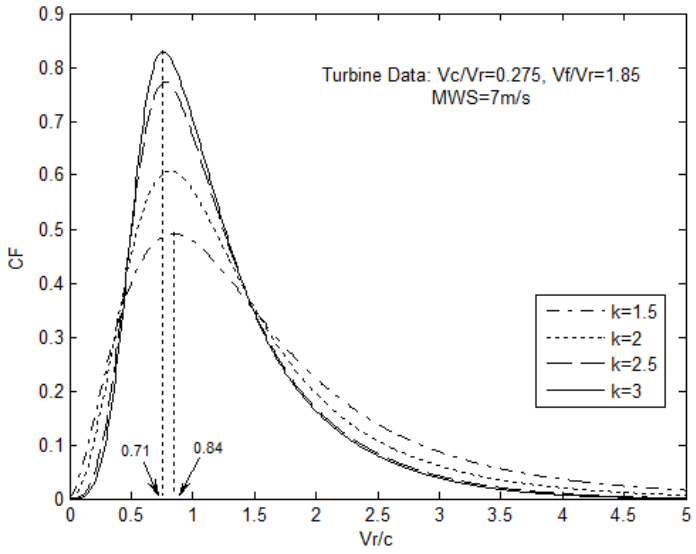

Figure 5-11: Effect of the shape factor, k, on (V_r/c) design

Figure 5-12 illustrates the effect of the shape factor, k, on the CF calculated for different MWS scenarios. It is worth mentioning that for each MWS scenario, there exists a value for k, at which point the CF is at its maximum value. Additionally, the calculated CF drops dramatically for k values less than 1. However, it is worth noting that this phenomenon does not happen in practice for most potential wind project sites, as the shape factor of the annual wind speed pdf takes values between 1.5 and 3.5.

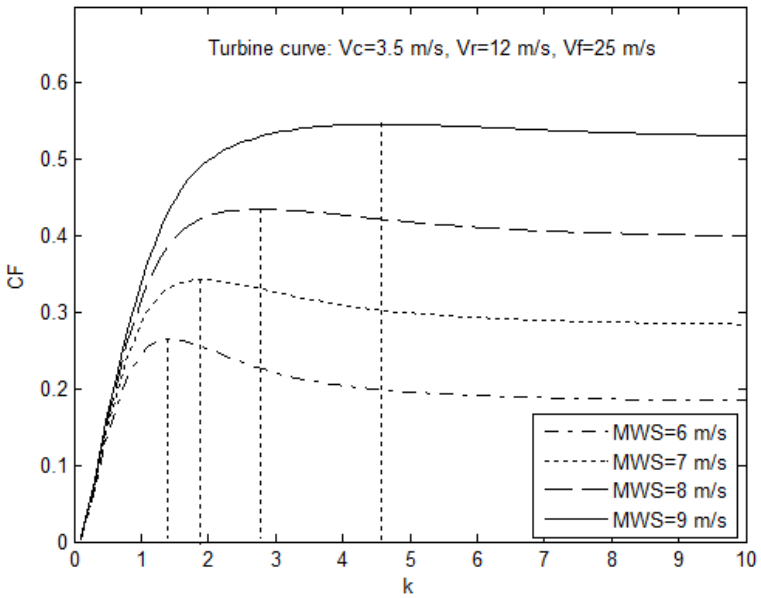

Figure 5-12: *CF* as a function of the shape factor for different *MWS*

In Figure 3-13, the CF, as a function of the MWS, is plotted for different values of k. There exists an approximately linear relationship between the calculated CF and the MWS. The results illustrate that for MWS less than 7m/s, lower values for k result in better wind energy capture. On the other hand, for MWS higher than 7.5m/s, better CF values are achieved for sites at higher k values than those obtained from sites at which wind speed is characterized by lower k values.

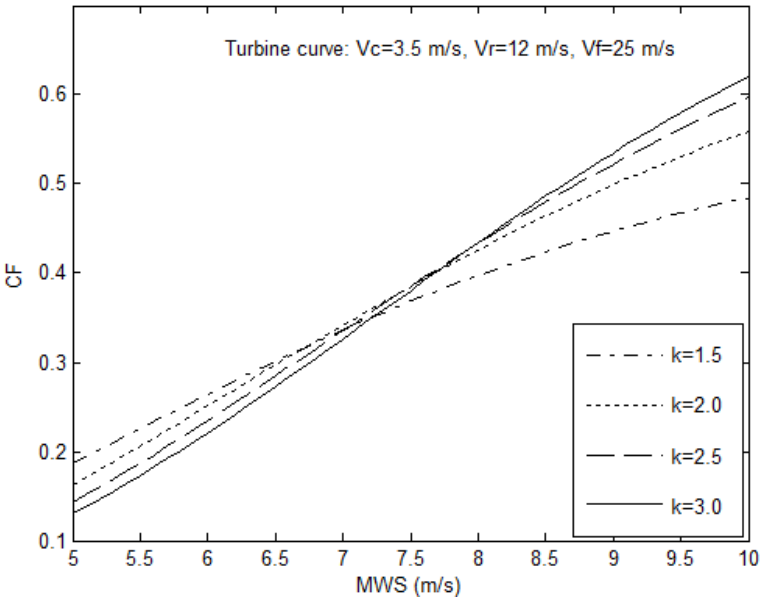

Figure 5-13: Effect of *MWS* on *CF* for different *k* factor scenarios

5.6 Summary

This chapter presents a new, generic and simple formulation for a pitch-regulated wind turbine capacity factor model, based on the Weibull pdf parameters of the wind speed at any site and any 'n' order turbine power performance curve model. The improved accuracy of the proposed CF model, which is based on the most accurate generic power curve model available in open literature, over that of the existing one, is verified using measured data from an existing wind power facility. While the existing CF model overestimates the annual wind potential at the site under study by 34%, the mismatch between the measured and estimated CF using the proposed model is less than 6%. Four illustrative case studies and parameter sensitivity analysis are presented to highlight the effectiveness of the new model in turbine-site matching applications. Due to its accuracy, using the proposed model leads to more accurate ranking of wind turbine candidates for installation at certain potential sites. Moreover, when used to design the optimum normalized nominal speed of a turbine for a specific location, the proposed model can lead to about 5% more wind energy capture than with the existing model. Finally, sensitivity analysis is presented to illustrate the effect of model parameter change on the estimated CF values.

Chapter 6
New Turbine-Site Matching Index[8]

6.1 Introduction

There are many different types of commercially available wind turbines, as illustrated in Table 6-1. For every manufacturer, different turbine sizes (MW), cut-in, rated, cut-out speeds, and hub heights are available. The optimum selection of wind turbine characteristics for specific sites can make wind power more economically competitive. Previous work on turbine-site matching was based solely on the turbine's CF with no comprehensive consideration of the impact of the available turbine size and hub heights [97-101].

The main objective of this chapter is to develop a new Turbine-Site Matching Index ($TSMI$) based on wind speed characteristics at any site and the power performance curve parameters of any pitch-regulated wind turbine. To develop the proposed $TSMI$, the new CF model proposed in the previous chapter is used. Moreover, the proposed CF model is modified to include wind shear effect by using the wind shear power law exponent and therefore is a function of turbine hub height. From an investor's perspective, CF is not enough for optimum turbine-site matching. The levelized Cost of Energy (COE) is commonly used to assess project viability. Therefore, the proposed $TSMI$ takes into account the benefits related to the economies of scale of using larger turbines and the cost associated with selecting higher towers.

After this introduction, this chapter proceeds with the main assumptions adopted to derive the $TSMI$. Section 6.3 is devoted to modeling the impact of the hub height on the CF formulation. A simplified model for the effect of turbine size and tower height on ICC ($/kW) is presented in 6.4. The proposed $TSMI$ is presented in section 6.5. The effectiveness of the proposed index is illustrated by five case studies in section 6.6. Finally, conclusions are presented.

6.2 Assumptions

To derive a universal $TSMI$ that can be used to rank different turbines, the following assumptions are adopted:

[8] Some parts of this chapter have been reported in:
[110] M. H. Albadi and E. F. El-Saadany, "Optimum Turbine-Site Matching," submitted to Energy.
An earlier version have been published in:
[111] M. H. Albadi and E. F. El-Saadany, "Novel Method for Estimating the CF of Variable Speed Wind Turbines," in *IEEE PES 2009 General Meeting (GM '09)* Calgary, Alberta, Canada, 2009.

- *The power curves of all turbines are represented by the quadratic model, equation (5-6).*
- *For the same turbine size and tower height, all turbines have the same Initial Capital Cost (ICC) per installed capacity.*
- *For the same size and tower height, all turbines have the same annual Operation and Maintenance (O&M) costs.*
- *A base-case turbine of 2MW with 80m hub height is adopted.*
- *Economies of scale effect is represented by a linear variation in the ICC ($/kW) as a function of turbine size.*
- *Tower height effect on the ICC is represented by a linear cost function.*

6.3 Effect of Tower Height on CF

As discussed in chapter 4, wind speed measurements should be adjusted for height according to equation (4-3). The friction coefficient, α, can be found using the following equation.

$$\alpha = \frac{log\left(\frac{\bar{v}_1}{\bar{v}_3}\right)}{log\left(\frac{h_1}{h_3}\right)} \tag{6-1}$$

where $\bar{v}_1$ and $\bar{v}_3$ are the measured MWS at h_1 and h_3, respectively.

The authors in [112] presented the following extrapolation model to estimate the CF with different tower heights.

$$CF_{new} = CF_{old}\left(\frac{h_{new}}{h_{old}}\right)^{3\alpha} \tag{6-2}$$

Although (6-2) is simple and easy to use, it is not accurate, as illustrated by the following two arguments:

1. This model does not capture the fact that the increase in MWS, which results from using a higher tower, actually increases the number of hours in which wind speed is higher than the V_f.
2. In the derivation of (6-2), the authors in [112] presume that the overall efficiency of a wind turbine (P_e/P_{wind}) is constant throughout the power curve. This assumption is, in fact, not accurate as the efficiency varies with wind speed, Figure 5-1.

In fact, with high values of MWS and the ground friction coefficient, the extrapolation of CF as estimated by (6-2) can result in unrealistically high CF values, as will be demonstrated later. To capture the effect of wind shear at ground level, the scale factor is represented by the MWS, which, in turn, is a function of friction coefficient α and height h. Using equations (4-3) and (2-7), the scale factor can be expressed by the following equation:

$$c(h) = \left(\frac{h}{h_{ref}}\right)^{\alpha} \frac{\bar{v}_1}{\Gamma\left(1+\frac{1}{k}\right)} \tag{6-3}$$

where h_{ref} and $\bar{v}_1$ are the reference height and MWS, respectively.

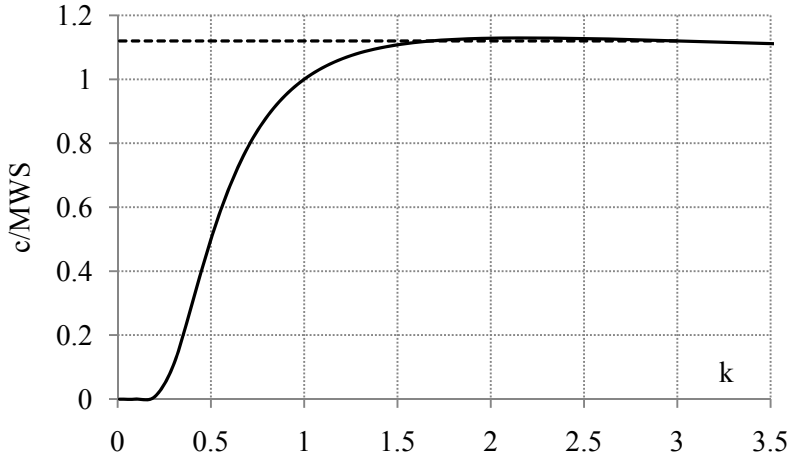

Figure 6-1: "*c/MWS"* ratio as a function of the shape factor

As illustrated by Figure 6-1, the ratio c/MWS is almost constant for k values between 1.5 and 3.5; therefore, the scale factor can be estimated by the following equation.

$$c = 1.12\bar{v} \tag{6-4}$$

Therefore, the scale factor as a function of tower height is

$$c(h) = 1.12\bar{v}\left(\frac{h}{h_{ref}}\right)^{\alpha} \tag{6-5}$$

Substituting (6-5) into (5-25), the CF model can be written as follows:

$$CF = \frac{2.51\bar{v}_1{}^2 H^{2\alpha}}{(V_r{}^2 - V_c{}^2)k}\Gamma\left(\frac{2}{k}\right)\left[\gamma\left(\left(\frac{V_r}{1.12\bar{v}_1 H^{\alpha}}\right)^k, \frac{2}{k}\right) - \gamma\left(\left(\frac{V_c}{1.12\bar{v}_1 H^{\alpha}}\right)^k, \frac{2}{k}\right)\right] - e^{-\left(\frac{V_f}{1.12\bar{v}_1 H^{\alpha}}\right)^k} \quad (6\text{-}6)$$

where $H=h/h_{ref}$.

To verify the accuracy of the model, the CF of a Vestas V90-1.8 MW turbine is calculated for different tower heights using three methods: the conventional complete enumeration method used in chapters 3 and 4, the extrapolation model [112], and the proposed CF model. In the conventional complete enumeration method, the CF is calculated using discretized forms of power curve and wind profiles models, as in chapters 3 and 4. A 92% adjustment loss factor is considered. The values of MWS, k, and α assumed in the analysis are 6 m/s, 2, and 1/7, respectively.

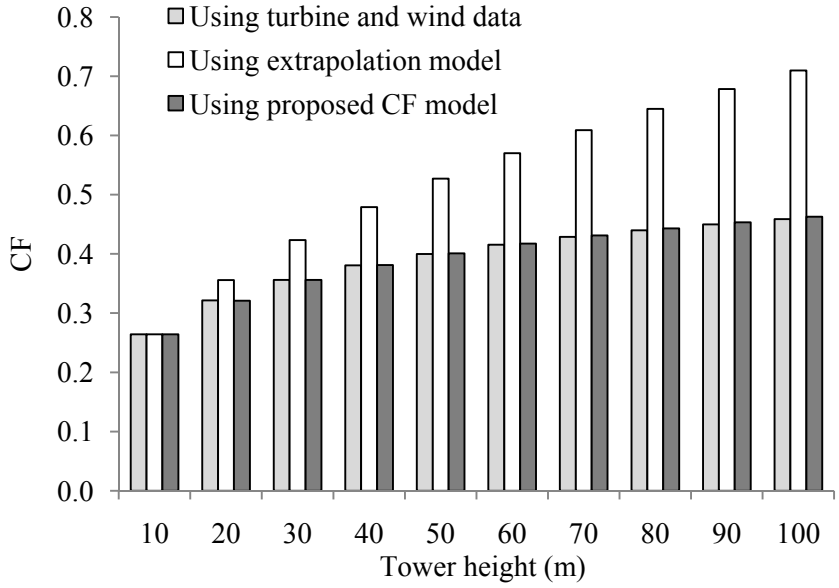

Figure 6-2: Comparison between the extrapolation model and the proposed one

The use of the extrapolation model results in an overestimation of CF, as illustrated in Figure 6-2. On the other hand, the proposed model yields appealing results. It should be mentioned that using (6-2) to extrapolate the CF for other wind scenarios with higher MWS and α can result in unrealistically high CF values.

6.4 Effect of Turbine Size and Tower Height on Installation Cost

6.4.1 Turbine Size

Previous turbine-site matching studies [97-101] are based solely on turbine CF, with no consideration of the effect of turbine size on turbine cost. However, this criterion plays a key role in the feasibility of a wind power project. For example, according to [39], prices will roughly triple, rather than quadruple, in a move from a 150 kW machine to a 600 kW one. This effect is mainly due to the economies of scale of larger turbines. When compared to a 150 kW turbine, a 600 kW turbine requires the same manpower and almost the same safety features and electronics [39]. The economies of scale in operating wind parks rather than individual turbines are beyond the scope of this work.

A linear variation of ICC per installed capacity is considered to represent the economies of scale phenomenon in the range 1 to 3MW, which represents typical onshore turbine sizes of European and North American manufacturers [43, 113-119]. The 2MW size is considered as the base-size ($P_{Base\ size}$) for which the cost per installed capacity ($ICC_{Base\ size}$) is 2000 $/kW [62]. The ICC can be formulated as follows.

$$ICC(P_{rated}) = ICC_{Base\ size} + m(P_{Base\ size} - P_{rated}) \tag{6-7}$$

where P_{rated} is installed capacity in MW and m represents the economies of scale effect. In this analysis, 2160 and 1840 $/kW are the ICC of 1 and 3MW turbines, respectively, is considered.

6.4.2 Tower Height

There exist different tower heights for each wind turbine, as illustrated in Table 6-1. The effect of tower height on turbine-site matching has two aspects. On the one hand, the harvested wind power increases as tower height increases, depending on the ground surface friction, α. On the other hand, increasing tower height results in an increase in the ICC per installed capacity. Although the optimum tower height can be very site and turbine specific, the ICC can be modeled as a function of tower height, so that it can be included in a universal Turbine-Site Matching Index.

As mentioned in [86], the cost of wind turbines represents about 75% of wind farm ICC. According to [120], about a quarter of this amount is for towers and foundations. Therefore, the tower and its related foundation work amount to about 19% of the overall ICC. To adjust the ICC for different tower heights, h,

an 80m base-case tower height ($h_{Base\ height}$) is assumed. It is estimated that a 2% increase in the tower height would result in a 1% increase in the tower and related foundation costs mainly due to the increase in required materials [121]. Therefore, the ICC of wind turbines can be modeled as follows.

$$ICC(h) = ICC_{Base\ height}\left(1 + \frac{0.19}{2}\left(\frac{h - h_{Base\ height}}{h_{Base\ height}}\right)\right) \quad (6\text{-}8)$$

where $ICC_{Base\ height}$ is given by equation (6-7) and h is in meters. Note that equations (6-7) and (6-8) can be easily adapted for other base-case assumptions.

Table 6-1: Examples of typical 1-3MW range turbines

S. No.	Manufac.	Turbine Name	P_{rated}	V_c	V_r	V_f	Tower Height
			MW	m/s			m
T1	Vestas	V82-1.65	1.65	3.5	13	20	70, 80
T2	Vestas	V80-2.0	2.0	4	15	25	60, 67, 78, 100
T3	Vestas	V90-1.8	1.8	3.5	12	25	80, 95, 105
T4	Vestas	V90-2.0	2.0	2.5	13	25	80, 95, 105
T5	Vestas	V90-3.0	3.0	4	15	25	80, 105
T6	GE	1.5sle	1.5	3.5	14	25	65,80
T7	GE	1.5xle	1.5	3.5	12.5	20	80
T8	GE	1.5xl	2.5	3.5	12.5	22	75, 85, 100
T9	AAER	A/1500-70	1.5	3	12	25	65, 80
T10	Enercon	E-70	2.3	2	16	25	64 – 113
T11	Enercon	E-82	2.0	2	13	25	78 – 138
T12	Siemens	SWT-82 VS	2.3	3	14	25	80/ site-specific
T13	Siemens	SWT-93	2.3	4	14	25	70, 80/ site-specific
T14	Fuhrlaender	FL 1500	1.5	3	12	25	65, 80, 100
T15	Fuhrlaender	FL 2500	2.5	4	14	25	65, 85, 100, 117, 141, 160
T16	Fuhrlaender	FL MD 70	1.5	3	12	25	65, 85, 114.5
T17	Gamesa	G83	2.0	4	15	25	67, 78
T18	Gamesa	G87	2.0	4	14	25	67, 78, 100
T19	Gamesa	G90	2.0	3	14	21	67, 78, 100
T20	Nordex	S70	1.5	3	13	25	65, 85, 98, 114.5
T21	Nordex	S77	1.5	3	13	25	61.5, 80, 85, 90, 100
T22	Nordex	N80	2.5	3	15	25	60, 70, 80
T23	Nordex	N90	2.3	3	13	25	70, 80, 100, 105
T24	Nordex	N90/2500	2.5	3	15	25	70, 75, 80, 100, 120
T25	Nordex	N100	2.5	3	12.5	20	100

6.5 Proposed Turbine-Site Matching Index

From a wind project developer's perspective, the Cost of Energy (COE) determines a project's economic viability. The COE depends mainly on the amount of harvested energy, which is represented by the turbine's CF, and the overall cost of the project, which can be represented by its upfront ICC. Other parameters affecting the COE include: project financing, operation and maintenance costs, location, and whether the project has a Power Purchase Agreement (PPA) or not. In this work, a universal Turbine Site Matching Index ($TSMI$), based on CF and ICC, is proposed for turbine-site matching problems. The proposed index is given by the following formula:

$$TSMI = \frac{CF\left(h, \alpha, \bar{v}, k, V_c, V_r, V_f\right)}{ICC(h, P_{rated})/ICC_{base\ case}} \tag{6-9}$$

where CF and ICC are given by equations (6-6) and (6-8), respectively. The proposed optimization index takes into account the local wind characteristics, the turbine power curve parameters, and the size and height of the turbine. As illustrated by equation (6-9), the proposed $TSMI$ can be adapted for any detailed cost function formulation that includes the effect of turbine capacity and tower height.

6.6 Illustrative Case Studies

In this section, five case studies are presented. In the first four, the turbines presented in Table 6-1 are ranked for given site parameters. In the fifth case study, the optimum tower height for given turbine characteristics is determined for various wind characteristics.

6.6.1 Turbine Ranking for a Specific Site

The wind characteristics of the site under study in this subsection are given in Table 6-2. The ten best matches of turbine to wind speed characteristics for this site are presented in Table 6-3.

Table 6-2: Wind characteristics base-case assumptions

MWS @ 10m above ground	6 m/s
Weibull shape factor, k	2
Scale factor, c	6.77 m/s
friction coefficient, α	1/7

Two indices are used to rank different turbines of different tower heights: the newly formulated CF and the proposed $TSMI$. Taking into account the wind characteristics of the site under study and the economic assumptions related to turbine size and tower height, T16 with a tower height of 114.5m is the best match for both rankings. This result is attributable to the low rated speed of T16 (12m/s) and the availability of high tower heights.

For the second best match and beyond, different ranking orders result when the CF and the $TSMI$ are used. For example, while T25 with a tower height of 100m is the second-best match according to proposed $TSMI$, it did not appear in the list of turbines ranked according to CF. Although T25 with a tower height of 100m yields a lower CF (0.4292) than that of T14 with the same tower height (0.4625), T25 is better from an investor's perspective due to economies of scale related to its size. Moreover, although T11 with a tower height of 138m is the third-best option when the CF ranking basis is used, it is the seventh-best option according to the proposed $TSMI$. This result is attributable to the increase in ICC for the higher tower.

Table 6-3: Turbines ranking

	Using $TSMI$			Using proposed CF only		
Rank	Turbine	Height	$TSMI$	Turbine	Height	CF
1	T16	114.5	0.4382	T16	114.5	0.4744
2	T25	100	0.4367	T14	100	0.4625
3	T3	105	0.4363	T11	138	0.4597
4	T14	100	0.4344	T3	105	0.4564
5	T8	100	0.4332	T16	85	0.4481
6	T3	95	0.4327	T3	95	0.4474
7	T11	138	0.4300	T11	115	0.4442
8	T16	85	0.4284	T9/T14	80	0.4428
9	T8	85	0.4266	T11	100	0.4323
10	T11	115	0.4265	T3	80	0.4320

6.6.2 Effect of MWS on Turbine-Site Matching

As illustrated in Figure 6-3, the increase in the site's MWS shifts the pdf towards the right. Therefore, the probability of having a speed within the P_{rated} range is higher. However, too-high MWSs result in higher probabilities that the wind speed is greater than the cut-out speed. Therefore, the optimum turbine matching for the same wind characteristics, represented by the same value of k, might change as the site MWS changes.

Table 6-4 presents a summary of the best 10 turbines, according to the proposed index, for different MWS scenarios. The results reveal that for the same α and k, higher tower heights are not always optimal. In fact, although higher tower heights are required for low wind speed scenarios, e.g., 4 and 5m/s, lower heights are preferable when wind speed is high, e.g., 7 and 8m/s. For example, while T11 with a tower height of 138 is the best and the third-best match for 4 and 5 m/s, respectively, it does not appear in the list for 7 and 8 m/s mean wind speed scenarios.

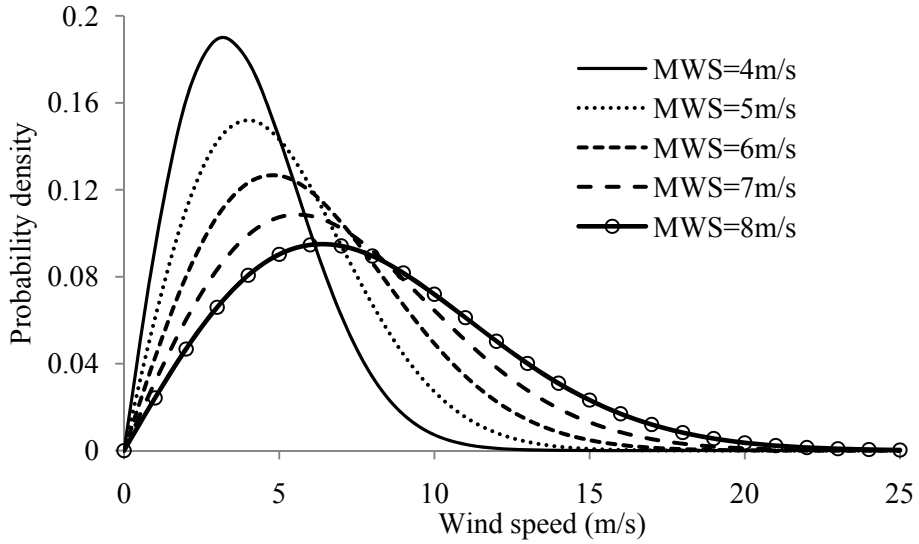

Figure 6-3: Effect of increased *MWS* on the Weibull pdf model (k=2)

Table 6-4: Effect of *MWS* on turbine-site matching problem

Rank	Mean wind speed @ 10m above ground, k=2, α=1/7											
	4 m/s			5 m/s			7 m/s			8 m/s		
	T	h	$TSMI$	T	h	$TSMI$	T	h	$TSMI$	T	h	$TSMI$
1	T11	138	0.2180	T16	114.5	0.3337	T3	105	0.5233	T3	80	0.5849
2	T16	114.5	0.2162	T25	100	0.3319	T3	95	0.5218	T3	95	0.5848
3	T11	115	0.2122	T11	138	0.3288	T16	114.5	0.5198	T3	105	0.5835
4	T25	100	0.2110	T14	100	0.3282	T14	100	0.5189	T16	85	0.5790
5	T14	100	0.2106	T3	105	0.3266	T8	100	0.5179	T9	80	0.5789
6	T11	100	0.2072	T11	115	0.3231	T3	80	0.5175	T14	80	0.5789
7	T3	105	0.2050	T3	95	0.3218	T16	85	0.5160	T14	100	0.5778
8	T16	85	0.2034	T8	100	0.3212	T8	85	0.5155	T9/14	65	0.5763
9	T9/14	80	0.2006	T16	85	0.3206	T9/14	80	0.5144	T16	65	0.5763
10	T3	95	0.2005	T11	100	0.3176	T8	75	0.5122	T16	114.5	0.5749

Table 6-5: Effect of k on turbine-site matching problem (MWS=6 m/s 10m above ground, α=1/7)

Rank	Shape factor, k											
	1.5			2.5			3.0			3.5		
	T	h	$TSMI$	T	h	$TSMI$	T	h	$TSMI$	T	h	$TSMI$
1	T3	105	0.4002	T25	100	0.4550	T16	114.5	0.4594	T16	114.5	0.4615
2	T16	114.5	0.4000	T16	114.5	0.4530	T25	100	0.4577	T25	100	0.4555
3	T14	100	0.3992	T3	105	0.4494	T3	105	0.4544	T3	105	0.4552
4	T3	95	0.3990	T14	100	0.4472	T14	100	0.4520	T14	100	0.4526
5	T16	85	0.3968	T8	100	0.4450	T3	95	0.4479	T3	95	0.4476
6	T3	80	0.3956	T3	95	0.4442	T8	100	0.4461	T8	100	0.4434
7	T9/T14	80	0.3955	T11	138	0.4408	T11	138	0.4432	T11	138	0.4419
8	T11	115	0.3949	T16	85	0.4387	T16	85	0.4414	T16	85	0.4404
9	T11	138	0.3945	T9/T14	80	0.4351	T9/T14	80	0.4371	T9/T14	80	0.4355
10	T11	100	0.3938	T8	85	0.4350	T3	80	0.4353	T3	80	0.4332

Table 6-6: Effect of α on turbine-site matching problem (MWS=6 m/s 10m above ground, k=2)

Rank	Ground friction coefficient, α											
	0.1			0.2			0.3			0.40		
	T	h	$TSMI$	T	h	$TSMI$	T	h	$TSMI$	T	h	$TSMI$
1	T25	100	0.3809	T3	105	0.5129	T3	105	0.6094	T3	80	0.6471
2	T16	114.5	0.3783	T16	114.5	0.5125	T3	95	0.608	T23	70	0.6457
3	T14	100	0.3767	T3	95	0.508	T23	105	0.6028	T23	80	0.6448
4	T3	105	0.3754	T11	138	0.508	T23	100	0.6018	T9/T14/T16	65	0.6399
5	T3	95	0.3737	T14	100	0.5073	T14	100	0.6012	T11	78	0.6383
6	T16	85	0.3737	T8	100	0.5068	T3	80	0.601	T9/T14	80	0.6374
7	T8	100	0.3726	T11	115	0.5031	T16	114.5	0.6005	T3	95	0.6349
8	T9/T14	80	0.3723	T25	100	0.4994	T11	115	0.5978	T16	85	0.634
9	T3	80	0.3697	T16	85	0.4988	T11	100	0.5972	T4	80	0.6338
10	T8	85	0.369	T8	85	0.4986	T16	85	0.597	T23	100	0.6298

6.6.3 Effect of Shape Factor on Turbine-Site Matching

The irregularity of the wind regime is measured by the standard deviation, σ. Equation (2-10) reveals that the shape factor, *k*, is inversely proportional to σ. Therefore, the higher the value of *k*, the greater the regularity of the wind regime. In general, irregular wind regimes in mountainous and urban areas are commonly characterized by low *k* values, of about 1.5. On the other hand, coastal areas that are affected by monsoon systems are characterized by higher *k* values, between 3 and 3.5. In continental climate areas, such as southern Ontario, the *k* values are around 2. The effect of various values of *k* on wind pdf is demonstrated in Figure 6-4; as *k* becomes larger, the wind speed becomes more regular, and therefore, is concentrated around the MWS, 6 m/s.

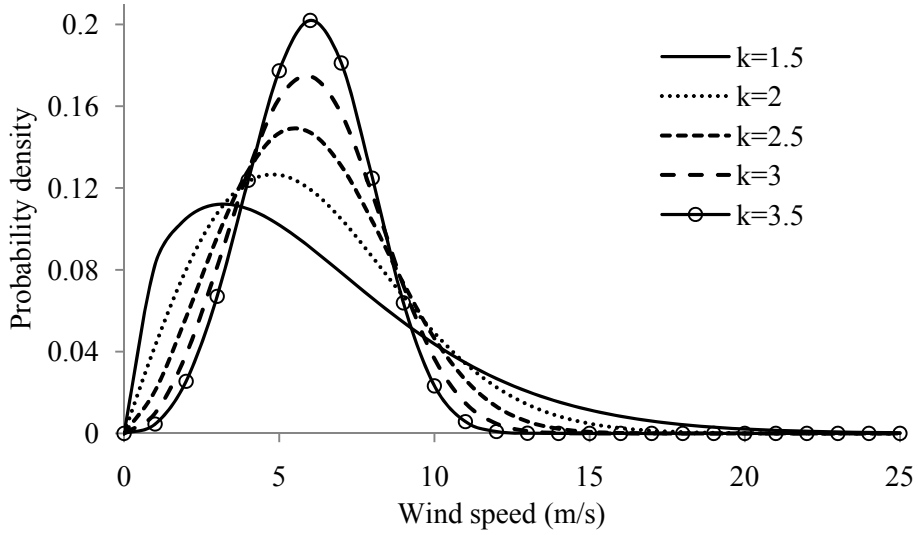

Figure 6-4: Effect of Weibull shape factor, *k*, on wind profile (*MWS*=6)

Table 6-5 presents a summary of the ten best turbines for an MWS of 6m/s, measured at 10m above ground level, and different *k* scenarios. In general, for each turbine there exists an optimal value for *k* at which $TSMI$ is maximized: for example, T16 with a tower height of 114.5m has the maximum $TSMI$ at *k*=3.5. Another tentative conclusion for the results presented in Table 6-5 involves the absence of T25 with a 100m tower height for *k*= 1.5 scenario, despite being among the best three options for all $k \geq 2$ scenarios. This result is attributable to the fact there is a high probability of having wind speed higher than the relatively low cut-out speed of T25, V_f =20 m/s, for irregular wind regimes (k=1.5).

6.6.4 Effect of Ground Friction Coefficient on Turbine-Site Matching

As mentioned in chapter 4, the friction coefficient α, ranges between 0.1 and 0.4 depending on the roughness of the terrain. Table 6-7 presents a summary of the ground friction coefficient with different terrain types [44].

Table 6-7: Ground friction coefficient according to terrain type [44]

Terrain type	α
Lake, oceans, and smooth hard ground	0.1
Tall grass on level ground	0.15
Tall crops, hedges, and shrubs	0.2
Wooded county with many trees	0.25
Small town with some trees and shrubs	0.30
City area with tall buildings	0.40

Table 6-6 presents a summary of the effect of α on turbine-site matching for a site with k=2 and a MWS of 6 m/s measured at 10 m above ground level. It should also be noted that new turbines with different tower heights enter the list as a result of variation in α. For example, T23 with different tower heights appears in all $\alpha \geq 0.25$ scenarios. In addition, the results reveal that turbines with lower tower heights are more effective than those with higher tower heights as the value of α increases. For example, T23 with a tower height of 70, 80, and 100m is the second-, third-, and tenth-best options, respectively, for an α=0.4 scenario.

Interestingly, while T16 with a tower height of 114.5m is the second-best site match for $\alpha \leq 0.25$ scenarios, it is the sixth-best match for α=0.3 scenario. Moreover, this turbine is not among the ten best options for $\alpha \geq 0.35$ scenarios. This result is attributable to the fact that for a high α scenario and an altitude of 114.5m, there is a higher probability that the speed is higher than the cut-out speed of the turbine, therefore, the harvested energy decreases significantly.

6.6.5 Optimal Tower Height Design

In this subsection, this research investigates the optimum turbine tower height for a 2MW machine with cut-in, rated and cut-out speeds of 3, 13 and 25 m/s, respectively. A shape factor, k, of 2 is considered for all wind speed scenarios. The analysis covers a wide range of MWS scenarios: 4 to 8m/s. The proposed

$TSMI$ is investigated for tower height values between 30m and 160m and ground friction coefficient between 0.1 and 0.4; see Figure 6-5 to Figure 6-8. Optimum tower heights for all scenarios are summarized in Table 6-8.

Table 6-8: Optimal tower height for different MWS and α scenarios

MWS^*	α= 0.1		α= 0.2		α= 0.3		α= 0.4	
(m/s)	h^*	$TSMI$	h^*	$TSMI$	h^*	$TSMI$	h^*	$TSMI$
4.0	160	0.1554	160	0.2818	160	0.4343	160	0.5526
4.5	160	0.2037	160	0.3460	160	0.4943	130	0.5801
5.0	160	0.2539	160	0.4047	160	0.5361	107	0.6012
5.5	160	0.3038	160	0.4559	133	0.5653	87	0.6176
6.0	140	0.3520	160	0.4982	111	0.5888	73	0.6306
6.5	128	0.3979	135	0.5323	91	0.6067	62	0.6410
7.0	109	0.4406	113	0.5611	76	0.6228	52	0.6494
7.5	96	0.4789	94	0.5852	64	0.6351	45	0.6561
8.0	84	0.5151	78	0.6052	55	0.6451	39	0.6616

* measured at 10m above ground level

Based on Table 6-8 and Figures 6-5 to 6-8, one can observe that there exists an optimal tower height, h^*, at which the value of the $TSMI$ is at its maximum. The value of h^* depends on the MWS and α scenario. In general, for a given MWS scenario, the optimal tower height decreases as α increases, with an exception of α=0.1. This result is attributable to the fact that with higher values of α, the increase in wind speed with tower heights is more than that for lower α values. Therefore, for the same MWS scenario, the probability of having wind speeds higher than V_f is higher for higher values of α. Similarly, for the same α, the lower values of h^* obtained for higher MWS scenarios can be attributed to having more wind speeds higher than the cut-out speed as the MWS increases. For α=0.1 scenario, the optimum tower height for MWS scenarios of 6, 6.5 and 7 m/s are lower than that for an α=0.2 scenario. This result reveals that the rate of increase in wind speeds with heights beyond the calculated h^* values do not justify the increase in cost related to higher towers.

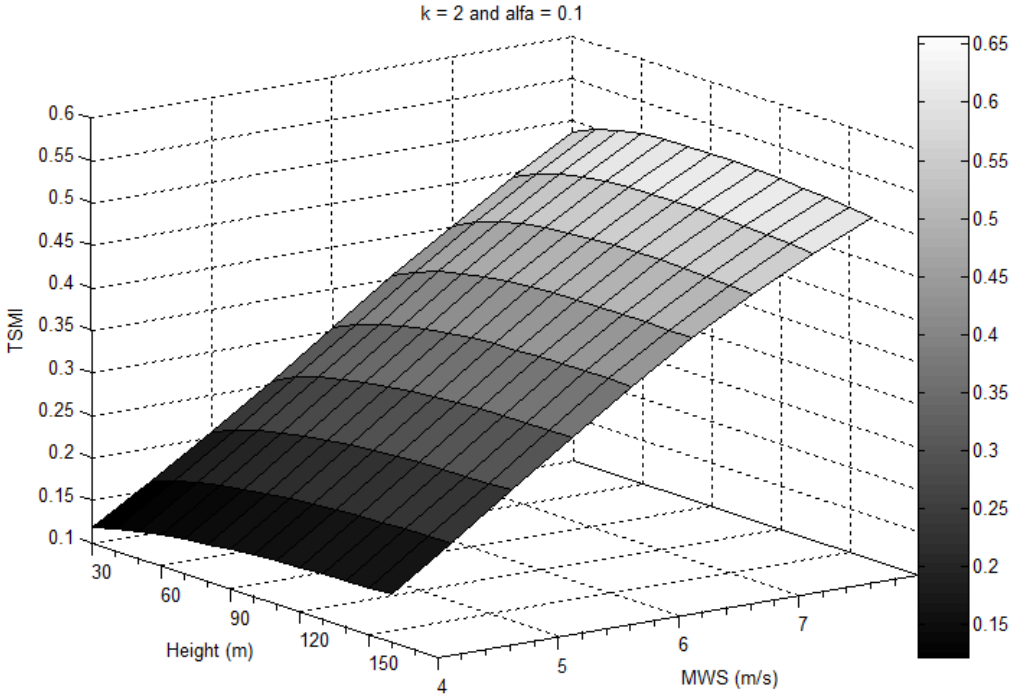

Figure 6-5: *TSMI* as a function of *MWS* and tower height for α=0.1

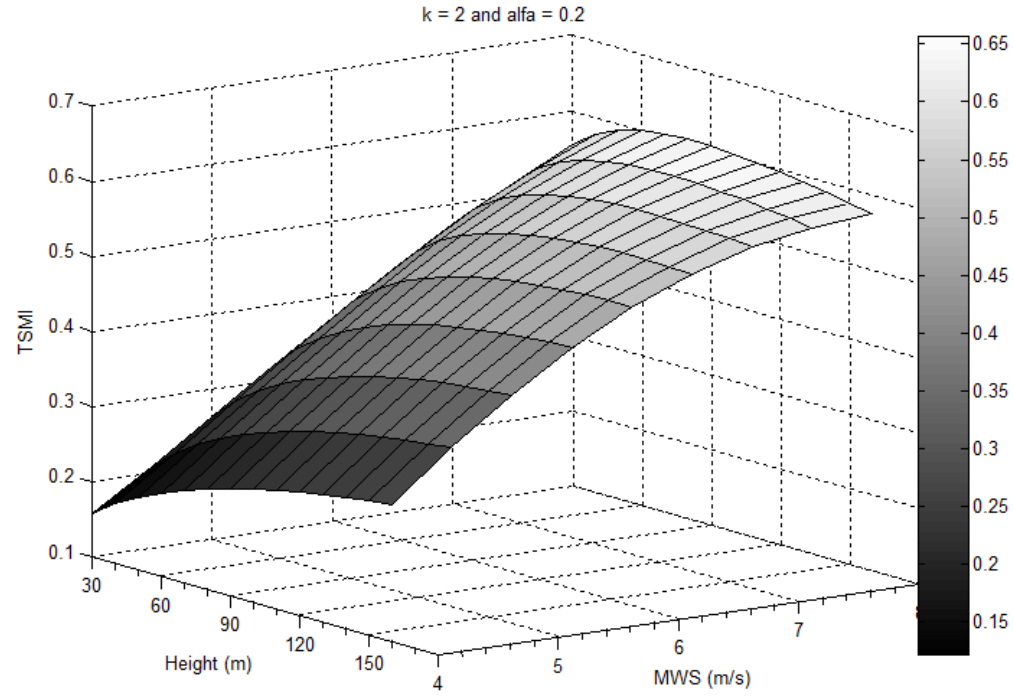

Figure 6-6: *TSMI* as a function of *MWS* and tower height for α=0.2

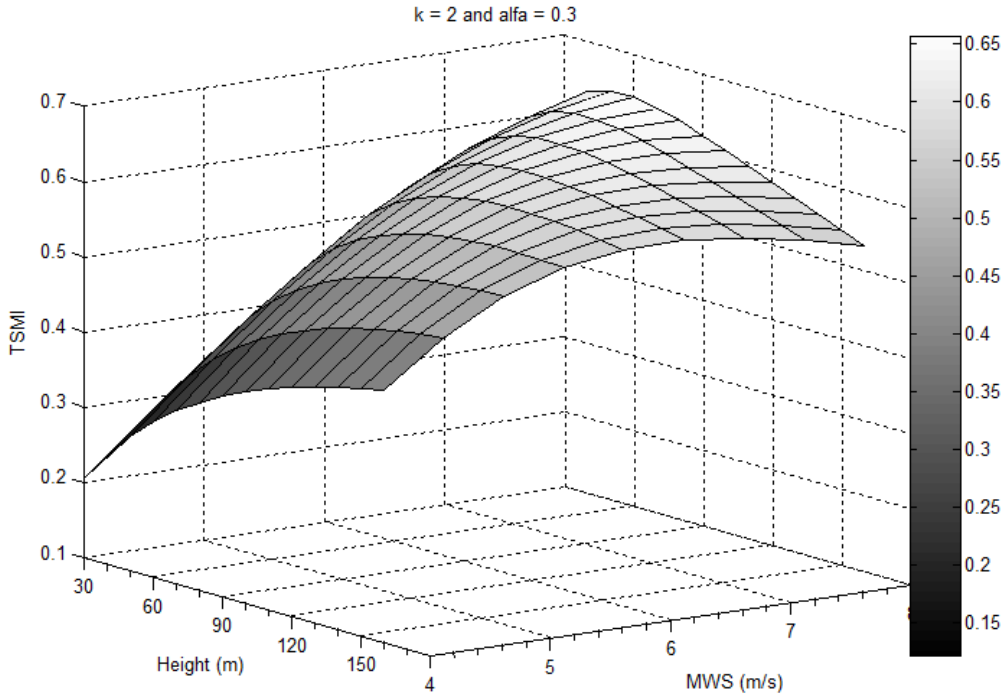

Figure 6-7: *TSMI* as a function of *MWS* and tower height for α=0.3

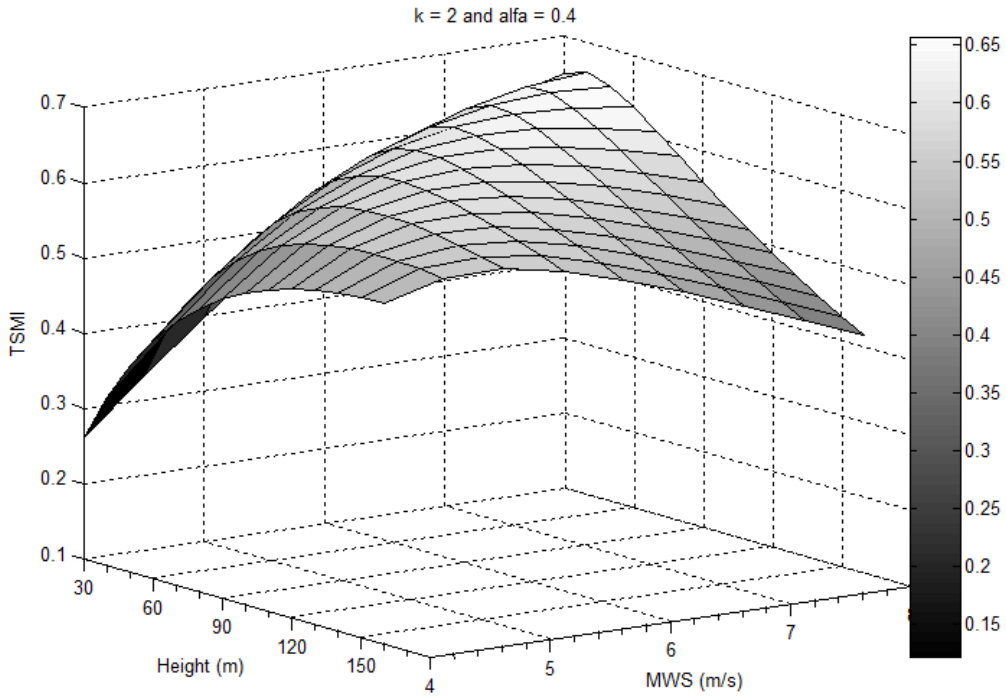

Figure 6-8: *TSMI* as a function of *MWS* and tower height for α=0.4

It is worth mentioning that although the $TSMI$ is calculated for all tower heights between 30m and 160m, these tower height limits might vary depending on turbine manufacturers. The lower limit (h_{LL}) for h^*, which mainly depends on P_{rated} of the turbine, could be about 60m for a 2MW turbine, as shown in Table 6-1. Therefore, for the cases for which h^* is lower than h_{LL}, it might be more economically effective to install turbines with smaller P_{rated} that have lower h_{LL}, despite the economies of scale associated with higher ratings.

Finally, it should be mentioned that there are other aspects that can affect the optimal Turbine-Site matching, but which are beyond the scope of this study. These aspects include the effects of other turbine properties related to different grid connection requirements, which can limit the size or technology used. Additionally, the effect of manufacturer location on the ICC of turbines might limit the available options because domestic manufacturers might be preferred over foreign ones.

6.7 Summary

When the ranking of different turbines is based solely on the CF, the results are based on the three speeds of the turbine power performance curve: cut-in, rated, and cut-out speeds, with no consideration of the costs associated with turbine installed capacity and tower height. Therefore, using the CF as the sole basis for turbine-site matching produces results that are biased towards higher towers, but which do not include the associated costs. In this chapter, a new universal formulation for the turbine-site matching problem, based on a new formulation for CF that does include turbine tower height, is presented. The accuracy of the proposed CF model that includes tower height over the existing CF extrapolation model is verified.

A new and universal Turbine-Site Matching Index ($TSMI$) is proposed for turbine site ranking based on the derived CF formulation and including the effects of turbine size, P_{rated}, and tower height on the upfront Initial Capital Cost (ICC) of wind turbines. The proposed $TSMI$ can be adapted for any detailed cost function formulation that includes the effect of turbine capacity and tower height. The effectiveness and the applicability of the proposed index are illustrated by five case studies. These studies include ranking different turbines for a given wind profile, sensitivity analysis, and optimum tower height selection for given turbine design features. In general, for each turbine, there exists an optimal tower height, at which the value of the $TSMI$ is at its maximum. The results reveal that higher tower heights are not always desirable for optimality.

Chapter 7

Impacts of Temporal Wind Profiles in Thermal Units Scheduling Costs[9]

7.1 Introduction

Due to the intermittent nature of wind power, the effects of high wind power penetration levels need to be carefully assessed. Although it is technically possible to integrate a large amount of wind power, higher wind penetration levels normally result in higher wind power integration costs. The impacts of wind power integration on power systems are twofold: wind power uncertainty and variability [125]. From an operational perspective of generation units, wind integration impacts can be divided into three main components: regulation, load-following and unit-commitment [48]. The dominant wind integration cost component occurs in the unit-commitment time frame [45].

The results of many case studies investigating such costs related to wind power balancing requirements are presented in [56], [45] and [48] and are summarized in Figure 7-1. The scattered nature of these results can be attributed to the use of different methodologies, tools and data, the use of different terminologies and metrics in representing the results, as well as different system characteristics [45]. For example, different time scales are used by different studies to estimate additional reserve requirements. Additionally, some studies consider only operating costs, whereas others consider investments for new reserves. These discrepancies also occur because some studies consider the transmission capacities needed to maintain the supply-demand balance, while others do not. In spite of the scattered results, one can draw the following conclusions:

- The incremental cost of balancing requirement is low at low wind penetration levels and increases as the wind penetration level increases [45]. At high penetration levels the cost of required reserves is significantly less when considering the net load variations (load - wind) compared with wind power variability.

[9] Some parts of this work have been reported in:

[122] M. H. Albadi and E. F. El-Saadany, "Overview of Wind Power Intermittency Impacts on Power Systems," *Electric Power Systems Research,* Accepted 30 October 2009.

[123] M. H. Albadi and E. F. El-Saadany, "Comparative Study on Impacts of Wind Profiles on Thermal Units Scheduling Costs," submitted to *IET Renewable Power Generation*.

Preliminary results of were published in:

[124] M. H. Albadi and E. F. El-Saadany, "The effects of wind profile on thermal units generation costs," in *IEEE PES 2009 Power Systems Conference and Exposition (PSCE '09)*, Seattle, WA, USA, 2009, pp. 1-6.

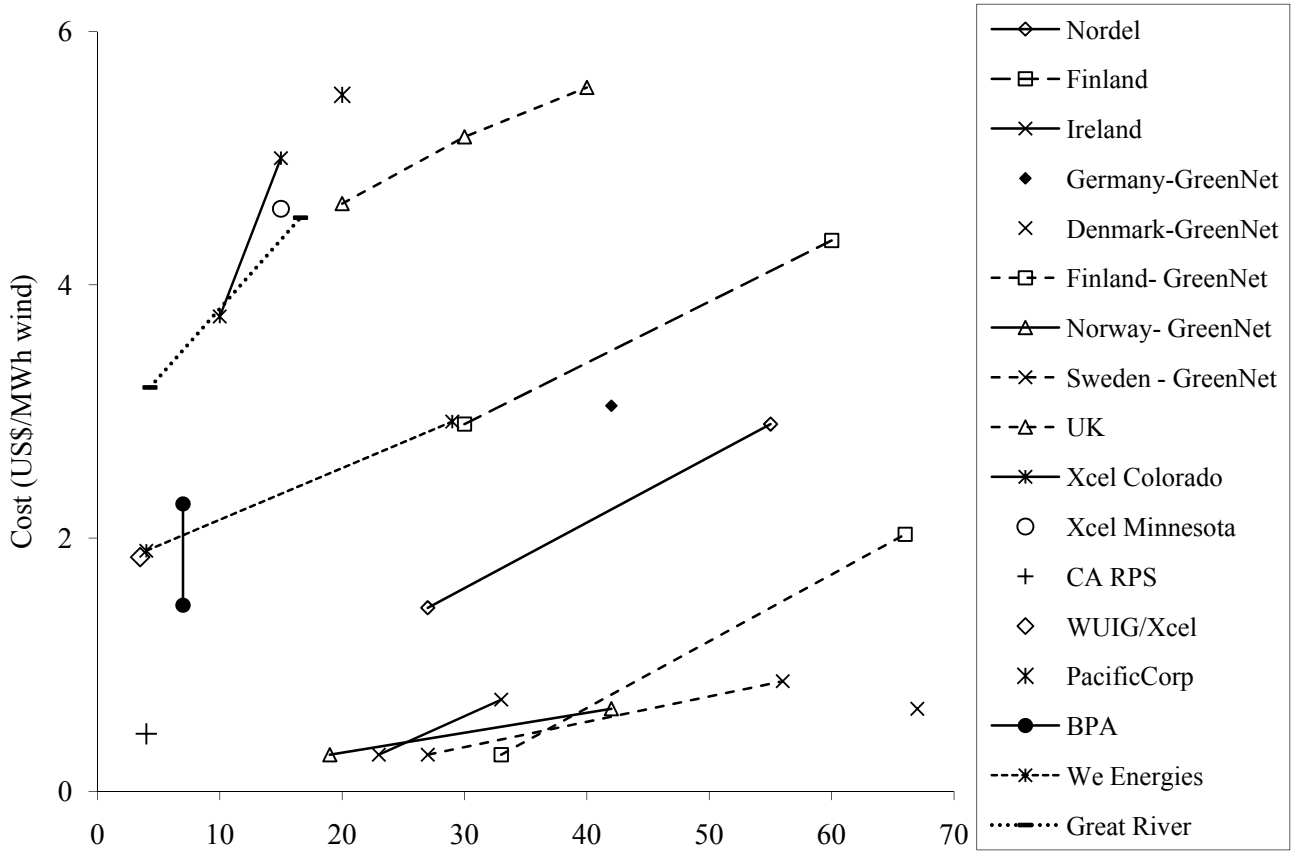

Figure 7-1: Wind power balancing requirements related costs
(Currency conversion rates are £ = US$1.95 US and € = US$1.45US).
Note: BPA,UWIG/Xcel, We Energies, PacificCorp, and Great River data is from [56];
Nordel, Finland, Ireland, GreenNet studies, and UK data is from[45];
WUIG/Xcel, PacificCorp, BPA, We Energies, Great River, and CA RPS data is from [48].

- The flexibility of conventional (dispatchable) generation plays a crucial role in reducing wind power integration costs. Therefore, hydro-dominated countries, e.g., Norway, have lower costs than thermal stations-dominated countries, e.g., Germany. The coordination of the operation of hydro generating systems with the electricity produced from wind farms opens up new possibilities to system operators and utilities. The output of wind facilities can be stored in water reservoirs using pumped hydro storage facilities and delivered later at times when needed most [56].

- Available transmission capacities to neighboring systems, e.g., the case of Denmark, facilitate the increase in wind penetration levels without increasing balancing requirements, to a certain extent. For example, the GreenNet study expected balancing costs of US$0.65 per MWh wind production at 67%

penetration level (peak wind production / peak demand) [126]. Nevertheless, wind power integration costs increases when a neighboring country gets more wind power as exporting possibilities decrease.

- To minimize integration costs, wind power production facilities should be geographically dispersed, especially when transmission capacity is limited. Germany has a relatively high integration cost compared with Denmark, Norway and Sweden, partly because of concentration of wind power production in the north-west region [45].

As the aforementioned studies are case-specific, none of them investigates the effect of changing wind profile, to the author's knowledge. In this work, a test system, which is modified from the IEEE Reliability Test System (IEEE-RTS), is used to study the effect of two generic temporal wind profiles on the system operating costs, which include fuel and startup costs, the value of wind power, and wind power curtailments, at different wind power penetration levels.

After this introduction, this chapter presents a Unit Commitment (UC) model with wind power included. This model takes into consideration uncertainties related to both wind power and load forecasting errors. The test system data and assumptions used in the study are presented in section 7.3. In section 7.4, the effects of two different temporal wind power patterns on total operation, fuel, and cycling costs, as well as curtailed wind energy are discussed. Finally, the main conclusions are summarized in section 7.5.

7.2 Unit Commitment with Wind Power

Unit commitment is the optimum selection of on-line dispatchable generators to satisfy different operating constraints, including supply-demand balance, spinning reserve requirements, and thermal unit and network component constraints. In [127] a bibliographical survey of this problem is presented. The UC problem involves two sources of uncertainties: generation units' outages and load forecast errors [128]. Similar to [129-131], the focus of this work is on forecasting errors, and thermal units are assumed to be reliable for the day-ahead UC problem.

7.2.1 Modeling Forecasting Uncertainties

7.2.1.1 Load Forecasting

In this study, hourly day-ahead expected demand and wind production are considered available. Short-term electricity demand forecasting has been the focus of extensive research [132]. The hourly demand

forecast consists of two components: an expected value ($PD_t{}^{mean}$) and a forecasting error ($e_{PD,t}$). Due to the repeated nature of daily/weekly variations, demand forecasts are commonly assumed to be accurate, and the error is modeled as a zero-mean normally-distributed random variable with a standard deviation of $\sigma_{PD,t}$ [133]. $\sigma_{PD,t}$ is commonly considered to be a percentage of the expected demand. In this work, $\sigma_{PD,t}$ is considered to be 2% of the hourly expected demand as in [133, 134].

$$PD_t{}^{f} = PD_t{}^{mean} + e_{PD,t} \tag{7-1}$$

7.2.1.2 Wind Power Forecasting

Currently, wind power forecasting techniques are the subject of extensive research [135]. Wind power forecasting can significantly reduce costs associated with day-ahead uncertainty. Smith et al., reported that state-of-the-art, commercially available forecasting tools can provide 80% of the benefits that would have been achieved from perfect forecasting [47].

Wind power forecasting error is commonly assumed to follow a normal distribution [130, 133, 134, 136, 137]. Motivated by the nonlinear characteristics of wind turbine power curves, some authors propose using beta distribution to represent wind forecast error [138, 139]. However, for a large number of wind power facilities and a wide geographical dispersion, the assumption of the forecasting error following normal distribution can be justified using central limit theorem [140]. In this work, the aggregate wind power forecast is represented by an expected value ($P_{wind,t}{}^{mean}$) and an error ($e_{wind,t}$) that is modeled as a zero-mean normally-distributed random variable with a standard deviation of $\sigma_{wind,t}$.

$$P_{wind,t}{}^{f} = P_{wind,t}{}^{mean} + e_{wind,t} \tag{7-2}$$

Wind power forecast error is commonly represented by a normalized standard deviation, which is standard deviation of the error divided by wind power installed capacity. The normalized forecast error of an individual wind farm increases as the forecast horizon increases [136, 141], Figure 7-2. The forecast error can be reduced by an increase in the number of turbines within a farm and a wider geographical dispersion of wind facilities, since not all wind turbines experience the same wind speed at the same time. The reduction due to an increase in the number of wind turbines within the same region quickly approaches a saturation level controlled by the region diameter [142, 143]. As well as by the forecasting horizon and the region diameter, forecast error is also affected by the expected wind power value [139].

For a 36-hour forecasting horizon, the hourly value of σ_{wind} as a function of the predicted value is represented by the following linear equation.

$$\sigma_{wind}\left(t, {P_{wind,t}}^{mean}\right) = \left(0.875\frac{{P_{wind,t}}^{mean}}{P_{wind,installed}} + 0.125\right)\sigma_{wind,t} \quad (7\text{-}3)$$

where $\sigma_{wind,t}$ is represented by Figure 7-2. The constants in the above equation are based on [139].

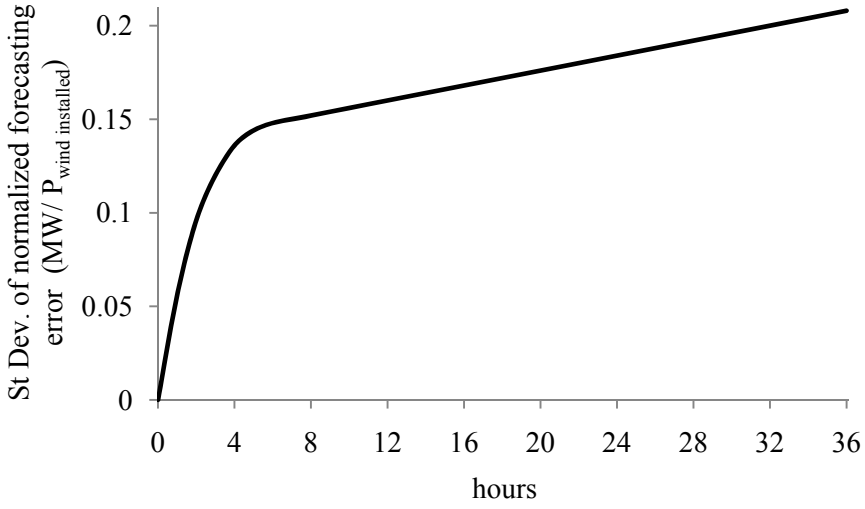

Figure 7-2: Standard deviation of normalized wind power forecast errors as a function of forecast horizon for one turbine

7.2.1.3 Net Demand Modeling:

Assuming no correlation between demand and wind forecasts [133], the net demand (ND) is the difference between the demand and the wind power forecasts.

$${ND_t}^f = {PD_t}^f - {P_{wind,t}}^f = {ND_t}^{mean} + e_{ND,t} \quad (7\text{-}4)$$

where $e_{ND,t}$ is the net demand forecast error for which the standard deviation is given by the following formula:

$$\sigma_{ND,t} = \sqrt{{\sigma_{PD,t}}^2 + \sigma_{wind}\left(t, {P_{wind,t}}^{mean}\right)^2} \quad (7\text{-}5)$$

where σ_{wind} is given by equation (7-3).

7.2.2 Handling Uncertainties in UC

There exist two approaches to handling uncertainties in the unit commitment problem: reserve requirement [129, 134, 136, 137, 144] and scenario-based stochastic programming [130, 133, 145]. The first approach applies the reserve requirement to handle uncertainties *explicitly* in the UC problem formulation, while the second one does it *implicitly*, through considering a set of scenarios to describe the stochastic nature of the uncertainties [128]. The disadvantage of the scenario-based approach is that a huge number of scenarios are required to represent the stochastic nature of uncertainties. For example, the authors in [133] generated a scenario tree with 2401 paths, using seven intervals of the discretized normal distribution of the net load forecast error and a 4-hour planning horizon. Using the aforementioned approximation of the normal distribution, a set of 7^{24} scenarios is required for a 24-hour planning horizon. Although scenario reduction techniques [146] can be used to discard part of the scenario tree, this approach remains computationally intensive for systems of a realistic size. In this work, the stochastic nature of net load uncertainty is considered using the reserve requirement approach.

7.2.3 Specifying Reserve Requirements

Conventionally, the spinning reserve requirement is planned based on deterministic criteria, such as the largest generator size, a certain percentage of the load, and the use of n-1 criterion when transmission constraints are considered [147]. These deterministic criteria lack flexibility and neglect economic factors [147]. Due to the intermittent nature of wind power, stochastic criteria based on the probabilistic confidence level of meeting the expected net demand have become more appealing. This approach uses chance-constrained stochastic formulation to represent the stochastic constraints, which can then be converted into deterministic equivalents based on some predetermined confidence levels [129, 144, 147]. Equation (7-6) below illustrates this approach.

$$Pro\left({ND_t}^{f} \leq {ND_t}^{mean} + \lambda\sigma_{ND,t}\right) = 1 - a_\lambda \qquad (7\text{-}6)$$

where the left hand side of the equation is the probability of the net demand being less than or equal to $({ND_t}^{mean} + \lambda\sigma_{ND,t})$ and $(1 - a_\lambda)$ is the associated confidence level. Assuming a normal distribution, when λ is assigned values of 1, 2, and 3, the probabilistic confidence levels of having enough committed capacity to meet the net expected demand are 84.1, 99.7, and 99.9%, respectively. The value of the confidence level can be assigned based on the system operator's experience. A graphical illustration of

equation (7-6), when $\lambda = 1$, is presented in Figure 7-3.

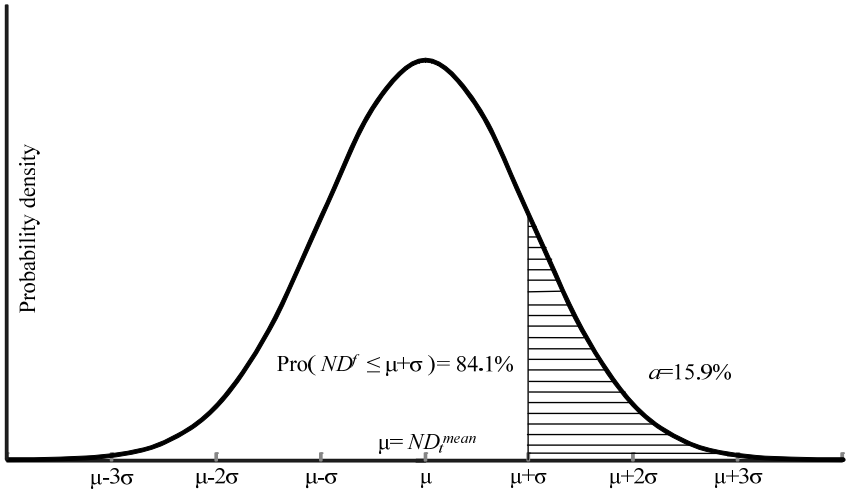

Figure 7-3: Graphical illustration of chance-constrained formulation (λ=1 and 1-a_λ=84.1%)

7.2.4 UC Mathematical Formulation

In this subsection, the mathematical formulation of the UC problem is presented. The objective is to minimize the dispatchable generation Operational Costs (OC) as described below.

$$\min OC = \sum_{i=1}^{NG} \sum_{t=1}^{T} [FC_{it}(P_{it}) + U_{it} MC_{it} + Ust_{it} ST_{it}] \tag{7-7}$$

where NG is the number of units; T is the number of hours in the planning period; FC_{it}, P_{it}, MC_{it}, and ST_{it} are the fuel cost, the level of power generation, the maintenance cost, and the start-up cost of the i^{th} unit during hour t, respectively. U_{it} is a binary variable for the status of the i^{th} unit (1 indicates that the unit is committed). A fixed maintenance cost (MC) of US$0.8 /MW is considered for all online units. This portion of OC cost is considered to calculate the overall cost of the system. More details of the thermal units are presented in Table 7-1.

In this study, a linearized FC function is considered.

$$FC_i = a_i P_i + b_i \tag{7-8}$$

where a_i and b_i are the average incremental fuel cost (US$/MWh) and the fixed fuel cost (US$), respectively, for the i^{th} unit.

A stair-wise startup cost function is typically used for thermal generation units [148]. In this work, a two-segment startup cost function is considered for each unit group, depending on how many hours the unit was off, as described by the following equation.

$$ST_{it} = \begin{cases} HSC_i & : if \;\; U_{off,it} < CST_i \\ CSC_i & : if \;\; U_{off,it} \geq CST_i \end{cases} \tag{7-9}$$

where HSC_i and CSC_i are the hot and cold start costs, respectively, of the i^{th} unit; $U_{off,it}$ is the number of hours the unit was turned off, and CST_i is the number of U_{off} hours at which CSC would be incurred if the unit is started up.

This objective function is subject to three types of constraints: thermal units, system, and wind power constraints. These constraints are described as follows.

7.2.4.1 System Constraints

1. Power balance constraints to ensure that the scheduled generation is equal to the expected net demand during each hour t. The losses are neglected for simplicity.

$$\sum_{i=1}^{NG} P_{it} = {ND_t}^{mean} \tag{7-10}$$

In network constrained UC, the DC power equation is commonly used to ensure a supply-demand balance.

$$P_{k,t} - {ND_{k,t}}^{mean} = \sum_j \frac{1}{X_{kj}} \left(\delta_{j,t} - \delta_{k,t}\right) \;\; \forall \; k = 1 \; to \; 24 \tag{7-11}$$

where ${ND^{mean}}_{k,t}$ and $P_{k,t}$ are the expected net demand at bus k and the output of the thermal units connected to bus k, respectively, during hour t. X_{kj} is the reactance of the line between buses k and j. $\delta_{j,t}$ is the power angle at bus j during hour t.

2. Thermal limits constraints to ensure that the lines are not overloaded.

$$-{P_{kj}}^{max} \leq \frac{1}{X_{kj}} \left(\delta_k - \delta_j\right) \leq {P_{kj}}^{max} \tag{7-12}$$

where ${P_{kj}}^{max}$ is the capacity limit of line kj and X_{kj} is the reactance of the line. The data of the test system lines are presented in Table 7-2

3. Spinning reserve (SR) requirement, which is necessary to ensure that enough committed capacity is available to meet the net expected demand. The chance-constrained stochastic formulation of the spinning reserve constraints is given by the following equation [129].

$$Pro\left(\sum_{i=1}^{NG} U_{it}{P_{it}}^{max} \geq {ND_t}^{f}\right) \geq 1 + a_{\lambda} \tag{7-13}$$

where ${P_{it}}^{max}$ denotes the maximum power generation of the i^{th} unit during hour t. The deterministic equivalent of the stochastic formulation can be written as follows [129].

$$\sum_{i=1}^{NG} U_{it}{P_{it}}^{max} \geq {ND_t}^{mean} + \lambda\sigma_{ND,t} \tag{7-14}$$

Considering $\lambda = 2$, the probabilistic confidence levels of having enough spinning reserve capacity to meet the net expected demand is 99.7%. To improve this confidence level, a power system operator can consider higher values for λ to commit more spinning reserve, or use other types of operating reserve. ${P_{it}}^{max}$ denotes the maximum power generation of the i^{th} unit during hour t, as defined by the following equation.

$${P_{it}}^{max} = \begin{cases} 60RR_i + P_{i(t-1)} \\ P_{i,max} \end{cases} \tag{7-15}$$

where $P_{i,max}$ is the upper limit of P_i; RR_i is the ramping rate of the i^{th} unit in MW/minute, and $P_{i(t-1)}$ is the output of the unit during hour $(t-1)$. It is worth mentioning that at very high penetration levels, network constraints might limit the amount of wind power that can be accommodated. Therefore, σ_{wind} in equation (7-5) should be capped to avoid overcommitting SR requirements.

$$\lambda\sigma_{Wind} \leq LinesCap - {PD_{Local\ load}}^{f} \tag{7-16}$$

where $LinesCap$ is the exporting capacity of the transmission lines connected to the bus at which wind facilities are connected and ${PD_{Local\ load}}^{f}$ is the demand at that bus. In such cases, equation (7-14) can be written as follows:

$$\sum_{i=1}^{NG} U_{it}{P_{it}}^{max} \geq {ND_t}^{mean} + \sqrt{\left((\lambda\sigma_{PD})^2 + \left(LinesCap - {PD_{Local\ load}}^{f}\right)^2\right)} \tag{7-17}$$

7.2.4.2 Thermal Unit Constraints

The thermal unit constraints considered in this model include limits on generation output, ramping rate, minimum up/down time, as well as the must-run unit and initial condition constraints, as described below.

1. Maximum and minimum output limits on generators

$$U_{it}P_{i,min} \leq P_{it} \leq U_{it}P_{i,max} \tag{7-18}$$

where $P_{i,min}$ is the output lower limit of the i^{th} thermal unit.

2. Ramp rate limits for online generator

$$P_{i(t-1)} - 60\,RR_i \leq P_{it} \leq P_{i(t-1)} + 60\,RR_i \tag{7-19}$$

3. Minimum up-time ($t_{i,up}$) is the minimum number of hours that the i^{th} unit must remain on-line once it has been turned on. Minimum down-time ($t_{i,down}$) is the minimum number of hours that the unit must remain off-line once it has been turned off.

$$U_{it} = \begin{cases} 1, & if\ U_{on,i(t-1)} < t_{i,up} \\ 0, & if\ U_{off,i(t-1)} < t_{i,down} \end{cases} \tag{7-20}$$

where $U_{on,i(t-1)}$ and $U_{off,i(t-1)}$ are the number of hours the i^{th} unit is on-line and off-line, respectively, during hour $(t-1)$.

4. Initial states/conditions are considered to honor minimum up/down constraints. The initial conditions of the test system units are presented in Table 7-3.

5. A must-run unit is one that must remain on-line for the whole planning period due to operating reliability and/or economic considerations.

$$U_{it} = 1 \quad \forall i \in MR \tag{7-21}$$

where MR is the group of must-run units. Unit types U350 and U400 are considered in the MR group for this study.

6. Logic constraints are to ensure that thermal units are not started-up or shut-down at the same time.

$$Ust_{it} - Usd_{it} = U_{it} - U_{i(t-1)} \tag{7-22}$$

where Ust_{it} and Usd_{it} are binary variables for the i^{th} unit start-up and shut-down status, respectively. Ust_{it}/Usd_{it}=1 indicates that the i^{th} unit is started-up/shut-down during hour t.

7.2.4.3 Wind Power Constraints

In this analysis, wind power curtailment is considered. This option is illustrated by the following two inequality constraints.

$$0 \leq P_{wind,t} \leq {P_{wind,t}}^{mean} \tag{7-23}$$

where ${P_{wind,t}}^{mean}$ is the expected value of wind power and $P_{wind,t}$ is the accommodated wind power, respectively, during hour t.

It is worth mentioning that most wind production facilities around the world, especially the ones connected to local distribution networks, are operating based on feed-in tariff contracts. According to these contacts, wind facility operators can dump all available wind power into the grid. However, for higher penetration levels, even with a strong grid, the wind curtailment option would be exercised to maintain a reliable and economic operation of thermal units.

7.3 Test System

A 24-bus test system modified from IEEE RTS is used to examine the effect of two different temporal wind profiles on generation costs. The IEEE RTS was initially presented in [149] and later updated in [150]. The one area system has a generation capacity of 3405 MW. In this research, the hydro capacity (300MW) was replaced by three units of type U100. The minimum up/down and the Hot/Cold start times and the ramping constraints of thermal units are as in [148, 151]. These details of the systems are presented in Table 7-1. A typical winter week load profile is considered as in [150], see Figure 7-4. The annual peak demand of the system is 3135 MW.

The two wind profiles considered in this study are also depicted in Figure 7-4. In Profile 1, wind power production is dominated by synoptic effects; therefore, diurnal variation is not evident. West Denmark wind power production, presented in [152], is an example of this profile. On the other hand, the diurnal wind speed variation is very clear in Profile 2. The aggregated New York ISO system wind production pattern described in [153] is an example of this profile. In the NY ISO system, wind power has an

opposite profile to that of the load. The weekly capacity factor of both profiles is considered to be 35%, which means that the average production of these wind power facilities is 35% of their installed capacity.

From a geographical perspective, two wind integration scenarios are considered. In the first, a wide geographical dispersion of wind power facilities is considered. Here, wind generators are assumed dispersed at different nodes in proportion to the amount of load at each node. Compared to individual wind farm forecasts, a 35% reduction of the ensemble hourly wind forecast error is considered based on a region diameter of about 400 km [142, 143].

In the second scenario, all wind power facilities are concentrated in the Bus 14 zone. Due to the smaller geographical dispersion area, a 10% reduction of the ensemble hourly wind forecast error compared to individual wind farm forecast is considered. For both scenarios, this amount of reduction in the ensemble forecast error is assumed constant for all wind penetration levels, because forecasting error reduction within the same region quickly approaches a saturation level after a finite number of turbines are installed [142, 143]. This number is considered to be reached at a wind penetration level of 10%.

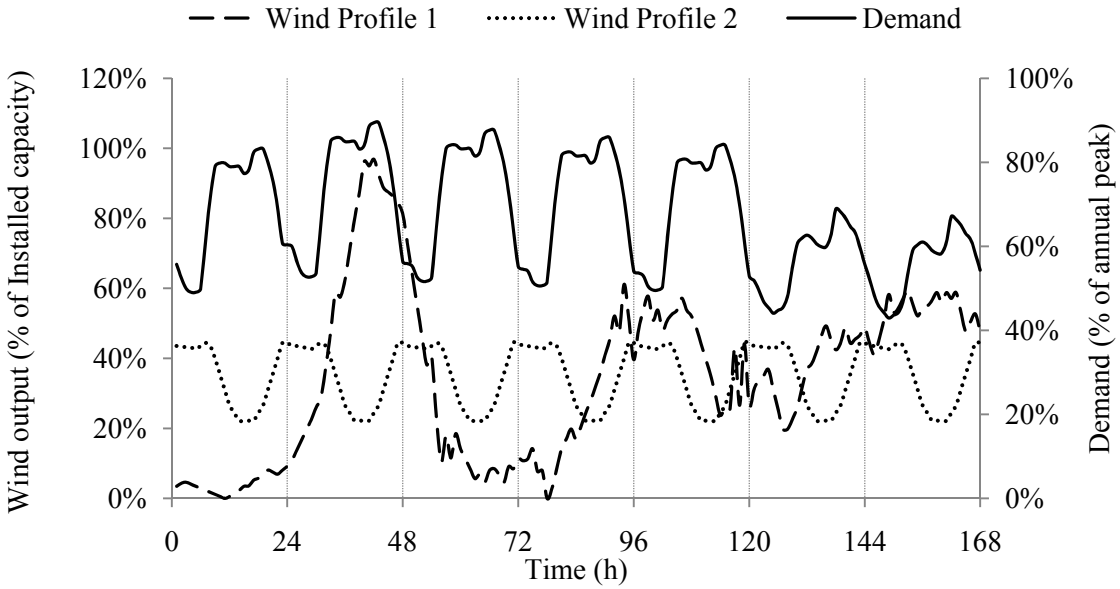

Figure 7-4: One-week load and wind profiles considered in the study

Table 7-1: Generation test system

Number of Units	*Unit Group*	*Unit Type**	$P_{i,max}$ *MW*	$P_{i,min}$ *MW*	RR_i *MW/min*	$t_{i,down}$ *hour*	$t_{i,up}$ *hour*	CST_i *hour*	HSC_i *US$*	CSC_i *US$*	a_i *US$/MWh*	b_i *US$/h*	MC *US$/MW*
5	U12	Oil St.	12	2.4	1	3	4	5	496	888	143.0	141.2	0.8
4	U20	Oil CT.	20	4	3	2	1	1	65	65	168.7	403.8	0.8
4	U76	Coal St.	76	15.2	2	5	8	12	1085	1085	19.4	158.3	0.8
6	U100	Oil St.	100	25	7	9	8	7	3265	7392	117.5	1215.6	0.8
4	U155	Coal St.	155	54.25	3	9	8	11	473	1734	15.8	239.9	0.8
3	U197	Oil St.	197	68.95	4	11	12	7	5786	10122	117.2	1484.2	0.8
1	U350	Coal St.	350	140	8	49	24	12	3485	8132	16.4	271.5	0.8
2	U400	Nuclear	400	100	20	-	-	-	-	-	6.9	238.4	0.8

* St.: Steam turbine; CT: Combustion Turbine

Table 7-2: IEEE RTS branch data

From bus #	*To bus #*	*X(pu)*	*Capacity (MVA)*
01	02	0.014	175
01	03	0.211	175
01	05	0.085	175
02	04	0.127	175
02	06	0.192	175
03	09	0.119	175
03	24	0.084	400
04	09	0.104	175
05	10	0.088	175
06	10	0.061	175
07	08	0.061	175
08	09	0.165	175
08	10	0.165	175
09	11	0.084	400
09	12	0.084	400
10	11	0.084	400
10	12	0.084	400
11	13	0.048	500
11	14	0.042	500
12	13	0.048	500
12	23	0.097	500
13	23	0.087	500
14	16	0.059	500
15	16	0.017	500
15	21	0.049	500
15	21	0.049	500
15	24	0.052	500
16	17	0.026	500
16	19	0.023	500
17	18	0.014	500
17	22	0.105	500
18	21	0.026	500
18	21	0.026	500
19	20	0.04	500
19	20	0.04	500
20	23	0.022	500
20	23	0.022	500
21	22	0.068	500

Table 7-3: Generators initial conditions

Generator	*Initial State 1=online, 0=offline*	*Hours since last change in State*	*Initial Output MW*
G1	0	10	0
G2	0	9	0
G3	0	8	0
G4	0	7	0
G5	0	6	0
G6	0	5	0
G7	0	4	0
G8	0	3	0
G9	0	2	0
G10	1	5	20
G11	1	8	20
G12	1	9	20
G13	1	10	20
G14	1	10	25
G15	1	5	25
G16	1	9	25
G17	0	9	0
G18	0	9	0
G19	0	10	0
G20	1	8	55
G21	1	8	55
G22	1	8	55
G23	1	12	100
G24	1	12	70
G25	1	12	170
G26	1	12	170
G27	1	50	350
G28	1	-	400
G29	1	-	400

7.4 Simulation Results

The unit commitment problem described in the previous section is modeled as a linear Mixed Integer Problem (MIP). A code in the General Algebraic Modeling System (GAMS) environment [154] is developed, and the CPLEX solver is used to solve the MIP. Figure 7-5 shows the methodology used to conduct the simulation.

Given system data and the units' initial conditions, the algorithm solves the day-ahead UC problem based on hourly expected demand, expected wind power, and associated forecasting errors. It is assumed

that the day-ahead UC problem is solved daily at 12pm, i.e., 12 hours before real time operation. Therefore, the 36-h forecasting horizon is used. Using a rolling planning technique [155], the algorithm solves the day-ahead UC problem for the whole week. For each day, the decision variables include unit states (0/1) and output levels (MW), the numbers of hours since the last change in unit states, and different components of OC. The model is used to study the effect of wind profiles on fuel cost, start-up cost, the value of wind power from a total operating cost saving perspective, and wind power curtailments, as wind power penetration levels increase.

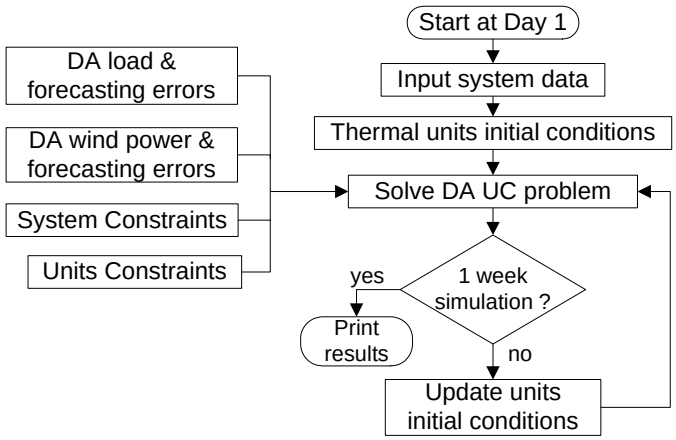

Figure 7-5: Rolling planning methodology used to quantify wind impacts

7.4.1 Impacts on Fuel Saving

Unlike thermal units, the operation of wind turbines does not require any fuel; therefore, they can be considered the cheapest generators from a UC perspective. Any energy produced by wind power facilities can displace a certain amount of thermal generation production. In fact, fuel saving, and its associated environmental impacts, is one of the main reasons for the promotion of wind power around the globe.

The effect of wind power on fuel savings for different penetration levels and wind profiles is illustrated in Figure 7-6. As can be seen, the fuel savings of both profiles are almost the same and increase linearly up to a penetration level of 20% for all scenarios. Beyond this level, it is clear that Profile 2 yields more savings than Profile 1 for the same geographical dispersion scenario. This result is attributable to the fact that with the Profile 1 scenario, the wind curtailment option is exercised more often as presented in subsection 7.4.3.

Figure 7-6 illustrates that at a penetration level of 40% and beyond, the difference between fuel saving benefits of different geographical dispersion scenarios becomes more evident. For example, at a penetration level of 80%, the fuel saving benefits of the wide geographical scenario overweigh those of the other scenario by about US$1.6 and US$0.7 million for Profiles 1 and 2, respectively. This effect is attributable mainly to wind power being spilled, due to the limited transmission capacity available for wind power in the scenario where all wind facilities are connected at Bus 14.

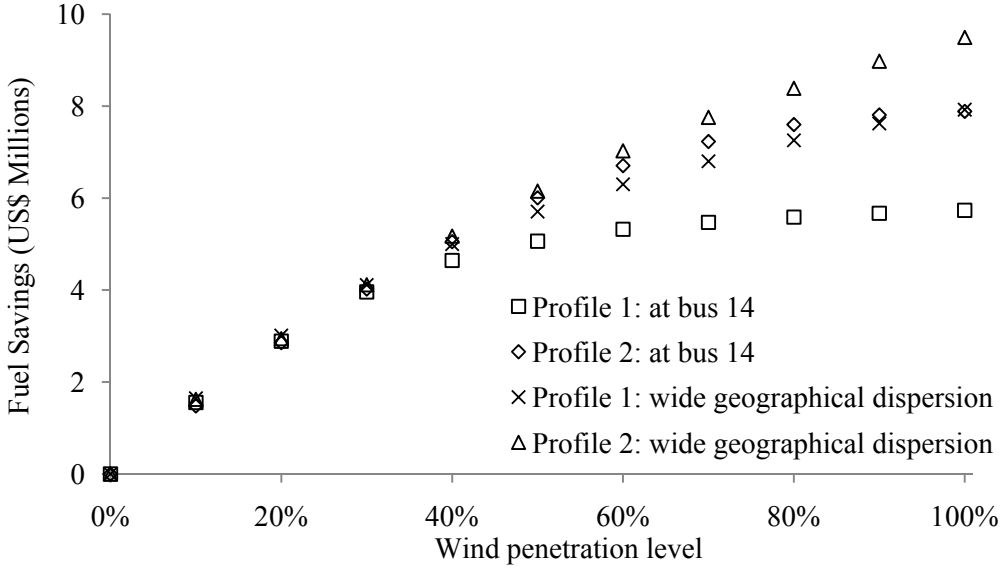

Figure 7-6: Fuel saving as a function of wind power penetration level

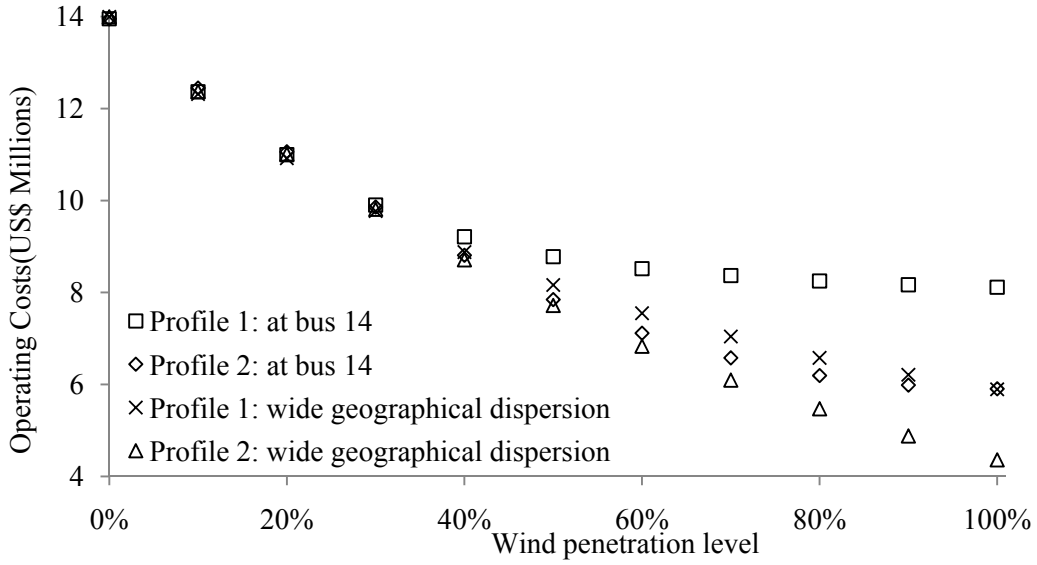

Figure 7-7: Total operating costs as a function of wind power penetration level

When all wind power facilities are connected within the Bus 14 zone, the fuel saving experiences a saturation effect. This result is attributable to the increase in wind energy being curtailed as well as the increase in costs associated with providing SR requirements.

The effect of wind power on total operating costs for different penetration levels and wind profiles is illustrated in Figure 7-7. As fuel costs are the dominant component of the total operating costs (OC), Figure 7-7 looks to be an inverse of Figure 7-6 with some positive offset.

7.4.2 Impacts on Cycling Costs

Cycling costs considered in this work are attributed to the two-segment fuel start-up cost function described by equation (7-9). In practice, the cycling costs of a thermal unit may include additional *O&M* costs, reduced unit efficiency caused by variable operation, increased auxiliary power, and shortening unit life caused by creep-fatigue interactions [156].

Figures 7-8 and 7-9 illustrate the effect of different wind profiles on cycling costs as a function of the penetration level for the two geographical dispersion scenarios. In general, systems with Profile 2 experience more start-up costs than those experienced by systems with Profile 1 for both geographical dispersion scenarios. This result is attributable to systems with Profile 1 experiencing higher wind power curtailments, which, in turn, result in a smoother accommodated wind power that better coincides with daily peak demand. The exception to this general conclusion is penetration levels of higher than 60% for the scenario in which all wind facilities are connected to Bus 14. In this case, high wind curtailments for both profile scenarios results in lower cycling costs in systems with Profile 2 scenario.

Another observation is that, generally, the start-up costs for systems with both wind profiles are less than those with no wind power (zero penetration level). This result is attributable to the fact that the SR, required to address the uncertainty of wind power, reduces the start-up/ shut-down actions.

7.4.3 Impacts on Wind Power Curtailments

During certain hours, wind turbine output needs to be curtailed to preserve a balanced, stable, and secure operation of the grid. In low load periods, the power system operator may consider curtailing wind power to ensure that sufficient dispatchable units are online to guarantee enough reserves and ramping capabilities to accommodate net demand fluctuation. The amount of curtailed energy depends not only on wind penetration levels, but also on system flexibility and wind profile.

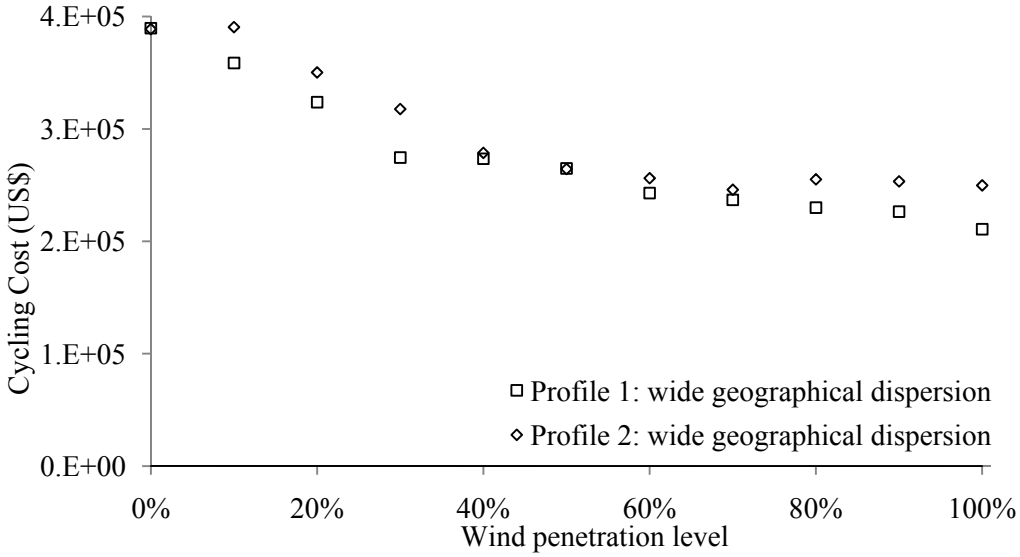

Figure 7-8: Cycling costs when a wide geographical dispersion of wind power is assumed

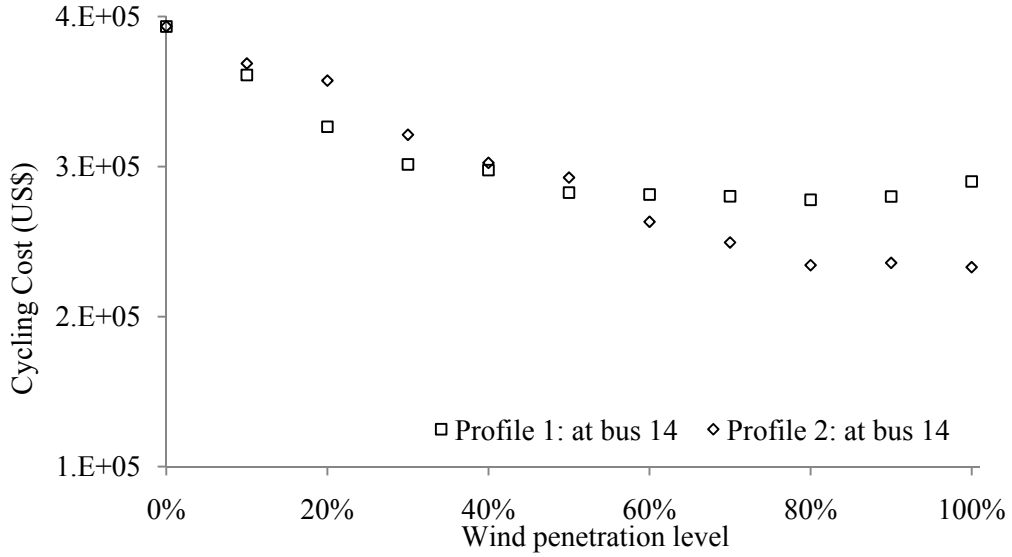

Figure 7-9: Cycling costs when all wind power facilities are connected at bus 14

As illustrated in Figure 7-10, when all wind power is considered at Bus 14, curtailments start at a penetration level of 30% and 50% for Profiles 1 and 2, respectively. For wind Profile 1, the two lines connecting Bus 14 to other buses become congested due to high wind power; therefore, the wind curtailment option is exercised for 8 consecutive hours, starting from the fortieth hour (Tuesday at 2 pm).

For wind Profile 2, the ninety-fifth hour is the first one during which wind curtailment would be exercised. During this hour, low local off-peak demand coincides with high wind production.

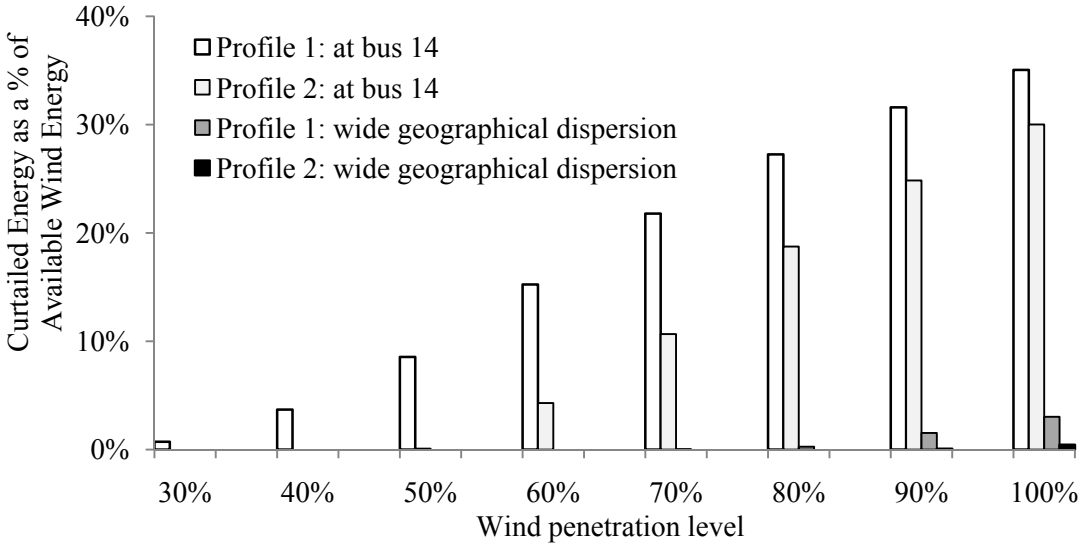

Figure 7-10: Curtailed wind energy at different wind power penetration level

When a wide geographical dispersion scenario of wind power facilities is considered, the system operator would start exercising the wind curtailment option at a penetration level of 70% and 90% for Profile 1 and Profile 2, respectively. For wind Profile 1, the first wind curtailment hours occur near Tuesday midnight (hours 48 and 49), during which a relatively high wind power coincides with low demand. During these hours, all online generation units are scheduled to operate at their minimum output limits. Similarly, the first wind curtailment hours for the wind Profile 2 scenario occur near Saturday midnight (hours 148-151), during which a high wind power coincides with low demand.

The amount of curtailed wind energy (as a percentage of available energy) increases sharply as penetration levels increase. Figure 7-11 to Figure 7-14 present curtailed and accommodated wind output at 100% penetration level for all profiles and geographical dispersion scenarios. At this specific penetration level, when all wind power facilities are considered to be installed at Bus 14, 35.06% and 30.01% of the potentially harvested wind power would be curtailed for both the wind Profile 1 and 2 scenarios, respectively. When the wide geographical dispersion scenario of wind power facilities is considered, this amount decreases to 3.03% and 0.44% for the former and the latter scenario, respectively. The effect of network constraints is clear in Figures 7-11 and 7-13, in which the output of wind power facilities is excluded above a certain production level.

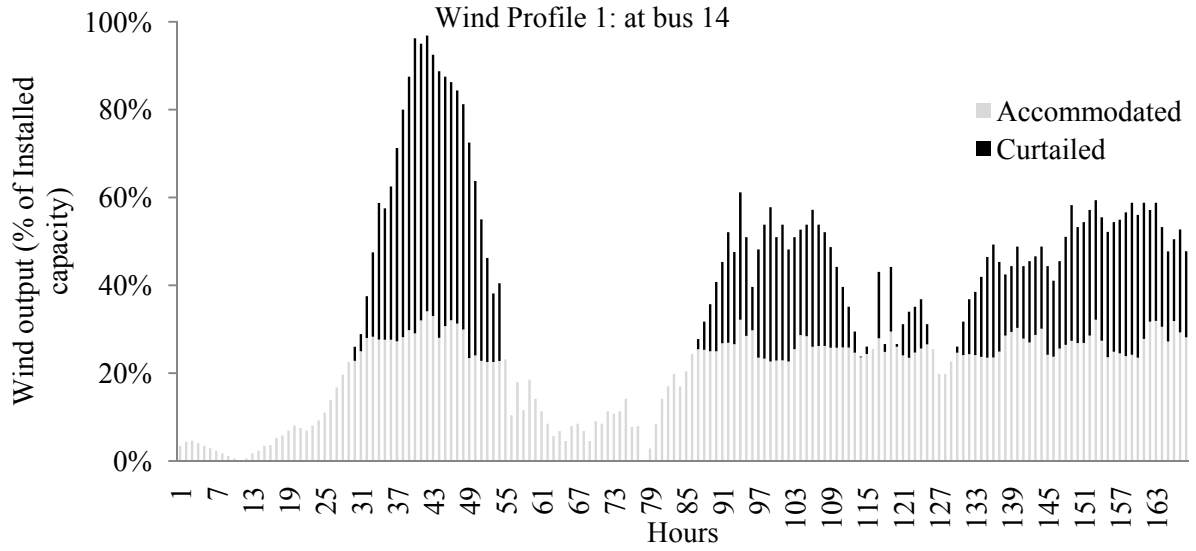

Figure 7-11: Curtailed versus accommodated wind output for Profile 1 at 100% penetration level with all wind resources connected at bus 14

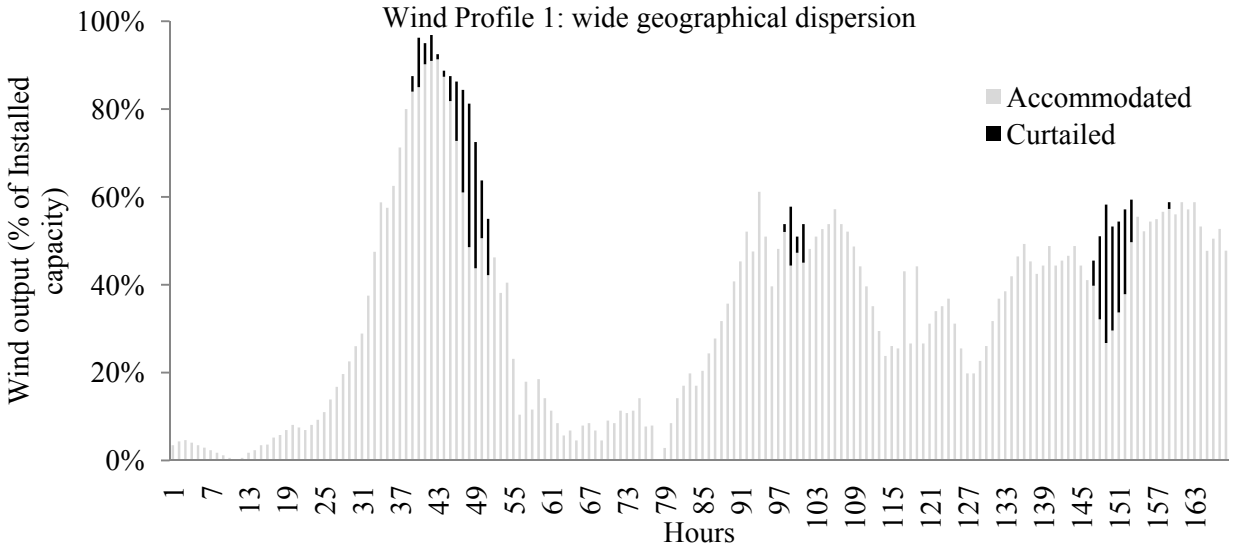

Figure 7-12: Curtailed versus accommodated wind output for Profile 1 at 100% penetration level with the wide geographical dispersion scenario

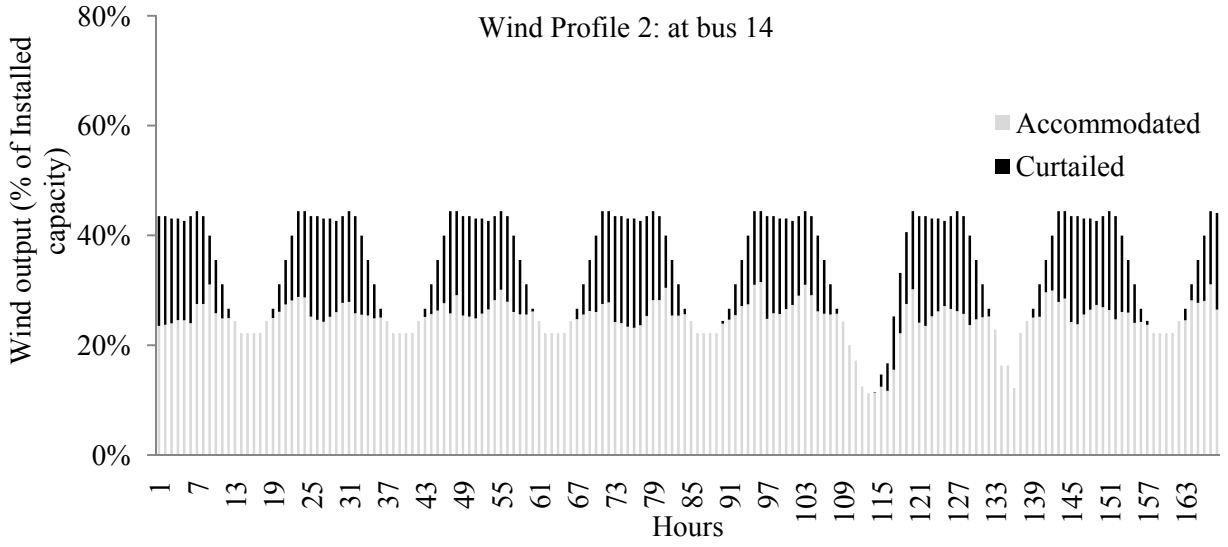

Figure 7-13: Curtailed versus accommodated wind output for Profile 2 at 100% penetration level with all wind resources connected at bus 14

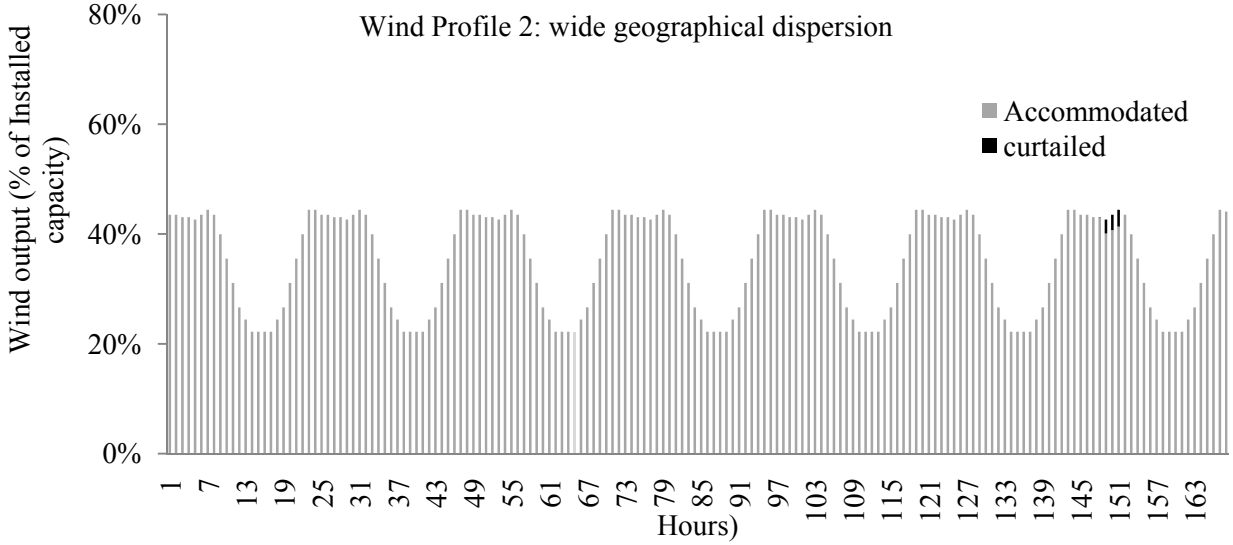

Figure 7-14: Curtailed versus accommodated wind output for Profile 2 at 100% penetration level with the wide geographical dispersion scenario

7.4.4 Impacts on Value of Wind Power

The effect of the penetration level on the marginal value of the harvested wind power is presented in Figure 7-15. The marginal value of wind energy at a certain penetration level scenario is calculated by

dividing the total operational cost savings in that scenario in comparison to savings at the previous penetration level scenario by the available wind energy (accommodated + curtailed).

Generally, this value decreases as the penetration level increases, for all wind profiles and geographical dispersion scenarios. This decrease occurs because the cost of electricity from marginal units decreases as wind power penetration levels increase, due to the decrease in net load (load-wind). In addition, wind power curtailments contribute to reducing the value, especially with high penetration levels.

For all penetration level scenarios higher than 20%, the marginal value of wind power in systems in which wind speed variations are dominated by diurnal effects, Profile 2, is higher than that where synoptic effects are dominant, Profile 1. This result is attributable to the fact that the wind curtailment option would be exercised more often in systems with Profile 1 than in those with Profile 2, as demonstrated in the previous subsection. At 10% and 20% penetration levels, the value of wind power in systems with wind Profile 1 is higher than that in systems having Profile 2. This result is attributable to Profile 2 having an almost opposite daily pattern of demand. This criterion reduces the fuel savings from marginal units as high wind production coincides with generators having low fuel costs and vice versa.

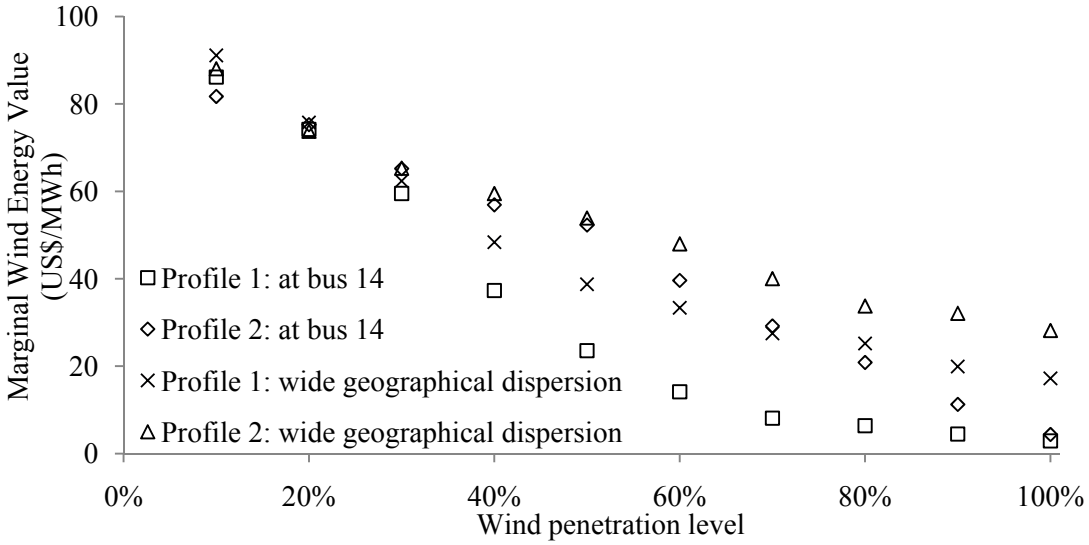

Figure 7-15: Marginal value of wind energy as a function of wind power penetration level

The effect of geographical dispersion scenarios on the marginal value of wind power is evident in all penetration level scenarios higher than 20% and 40% for Profile 1 and Profile 2, respectively. The value of wind power in systems with a wide geographical dispersion of wind power facilities is higher than that of those in which wind power is concentrated in one zone. For example, for wind Profile 1 and a

penetration level of 80%, the marginal value of wind energy for the former scenario is about 2.5 times that of the latter. This result is expected because of the limited transmission capacity and higher wind power forecasting error associated with concentrating power facilities within one zone.

7.5 Summary

The intermittent nature of wind power requires careful assessment of wind power impacts on system operations. Recent studies show that these impacts are system-specific, and conclude that the dominant wind integration cost component is related to the unit commitment time frame. This chapter investigates the impacts of different wind power profiles on fuel savings, startup costs, total operational cost, and wind power curtailments at different wind power penetration levels. A linear mixed-integer unit commitment model was formulated in a GAMS environment and tested on a modified IEEE-RTS generation system.

Two wind profile scenarios are considered: wind Profile 1 and wind Profile 2. Synoptic and diurnal effects of wind speed variations are dominant in the former and the latter, respectively. Two geographical dispersion scenarios of wind power facilities are studied. In the first, a wide geographical dispersion of wind power facilities is presumed. In the second, all wind power facilities are considered connected to Bus 14. Simulation results show that, for both profiles, fuel savings increase linearly up to a penetration level of 20%, after which, the rate of increase decreases continously due to the decrease in the fuel costs of marginal units, the execution of the wind curtailment option, and the increase in spinning reserve requirements associated with wind uncertainty. Beyond the 20% penetration level, Profile 2 yields more savings than Profile 1 because the wind curtailment option is exercised more often in systems with the latter than in those with the former. For the same reason, the value of wind power in systems with wind Profile 2 is higher than that in systems having Profile 1 for all penetration levels higher that 20%. At 10% and 20% penetration levels, the value of wind power in systems with wind Profile 1 is higher than that in systems having Profile 2 due to the fact that Profile 2 has an almost opposite daily pattern of the demand. In addition, a wide geographical dispersion of wind power facilities has a positive impact on the value of wind power in two aspects: 1) reducing the amount of curtailed wind energy attributed to network constraints; 2) reducing wind forecasting error and associated spinning reserve requirements. Finally, the results show that, in general, systems with wind Profile 2 experience higher start-up costs than systems having Profile 1. This result is attributable mainly to wind Profile 1 experiencing higher curtailments, which, in turn, results in a smoother accommodated wind power that better coincides with daily peak demand.

Chapter 8
Conclusions

8.1 Summary and Conclusions

This thesis is devoted to facilitating the integration of wind-based DG into the system without jeopardizing the system's economics, security or efficiency. To achieve this goal, this work is tackling wind power from three different perspectives: those of the policymaker, the investor and the system operator. From the policymaker perspective, the importance of policies in promoting wind power is investigated. Two case studies were presented, those of Ontario and Oman, in chapters 3 and 4 respectively. From an investor perspective, the thesis focuses on optimizing turbine-site matching to achieve more economical wind power. In this regard, a new *CF* model and a new Turbine-Site Matching Index (*TSMI*) were developed in chapters 5 and 6, respectively. Finally, in chapter 7 the effect of high penetration levels of wind power was investigated from a system operator perspective. These chapters' summaries are presented below.

In chapter 3, a thorough techno-economic evaluation of wind-based DG projects is presented to demonstrate the role of Ontario's taxation and incentive policies in the economic viability of investments under Ontario's SOP. The case study presented in this chapter considered different wind turbines and mean wind speed scenarios. The net capacity factor of each turbine for different wind speed scenarios was calculated. This chapter considers the effects of provincial income taxes, capital cost allowance (CCA), property taxes, and federal incentives to wind power production. It can be concluded that property taxes in Ontario do not have a major impact on the viability of wind project, compared to other factors under the current policy. However, income taxes result in a 13% decrease of the project' NPV, for the base-case parameters. Currently, incentives are considered taxable in Ontario. The project's economic viability can be improved considering non-taxable incentives. Additionally, the 50% accelerated declining balance depreciation rate used for the CCA calculation in Ontario delays tax payment compared to using the SL method, and improves the project's economic viability tremendously.

In chapter 4, the thesis proposes the utilization of wind power as a source of electricity in a new city being developed in the Duqm area of Oman. The investment in wind power is in line with the country's long-term development strategy, which aims for sustainable development. Recent wind speed measurements taken at the Duqm meteorological station are analyzed to obtain the annual and monthly wind probability distribution profiles represented by Weibull parameters. As Oman has no utility-scale

wind power projects, a techno-economic evaluation case study is presented to demonstrate the project's viability. The 5-turbine project case study shows that the COE ranges between US$0.05 and US$0.08 per kWh. This cost is higher than the average COE of the MIS (about US$0.024 per kWh) because of the low prices of domestically available natural gas (US$1.5 per MMBtu). However, when the actual high prices of natural gas in international markets are used to calculate the COE, wind power becomes cheaper. A feed-in tariff and capital cost allowance policies are recommended to facilitate investments in this sector.

In chapter 5, a generic formulation for wind turbine capacity factor (CF) based on wind speed characteristics at any site and the performance curve parameters of any pitch-regulated wind turbine is presented. The accuracy of the proposed CF model, which is based on the most accurate generic power curve model available in open literature, over that of the existing one, is verified using measured data. Illustrative case studies and parameter sensitivity analysis are presented to test the effectiveness of the model in turbine-site matching applications. The results demonstrate that using the proposed model leads to more accurate ranking of wind turbine candidates for installation at potential sites.

Using the CF as the sole basis for turbine-site matching produces results that are biased towards higher towers, but do not include the associated costs. Therefore, chapter 6 presents a new formulation for the turbine-site matching problem by proposing a new Turbine-Site Matching Index ($TSMI$). The $TSMI$ is based on formulation for CF that does include turbine tower height. In addition, the index includes the effects of turbine size (installed capacity) and tower height on the initial capital cost of wind turbines. The effectiveness and the applicability of the proposed $TSMI$ and CF are illustrated using case studies. Results show that for each turbine, there exists an optimal tower height, at which the value of the $TSMI$ is at its maximum. The results reveal that higher tower heights are not always desirable for optimizing the turbine-site matching solution.

Chapter 7 investigates the effects of different temporal wind profiles on the scheduling costs of thermal generation units. Two temporal wind variation scenarios are considered: Profile 1 and Profile 2. Synoptic and diurnal effects of wind speed variations are dominant in the former and the latter, respectively. Two geographical dispersion scenarios of wind power facilities are studied. In the first, a wide geographical dispersion of wind power facilities is presumed. In the second, all wind power facilities are considered connected at one bus, which represents one zone. To simulate the wind power impacts, a linear mixed-integer unit commitment problem is formulated in a GAMS environment. The uncertainty associated with wind power is represented using a deterministic equivalent of a chance constrained formulation. The

simulation results include the impacts on fuel savings, startup costs, total operational cost, and wind power curtailments at different wind power penetration levels.

8.2 Contributions

The main contributions of this thesis can be highlighted as follows:

- A thorough techno-economic study about the role of policies (taxes & incentives) in the economic viability of wind-based DG in Ontario under the SOP is presented.
- The thesis proposed the use of wind power in Duqm area in Oman and presents a model for wind characteristics there. To facilitate investments in this sector, wind power support policies are proposed.
- A new generic *CF* model that is based on wind profile and turbine characteristics has been presented. The thesis demonstrates that using *CMWS* instead of *MWS* to determine Weibull pdf parameters can results in an overestimation of *CF* and inaccurate design of turbine rated speed.
- The proposed *CF* model is modified to include the tower height effect on wind speed and captured energy. The thesis demonstrates that the existing extrapolation model used to estimate *CF* values at different altitudes is inaccurate and results in an overestimation of wind potential.
- A novel formulation of the turbine-site matching problem is presented through a new Turbine-Site Matching Index (*TSMI*). The *TSMI* is based on a *CF* model that includes the effect of tower height and a model for the Initial Capital Cost (ICC) that includes the effect turbine tower height and power rating.
- The thesis investigates the effect of temporal wind profiles on the scheduling costs of thermal units.

8.3 Directions for Future Work

In continuation of this work, the following subjects are suggested for future studies:

- The inclusion of a more detailed ICC function, which could include turbine capacity, rotor area, and tower height, in the proposed *TSMI*. This index can then be used for the turbine-site matching problem more effectively.
- As the penetration level of wind power increases, wind power curtailments increase which in turn deteriorates its value. Demand Response (DR) could have a high potential in reducing wind power

curtailments; therefore, facilitating more integration of wind power. Initial works in this direction has been conducted and presented in Appendix A.

- Another resource that could facilitate accommodating more wind power in the system is the use of energy storage systems. Optimal operation strategy of wind-storage hybrid system can reduce wind curtailments and increase the benefits of wind. The storage option could be included in the UC problem formulation by adding pumped hydro and/or compressed air energy storage-related constraints.
- As demonstrated in chapter 7, the value of wind power decreases as penetration level increases. From a policy maker perspective, it is important to estimate the optimal amount of wind power in a system. To find this amount, local wind power temporal profile, demand response options, and energy storage are required.

Appendix A: Demand Response in Electricity Markets[10]

A1. Introduction

For many reasons, electric utilities and power network companies have been forced to restructure their operations from vertically integrated mechanisms to open market systems [17]. With the restructuring and deregulation of the electricity supply industry, the philosophy of operating the system was also changed. The traditional approach was to supply all power demands whenever they occurred, however, the new philosophy states that the system will be most efficient if fluctuations in demand are kept as small as possible.

Reliable operation of the electricity system necessitates a perfect balance between supply and demand in real time. This balance is not easy to achieve given that both supply and demand levels can change rapidly and unexpectedly for many reasons, such as generation unit forced outages, transmission and distribution line outages, and sudden load changes. The electricity system infrastructure is highly capital-intensive; demand side (load) response is one of the cheaper resources available for operating the system according to the new philosophy.

This work presents an overview of new flexible resources for operating a reliable system. The work starts with defining the DR and how electricity consumers can be responsive. Highlighting different DR programs follows, including classical, new market-based and dynamic pricing scenarios. Potential cost savings and benefits related to different market components are also discussed. After that, measuring indices that are used to assess program success are presented. In addition, the effect of DR on electricity prices is simulated. The work is concluded with a few selected utilities' experience with DR programs.

A2. Definition and Classification

A2.1 Definition

Demand Response can be defined as the changes in electricity usage by end-use customers from their normal consumption patterns in response to changes in the price of electricity over time. Further, DR can

[10] Some parts of this work have been published in:

[22] M. H. Albadi and E. F. El-Saadany, "A summary of demand response in electricity markets," *Electric Power Systems Research,* vol. 78, pp. 1989–1996, 2008.

An earlier version appeared in:

[23] M. H. Albadi and E. F. El-Saadany, "Demand Response in Electricity Markets: An Overview," in *IEEE PES 2007 General Meeting (GM' 07)*, Tampa, FL, USA, 2007, pp. 1-5.

be also defined as the incentive payments designed to induce lower electricity use at times of high wholesale market prices or when system reliability is jeopardized [157]. DR includes all intentional electricity consumption pattern modifications by end-use customers that are intended to alter the timing, level of instantaneous demand, or total electricity consumption [158].

A2.2 Customer Response

There are three general actions by which a customer response can be achieved [157]. Each of these actions involves cost and measures taken by the customer. First, customers can reduce their electricity usage during critical peak periods when prices are high without changing their consumption pattern during other periods. This option involves a temporary loss of comfort. This response is achieved, for instance, when thermostat settings of heaters or air conditioners are temporary changed [159, 160]. Secondly, customers may respond to high electricity prices by shifting some of their peak demand operations to off-peak periods, as an example, they shift some household activities (e.g., dishwashers, pool pumps) to off-peak periods. The residential customer in this case will bear no loss and will incur no cost. However, this will not be the case if an industrial customer decides to reschedule some activities and rescheduling costs to make up for lost services are incurred. The third type of customer response is by using onsite generation – customer-owned DG [161, 162]. Customers who generate their own power may experience no or very little change in their electricity usage pattern; however, from the utility's perspective, electricity use patterns will change significantly, and demand will appear to be smaller.

A2.3 Program Classification

A classification of different DR programs is presented in Figure A1. DR programs can be classified into two main categories: Incentive Based Programs (IBP) and Price Based Programs (PBP) [157]. Some articles named these categories as system-led and market-led, emergency-based and economic-based, or stability-based and economic-based DR programs [158, 163, 164]. IBP are further divided into classical programs and market-based programs. Classical IBP include Direct Load Control programs and Interruptible/Curtailable programs. Market-based IBP include Emergency DR programs, Demand Bidding, Capacity Market, and the Ancillary services market. In classical IBP, participating customers receive participation payments, usually as a bill credit or discount rate, for their participation in the programs. In market based programs, participants are rewarded with money for their performance, depending on the amount of load reduction during critical conditions.

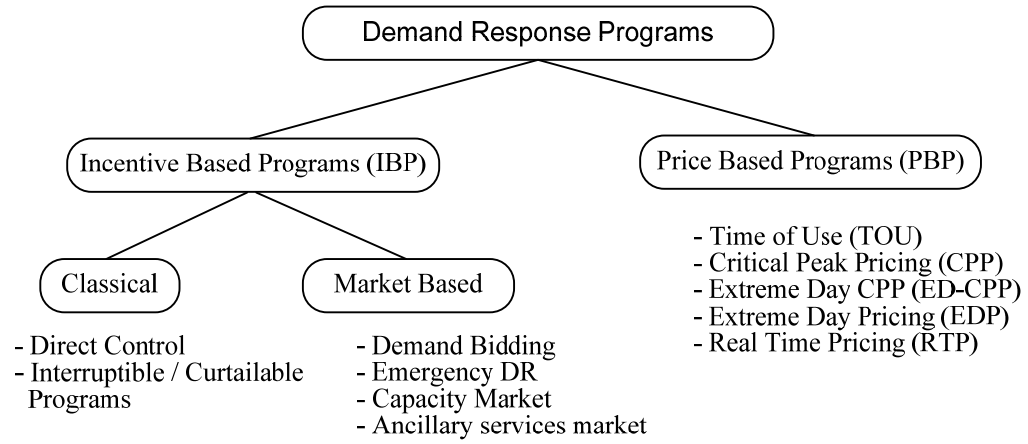

Figure A1: Classification of DR programs

- Classical IBP

In Direct Load Control programs, utilities have the ability to remotely shut down participant equipment on short notice. Typical remotely-controlled equipment includes air conditioners and water heaters. This kind of program is of interest mainly to residential customers and small commercial customers. As with Direct Load Control programs, customers participating in Interruptible/Curtailable Programs receive upfront incentive payments or rate discounts. Participants are asked to reduce their load to predefined values. Participants who do not respond can face penalties, depending on the program terms and conditions.

- Market-based IBP

Demand Bidding (also called Buyback) programs are those in which consumers bid on specific load reductions in the electricity wholesale market. A bid is accepted if it is less than the market price. When a bid is accepted, the customer must curtail his load by the amount specified in the bid or face penalties. On the other hand, in Emergency DR Programs, participating customers are paid incentives for measured load reductions during emergency conditions [157]. Furthermore, Capacity Market Programs are offered to customers who can commit to providing pre-specified load reductions when system contingencies arise [157]. Participants usually receive a day-ahead notice of events and are penalized if they do not respond to calls for load reduction. Ancillary services market programs allow customers to bid on load curtailment in the spot market as operating reserve. When bids are accepted, participants are paid the spot market

price for committing to be on standby and are paid the spot market energy price if load curtailment is required [157].

- Price Based Programs (PBP)

PBP programs are based on dynamic pricing rates in which electricity tariffs are not flat; the rates fluctuate following the real time cost of electricity. The ultimate objective of these programs is to flatten the demand curve by offering a high price during peak periods and lower prices during off-peak periods. These rates include the Time of Use (TOU) rate, Critical Peak Pricing (CPP), Extreme Day Pricing (EDP), Extreme Day CPP (ED-CPP), and Real Time Pricing (RTP). The basic type of PBP is the TOU rates, which are the rates of electricity price per unit consumption that differ in different blocks of time. The rate during peak periods is higher than the rate during off-peak periods. The simplest TOU rate has two time blocks; the peak and the off-peak. The rate design attempts to reflect the average cost of electricity during different periods. A TOU rate design process is described in [165]. CPP rates include a pre-specified higher electricity usage price superimposed on TOU rates or normal flat rates. CPP prices are used during contingencies or high wholesale electricity prices for a limited number of days or hours per year [157, 164]. On the other hand, EDP is similar to CPP in having a higher price for electricity and differs from CPP in the fact that the price is in effect for the whole 24 hours of the extreme day, which is unknown until a day-ahead [166]. Furthermore, in ED-CPP rates, CPP rates for peak and off-peak periods are called during extreme days. However, a flat rate is used for the other days [166]. RTP are programs in which customers are charged hourly fluctuating prices reflecting the real cost of electricity in the wholesale market. RTP customers are informed about the prices on a day-ahead or hour-ahead basis. Many economists are convinced that RTP programs are the most direct and efficient DR programs suitable for competitive electricity markets and should be the focus of policymakers [167].

A3. DR Benefits and Costs

This section covers and discusses both potential benefits expected from DR programs and the associated costs.

A3.1 DR Benefits

Figure A2 summarizes the benefits associated with DR, which fall into four main categories: participant, market-wide, reliability, and market performance benefits.

Customers participating in DR programs can expect savings in electricity bills if they reduce their electricity usage during peak periods [157, 163, 168]. In fact, some participants may experience savings even if they do not change their consumption pattern, if their normal consumption during high price peak periods is lower than their class average [165]. Some customers might be able to increase their total energy consumption without having to pay more money by operating more off-peak equipment. Moreover, participants in classical IBP are entitled to receive incentive payments for their participation, while market-based IBP customers will receive payments according to their performance.

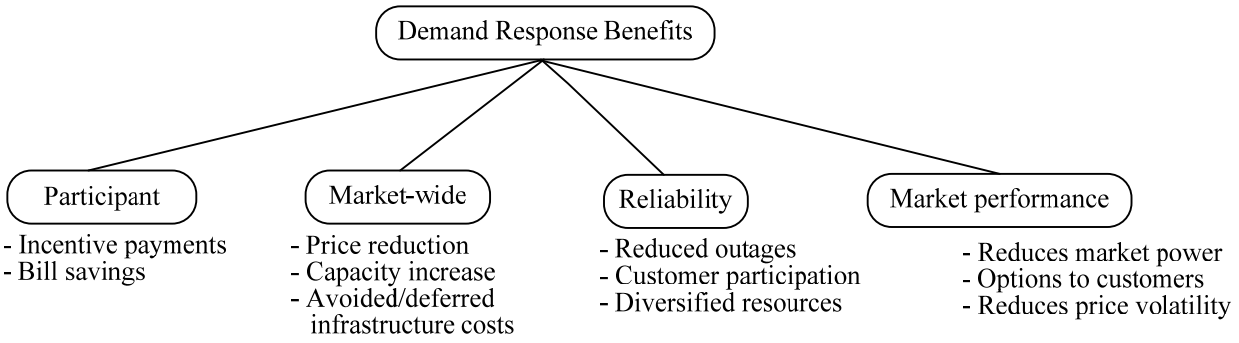

Figure A2: Benefits associated with DR

The benefits of DR programs are not only for program participants; some are market-wide. An overall electricity price reduction is expected eventually because of a more efficient utilization of the available infrastructure, as in, for example, the reduction of demand from expensive electricity generating units. Moreover, DR programs can increase short term capacity using market-based programs, which in turn, results in an avoided or deferred capacity costs. The cascaded impact of DR programs includes avoided or deferred need for distribution and transmission infrastructure enforcements and upgrades [157, 158, 163]. All of the avoided or deferred costs will be reflected in the price of electricity for all electricity consumers (DR programs participants and non-participants).

Reliability benefits can be considered as one of the market- wide benefits because they affect all market participants. Because of their importance, we have considered reliability benefits to be a category by itself. By having a well designed DR program, participants have the opportunity to help in reducing the risk of outages. Simultaneously and as a consequence, participants are reducing their own risk of being exposed to forced outages and electricity interruption. On the other hand, the operator will have more

options and resources to maintain system reliability, thus reducing forced outages and their consequences [169].

The last category of DR program benefits is improving electricity market performance [170]. DR program participants have more choices in the market even when retail competition is not available. Consumers can manage their consumption since they have the opportunity to affect the market, particularly with the market-based programs and dynamic pricing programs. In fact, this was the prime driver for many utilities to offer DR programs, particularly for large consumers [171]. Another important market improvement is the reduction of price volatility in the spot market. Demand responsiveness reduces the ability of main market players to exercise power in the market [172]. It has been reported that a small reduction of demand (5%) could have resulted in a 50% price reduction during the California electricity crisis in 2000-2001 [173]. This phenomenon is due to the fact that generation cost increases exponentially near maximum generation capacity. A small reduction in demand will result in a big reduction in generation cost and, in turn, a reduction in electricity price, as shown in Figure A3. In this example, the original demand curve is represented by a vertical line because it is assumed that the system is without DR programs. DR programs introduce a negative slope on the original demand curve, leading to a small reduction in demand and a huge reduction in price. Although some people might argue about environmental benefits associated with DR programs, those benefits are evident [165]. Environmental benefits of DR programs are numerous and include better land utilization as a result of avoided/deferred new electricity infrastructure such as generation units and transmission/distribution lines, air and water quality improvement as a result of efficient use of resources, and reduction of natural resources depletion [157].

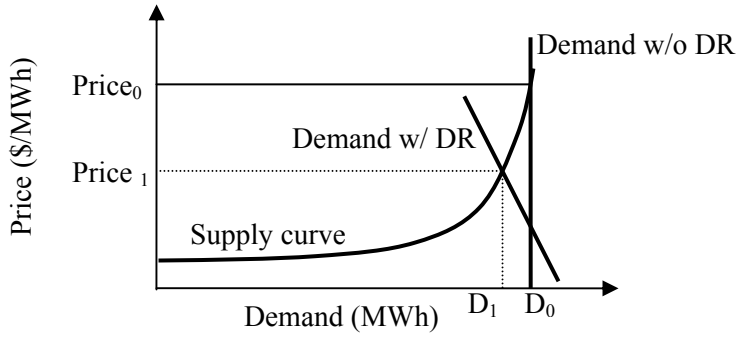

Figure A3: Simplified effect of DR on electricity market prices

A3.2 DR Costs

Any DR program involves different kind of costs; Figure A4 shows a classification of DR program costs, where both DR program owners and participants incur initial and running costs [157].

The program participant might need to install some enabling technologies to participate in a DR program: smart thermostats, peak load controls, energy management systems, and onsite generation units. A response plan or strategy needs to be established so that it can be implemented in case of an event. These initial costs are usually paid by the participant; however, technical assistance should be provided by the program.

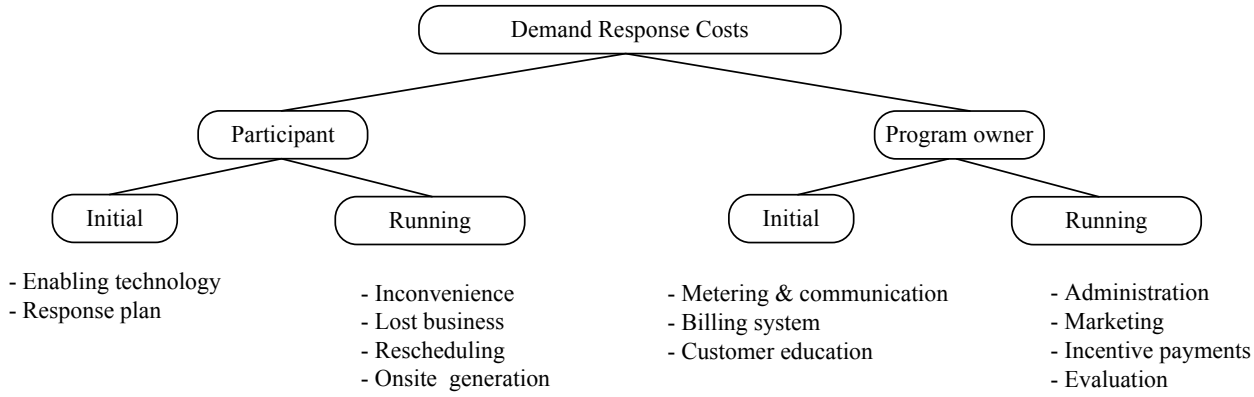

Figure A4: Classification of DR costs

Participants running costs are those associated with events. Depending on the response plan, these costs may vary. A reduction of comfort may result if a customer decides to reset the thermostat, which results in customer inconvenience that is difficult to quantify. Other event-relevant costs are easier to quantify, for instance, lost business or rescheduling of industrial processes or activities. If a participating customer decides to use a backup onsite generation unit, fuel and maintenance costs need to be considered. The program owner has to take care of initial and running systemwide costs. Most DR programs involve metering and communication costs as initial costs. Utilities need to install advanced metering systems to measure, store and, transmit energy usage at required intervals, e.g., hourly readings for real time pricings. Running costs of DR programs include administration and management cost of the program. As well, incentive payments should be considered as part of the running costs of IBP. Upgrading the billing system is necessary before most DR programs are deployed, especially PBP for enabling the system to deal with time varying cost of electricity.

Another important cost component before deploying any DR program is educating eligible customers about the potential benefits of the program. Different DR program choices need to be explained to potential participants and possible demand response strategies need to be defined. A successful DR program depends heavily on customer education. Continuous marketing is important to attract new participants. Further, a continuous evaluation and assessment of DR programs is important to develop a better approach for reaching the ultimate objectives of the programs [157].

A4. DR Measurement and Simulation

A4.1 DR Measurement

The ultimate objective of DR programs is to reduce peak demand. Therefore, actual peak demand reduction is used as an indication of how successful a DR program is and to compare DR programs in similar situations. To normalize this indicator, the percentage peak demand reduction is used. Percentage and actual peak demand reduction are used to evaluate IBP.

In addition to peak load reduction, the performance of dynamic pricing programs is measured using demand price elasticity which represents the sensitivity of customer demand to the price of electricity. This can be found by calculating the ratio of the percent change in demand to the percent change in price [158, 173, 174]. Usually, the price-demand curve of any commodity is not linear. Therefore, elasticity is linearized around the initial price-demand balance ($Quantity_o$, $Price_o$); as seen in Figure A5.

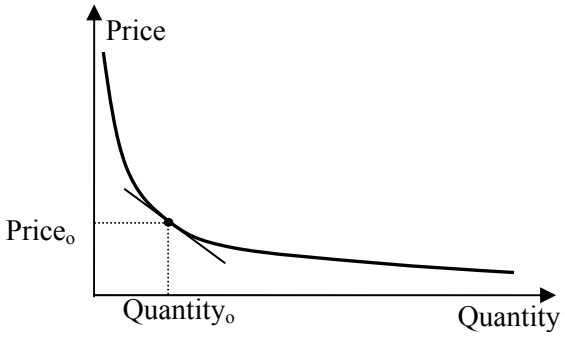

Figure A5: Price elasticity graphical definition

The elasticity of a substitution measures the rate at which the customer substitutes off-peak electricity consumption for peak usage in response to a change in the ratio of peak to off-peak prices [158]. This kind of elasticity is important in TOU and CPP pricing programs. In [175], elasticity is divided into self-

elasticity and cross-elasticity. Self-elasticity measures the demand reduction in a certain time interval due to the price of that interval. Cross-elasticity measures the effect of the price of a certain time interval on electricity consumption during another interval.

Two types of customers are described in [176]: long-range (LR) and short-range (SR) customers. LR customers maximize long term benefits by deciding their demands while considering all pricing periods. SR customers set their demand considering the current pricing period only. However, real world (RW) consumers, described in [175], consider both current prices and the prices of one step into the future.

As Figure A6 suggests, elasticity is used in conjunction with expected price to modify expected demand; consequently, demand and prices will be reduced if prices are above the equilibrium point (p_0,q_0); see Figure A5. The equilibrium point is defined as price and demand of the normal case. In this analysis, one equilibrium point is assumed for each period.

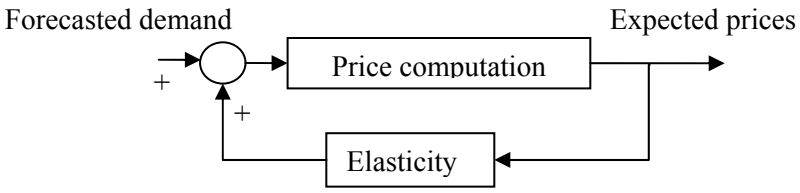

Figure A6: Effect of price elasticity in price computation

A4.2 Market Simulation

In this analysis, a single-sided uniform market price is considered in which the supply-side submits bids for supplying power to the market operator when the market operator has a forecast of demand [17]. These bids reflect generator cost functions. The operator announces the expected prices for the next 24 hours. These prices act as guidelines for customers to respond to in real time, depending on their elasticity and expected prices. This DR is very beneficial as it can reduce market prices as well as costs. The process used for simulating DR is shown in Figure A7 [177].

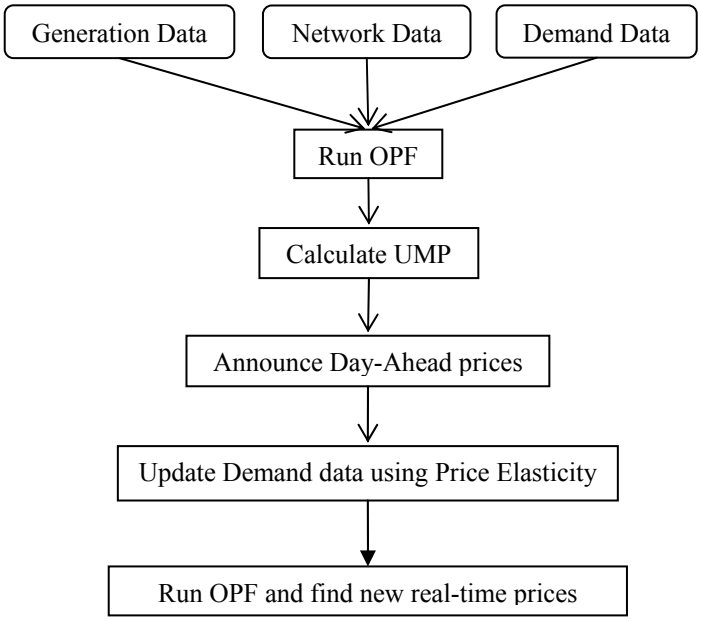

Figure A7: Simulation flow chart

A4.2.1 Optimal Power Flow Formulation

An Optimal Power Flow (OPF) code was developed in a GAMS environment to simulate market prices. The objective function of the OPF is to minimize the total cost of generation for social welfare maximization [17].

$$\min J = \sum_{i=1}^{NG} a_i {P_i}^2 + b_i P_i + c_i \qquad \text{(A-1)}$$

where J is the total generation costs; P_i is the power output of generator i; a_i, b_i, and c_i are the cost coefficients of generator i, and NG is the number of generators. Generators are assumed to be bidding their true cost of generation. The minimization objective function has the following constraints:

1. Power balance equations

$$P_k - PD_k = \sum_j |V_k||V_j|Y_{kj}\cos(\vartheta_{kj} + \delta_j - \delta_k) \qquad \text{(A-2)}$$

$$Q_k - QD_k = \sum_j |V_k||V_j|Y_{kj} sin\,(\vartheta_{kj} + \delta_j - \delta_k) \quad \text{(A-3)}$$

where V_k is the voltage at bus k; δ is the angle associated with the voltage at relevant buses; Y_{kj} is the element of the Y-bus admittance matrix; θ_{kj} is the angle associated with Y_{kj}; P_k and Q_k are real and reactive power generation at bus k, respectively. PD_k and QD_k are real and reactive power demand at bus k, respectively.

2. Generation limits

$$P_{i,min} \leq P_i \leq P_{i,max} \quad \text{(A-4)}$$

$$Q_{i,min} \leq Q_i \leq Q_{i,max} \quad \text{(A-5)}$$

3. Voltage limits

$$V_{k,min} \leq V_k \leq V_{k,max}\ \forall\ k \in 1\ to\ NL \quad \text{(A-6)}$$

$$|V_k| = const\ \ \forall\ k \in 1\ to\ NG \quad \text{(A-7)}$$

NL and *NG* are the number of load buses and generator buses, respectively. The voltages at load buses are bounded between minimum and maximum values; whereas the voltages at generation buses are kept at constant values.

There are two types of market price formulations: the Locational Marginal Prices (LMP) and the Uniform Market Price (UMP). In an LMP formulation, electricity prices are location dependent. The market price at each bus is represented by the Lagrangian multiplier β_k of the real power balance constraint at that bus. In an UMP formulation, the market price is the highest value of the bus incremental cost obtained by solving the above model:

$$MP \geq \beta_k \quad \text{(A-8)}$$

where *MP* represents the uniform electricity market price; β_k is the incremental cost of generation at bus k.

A4.2.2 Simulation Results

A six-bus system, presented in [17], was used for this simulation. The system is presented in Figure A8, and Tables A1 and A2 show the system data.

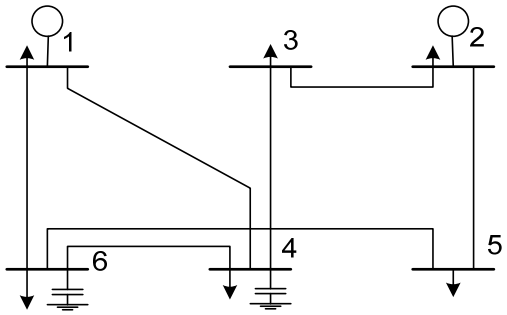

Figure A8: Six-bus test system

Table A1: Line Data

Line	R_{kj} *(p.u.)*	X_{kj} *(p.u.)*	$B_{kj}/2$ *(p.u.)*
1-4	0.0662	0.1804	0.003
1-6	0.0945	0.2987	0.005
2-3	0.0210	0.1097	0.004
2-5	0.0824	0.2732	0.004
3-4	0.1070	0.3185	0.005
4-6	0.0639	0.1792	0.001
5-6	0.0340	0.0980	0.004

Table A2: Bus Data (Base=100MVA)

	Demand (p.u.)		*Generation limits (p.u.)*			
#	*PD*	*QD*	P_{max}	P_{min}	Q_{max}	Q_{min}
1	0.73125	0.1950	5.0	1.0	3.0	-0.2
2	0.92625	0.2925	2.5	0.5	1.5	-0.2
3	0.78000	0.3900	0.0	0.0	0.0	0.0
4	1.12125	0.3120	0.0	0.0	0.0	0.0
5	1.26750	0.34125	0.0	0.0	0.0	0.0
6	0.67375	0.24375	0.0	0.0	0.0	0.0

The generation cost function ($/MWh) of the two generation units is represented by the quadratic functions: $C_1 = {P_1}^2 + 8.5P_1 + 5 \; and \; C_2 = 3.4{P_2}^2 + 25.5P_1 + 9$

A Load Scaling Factor (LSF) was used to represent load variation. Simulation results of the base-case are shown in Figure A9. The equilibrium point during each interval is the demand and the price of the base-case scenario. As shown in Figure A9, 12 price intervals were considered. The figure shows clearly that electricity prices are sensitive to increase in demand.

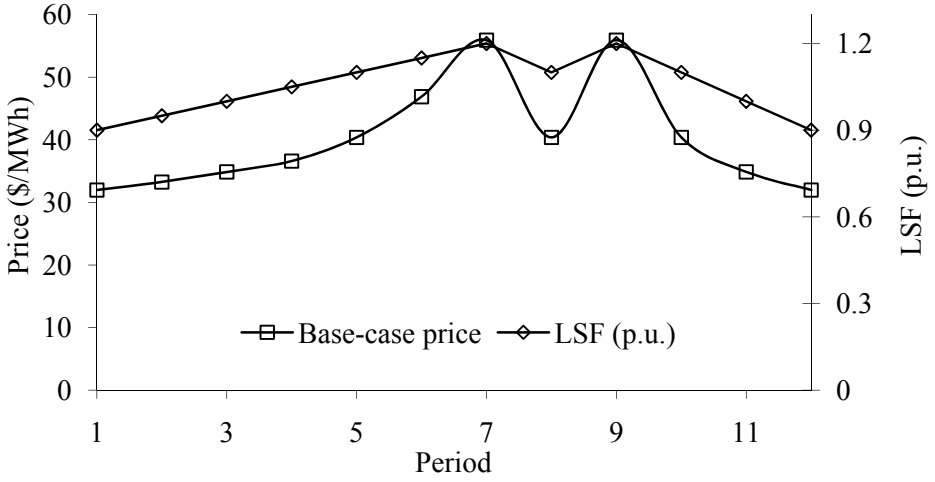

Figure A9: Base-case simulation results

A contingency in the system was introduced by removing line 4-6 from the network data. Obviously, this contingency causes a large increase in market price, with inelastic demand, especially during peak periods (Figure A10). These high prices will be announced 24 hours ahead. Note that we assume that the operator is aware that such a contingency will happen the next day and will last for the whole day.

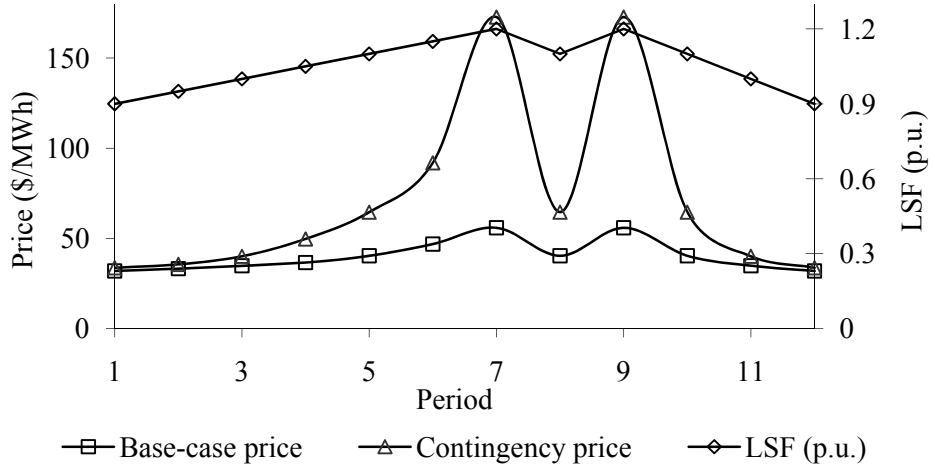

Figure A10: Comparison between base-case and contingency case prices

To illustrate the effect of demand elasticity, loads at all buses are assumed to have the same constant self-elasticity of -0.1, which means that a 100% change in price will reduce the load by 10%. All cross-

elasticities are neglected, which means that the customers are of the SR type. After calculating the change in LSF, the OPF model is solved, and the results are shown in Figure A11.

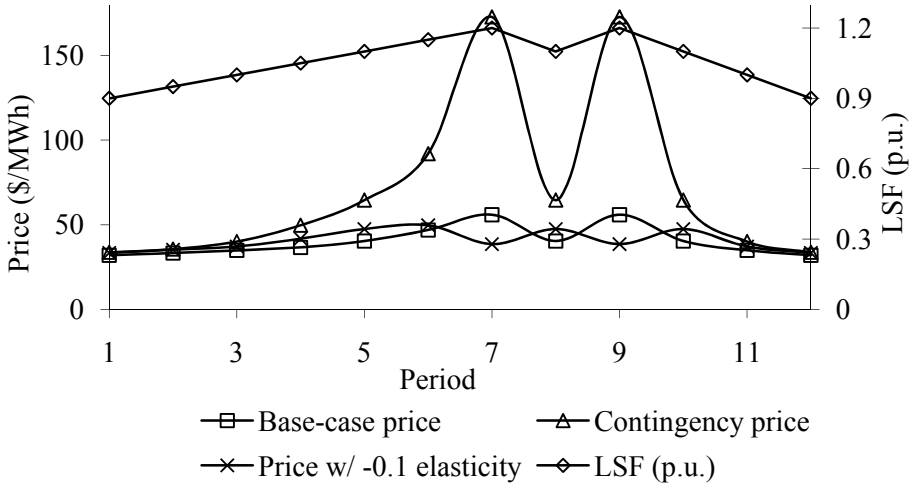

Figure A11: Comparison between base-case, contingency and prices when loads have -0.1 elasticity

It is notable that real prices were reduced below contingency prices. Moreover, due to the assumption that customers react in response to the day-ahead published prices, the very high expected prices of the two peaks were actually reduced even below the base-case prices. However, this will not happen in practice because elasticity is not constant, and it has a lower value during peak periods.

A4. DR Experiences

A4.1 Quantification Studies

Three types of DR quantization studies have been distinguished [157]: illustrative studies, integrated resource planning studies, and program evaluation studies. It has been shown that program evaluation studies revealed much lower benefits than the other two studies. Illustrative studies assume high penetration rates and long term sustained benefits. Similarly, integrated recourse planning studies consider long term benefits. On the other hand, program evaluation studies do not consider long term benefits, and suffer from low penetration rates.

A4.2 Incentive-based Programs

Many utilities in North America and around the globe have experiences with IBP. As an example, NYISO IBP paid out US$ 7.2 million in incentives to more than 14,000 program participants to release 700MW peak capacity in the summer of 2003 [166]. The load curtailment programs were estimated providing reliability benefits of more than US$ 50 million on August 15, 2003 [166]. In general, it was reported that the benefits of these programs exceeded the cost by a factor of 7:1 [166].

A4.2 Price-based Program

TOU pricing is the basic PBP and easiest to implement. Electricite De France (EDF) operates what is probably the most successful example of a TOU pricing program. This program was applied to large industrial customers in 1956 and introduced to residential customers in 1965. Currently, it is estimated that one third of its customers are on TOU pricing [166]. In 1993, EDF introduced a CPP pricing program called Tempo in which the year is divided into three types of days: Tempo Blue, Tempo White, and Tempo Red. 300 days of the year are Tempo Blue, during which time electricity is cheaper than the normal TOU prices. Tempo White days number 43, and are at a slightly higher rate compared to that of normal TOU. Tempo Red days number only 21 and are the most expensive. Customers can discover the color of the next day by several means.

TOU pricing was implemented by many utilities in North America. A CPP experiment implemented in Pennsylvania revealed that the elasticity of substitution ranges from -0.31 to -0.40 [166]. This means that a 100% price increase will correspond to reduction in demand between 31 and 40%. Another experiment in Florida, by the Gulf Power Company, used TOU pricing. Customers were provided with smart thermostats that automatically adjusted the temperature and other loads depending on a price signal. In this program, normal TOU prices were applied 99% of all hours in the year. In the remaining 1% of the hours, the utility had the option of charging a critical peak pricing, more than the normal peak period price. This program resulted in 42% peak demand reduction during critical peak periods [166].

A comprehensive survey of utility experience with RTP was presented in [171]. This survey covered 43 voluntary real time pricing programs offered in 2003. It has been reported that the most common utility motivation behind these programs was customer satisfaction by providing opportunities for bill savings. Encouraging peak demand reduction and load growth comes after the prime motivation. Complying with new regulations was also mentioned as a motivation. It has been reported that penetration rates were low in most programs. In some programs, penetration levels were dropping even lower. The problem of low

program participation was attributed to poor marketing and limited technical assistance provided to help participants managing price volatility. Most RTP participants were large industrial customers and some large institutional ones. This survey concluded that important aspects of required information about price-responsiveness were not available in most programs. In addition, some RTP participants are not price responsive at all. Price responsive customers generally employ on-site generation or simple strategies such as rescheduling. Some of these participants were found to be very sensitive to prices as low as US$0.20/kWh. The programs under study were reported to achieve 12-33% aggregate load reduction across a wide range of prices. Only one program was able to generate a load reduction of more than 1% of the utility system peak [171]. Another case study of the Niagara Mohawk RTP program in New York found that the average substitution elasticity was -0.14 [167].

A5. Summary

DR changes end-use customer electricity consumption patterns from those customers' normal patterns in response to changes in the price of electricity over time, or to incentive payments designed to induce lower electricity use at times of high wholesale market prices, or when system reliability is jeopardized. DR program benefits cover all electricity consumers. DR programs can reduce electricity prices, improve system reliability, and reduce price volatility. To employ DR programs, both participants and program owners incur initial and running costs. The performance of DR programs is measured by peak load reduction and demand elasticity. Although illustrative studies and integrated resource planning studies project more benefits from DR programs, program evaluation studies prove the substantial benefits of these programs. The above case study simulating the effect of elasticity in electricity prices demonstrates the effect of DG programs in cases of system contingency.

Appendix B: New Power Curve Model[11]

Figures B1 to B3 present examples of the power curve of pitch-regulated turbines from three manufacturers [43, 117, 119].

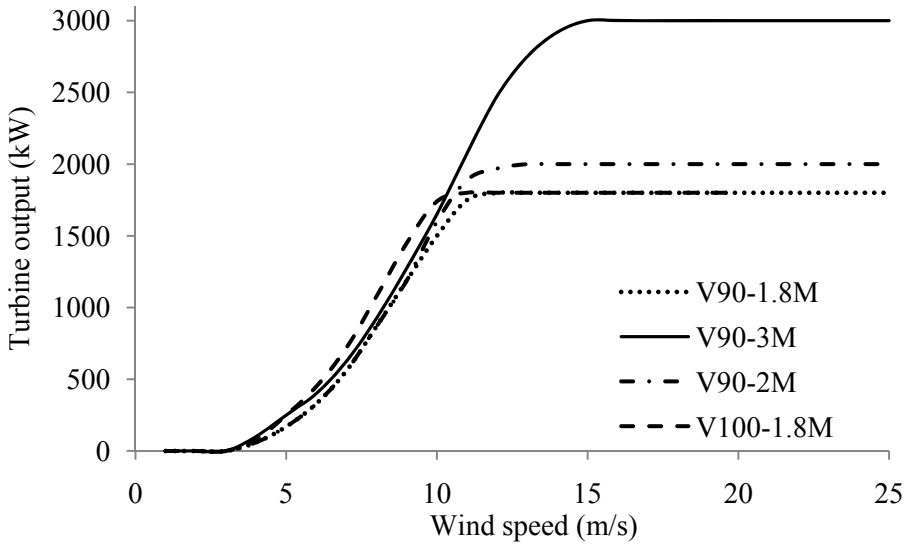

Figure B1: Vestus pitch-regulated turbines [43]

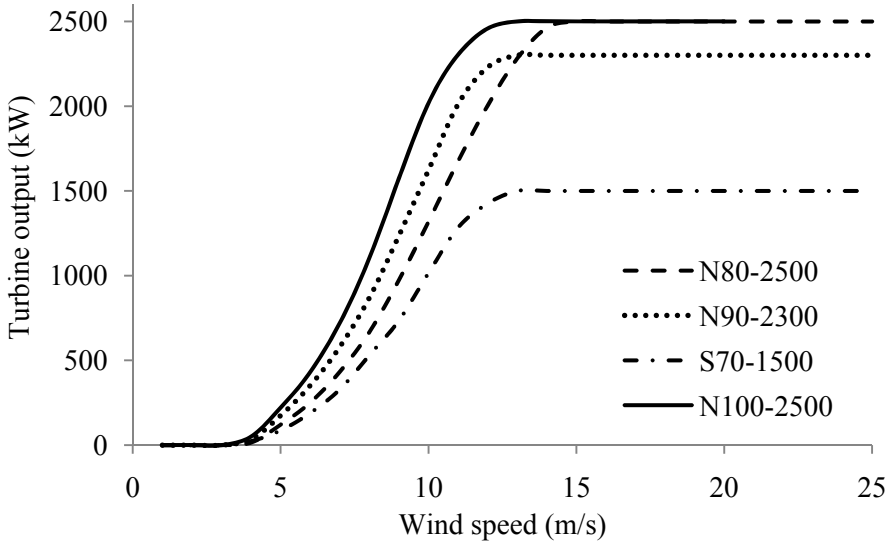

Figure B2: Nordex pitch-regulated turbines [117]

[11] This work has been published in:
[106] M. H. Albadi and E. F. El-Saadany, "Effect of Power Curve Model Accuracy on CF Estimation of Pitch-regulated Turbines," in *CIGRÉ Canada 2009 Conference on Power Systems* Toronto, ON, Canada, 2009, pp. 1-13.

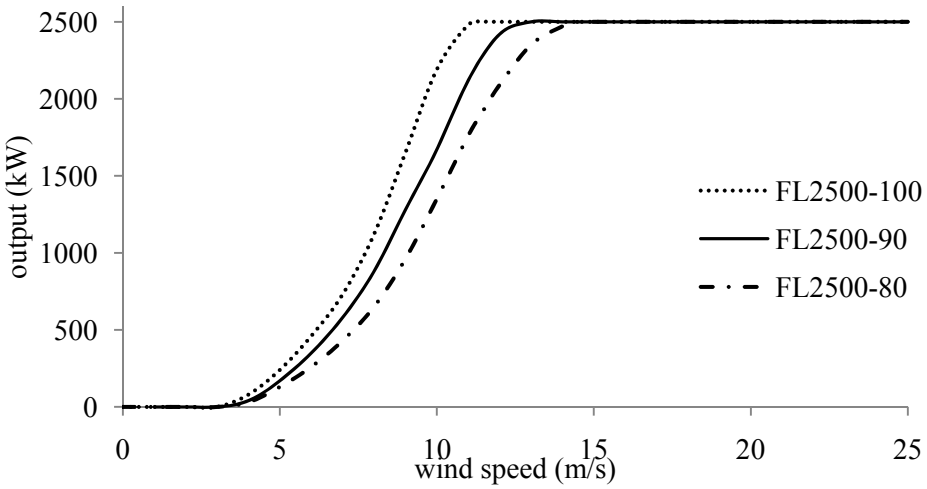

Figure B3: Fuhrlaender pitch-regulated turbines [119]

Similar to Figure 5-1, all turbine curves show their point of inflection in the second half of the ascending segment. This point is attributable to the decrease in turbine efficiency after it has reached its maximum value. Because none of the existing power curve models consider this property, all of them underestimate the power curve in the second half of the ascending segment.

For a more accurate representation of the ascending segment of the power curve, a fourth order polynomial function is proposed; please refer to equation (5-7). The coefficients, a_0 to a_4, of the polynomial function are obtained by solving the following equations:

$$\begin{gathered} P_e(V_c) = 0 \\ P_e(V_r) = 1 \\ P_e(V_1) = 0.03 \\ P_e(V_2) = 0.4 \\ P_e(V_3) = 0.75 \\ P_e(V_4) = 0.97 \end{gathered} \tag{8-1}$$

where

$$\begin{aligned} V_1 &= V_c + 0.1(V_r - V_c) \\ V_2 &= V_c + 0.5(V_r - V_c) \\ V_3 &= V_c + 0.75(V_r - V_c) \\ V_4 &= V_c + 0.9(V_r - V_c) \end{aligned}$$

As the coefficients of this model are based on a general estimation of turbine output at four wind speeds, they can be further tuned to obtain a better fit of turbine data from a certain manufacturer. Normalized turbine curves for different cut-in and nominal speeds are presented in Table B1. An example of the

proposed power curve model is presented in Figure B4, and a comparison of the proposed model and Quadratic model 2 for turbines with V_c=3 m/s and V_r=13m/s is presented in Figure B5.

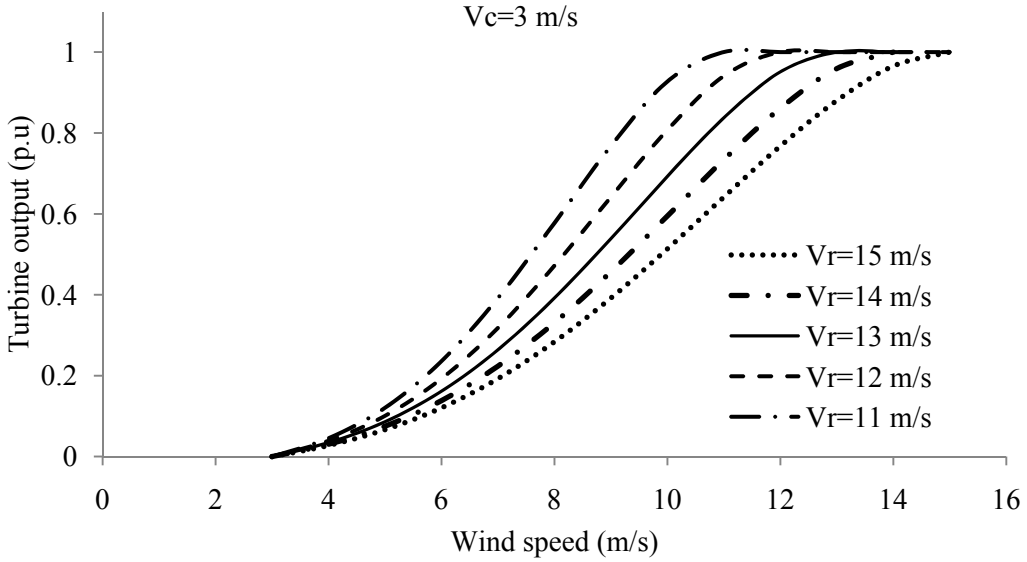

Figure B4: Proposed model when the cut-in speed is 3 m/s and different nominal speeds

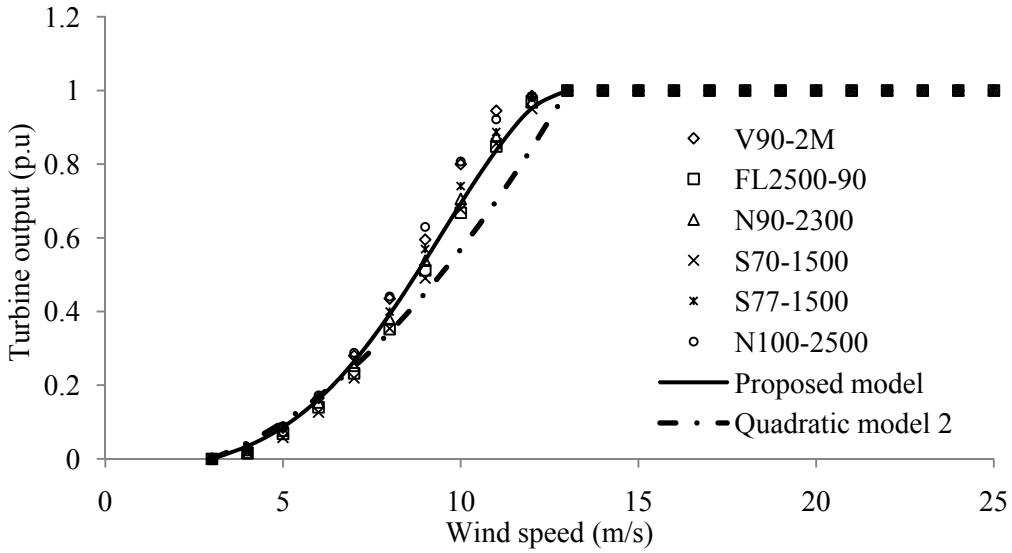

Figure B5: Proposed model versus Quadratic model 2 for turbines with V_c=3 m/s and V_r=13m/s

From Figure B5, one can conclude that although the power curve in the ascending segment is turbine specific, the proposed power curve model represents manufacturer data better than Quadratic model 2, which is the best generic model available in open literature. For V90-1.8 turbine data, presented in Table 5-1, the error in annual energy estimation of the proposed model is about -0.3%.

Table B1: Normalized turbine curves

V_c	V_r	Wind speed	2	3	4	5	6	7	8	9	10	11	12	13	14	15
2	11		0	0.0391	0.1006	0.1926	0.318	0.4718	0.6416	0.8073	0.9410	1	1	1	1	1
2	12		0	0.0343	0.0861	0.1615	0.264	0.3919	0.5388	0.6929	0.8376	0.9513	1		1	1
2	13		0	0.0305	0.0751	0.1383	0.2236	0.3309	0.4569	0.5947	0.7341	0.8613	0.9592	1	1	1
2	14		0	0.0275	0.0665	0.1205	0.1926	0.2836	0.3919	0.5134	0.6416	0.7677	0.8802	0.9654	1	1
2	15		0	0.0249	0.0597	0.1065	0.1684	0.2465	0.3400	0.4467	0.5624	0.6811	0.7953	0.8955	0.9704	1
3	11		0	0	0.0454	0.1205	0.2358	0.3919	0.5772	0.7677	0.9272	1	1	1	1	1
3	12		0	0	0.0391	0.1006	0.1926	0.318	0.4718	0.6416	0.8073	0.9410	1	1	1	1
3	13	Turbine output	0	0	0.0343	0.0861	0.1615	0.2640	0.3919	0.5388	0.6929	0.8376	0.9513	1	1	1
3	14		0	0	0.0305	0.0751	0.1383	0.2236	0.3309	0.4569	0.5947	0.7341	0.8613	0.9592	1	1
3	15		0	0	0.0275	0.0665	0.1205	0.1926	0.2836	0.3919	0.5134	0.6416	0.7677	0.8802	0.9654	1
4	11		0	0	0	0.0541	0.1491	0.2981	0.4955	0.7146	0.9080	1	1	1	1	1
4	12		0	0	0	0.0454	0.1205	0.2358	0.3919	0.5772	0.7677	0.9272	1	1	1	1
4	13		0	0	0	0.0391	0.1006	0.1926	0.318	0.4718	0.6416	0.8073	0.9410	1	1	1
4	14		0	0	0	0.0343	0.0861	0.1615	0.264	0.3919	0.5388	0.6929	0.8376	0.9513	1	1
4	15		0	0	0	0.0305	0.0751	0.1383	0.2236	0.3309	0.4569	0.5947	0.7341	0.8613	0.9592	1

Bibliography

[1] M. H. Albadi and E. F. El-Saadany, "The Role of Distributed Generation in Restructured Power Systems," in *IEEE PES 2008 North American Power Symposium (NAPS' 08)*, Calgary, AB, Canada, 2008, pp. 1-6.

[2] M. H. Albadi and E. F. El-Saadany, "Impacts of Wind Power Variability on Generation Costs- an Overview," *The Journal of Engineering Research (TJER),* vol. 7, to be published in June 2010.

[3] M. H. Albadi and E. F. El-Saadany, "Impacts of Wind Power Variability on Generation Costs: an Overview," in *International Conference on Computer Communication and Power (ICCCP' 09)*, Muscat, Oman, 2009, pp. 1-6.

[4] G. Pepermans, J. Driesen, D. Haeseldonckx, R. Belmans, and W. D'Haeseleer, "Distributed generation: definition, benefits and issues," *Energy Policy,* vol. 33, pp. 787-798, 2005.

[5] CIRED, "Dispersed generation: Preliminary report of CIRED working group WG04," June 1999.

[6] A. Chambers, *Distributed generation: a no technical guide*. PennWell, Tulsa, OK, 2001.

[7] T. Ackermann, G. Andersson, and L. Söder, "Distributed generation: a definition," *Electric Power Systems Research,* vol. 57, pp. 195-204, 2001.

[8] IEA, *Distributed Generation in Liberalised Electricity Markets*. Paris, 2002.

[9] IEEE Std 1547-2003, "IEEE Standard for Interconnecting Distributed Resources with Electric Power Systems", 2003.

[10] The Resource Dynamics Corporation, http://www.distributed-generation.com.

[11] W. El-Khattam, "Power Deleviry System Planning Implementing Distributed Generation." vol. PhD Waterloo: University of Waterloo, 2004.

[12] W. El-Khattam and M. M. A. Salama, "Distributed generation technologies, definitions and benefits," *Electric Power Systems Research,* vol. 71, pp. 119-128, 2004.

[13] International Association for Small Hydro. Definition of SHP.

[14] S. Doolla and T. S. Bhatti, "Automatic generation control of an isolated small-hydro power plant," *Electric Power Systems Research,* vol. 76, pp. 889-896, 2006.

[15] N. Jenkins and e. al, *Embedded Generation*. London: The Institute of Electrical Engineers, 2000.

[16] T. Au and T. Au, *Engineering Economics for Capital investment Analysis*. Boston: Allyn and Bacon Inc., 1983.

[17] K. Bhattacharya, M. H. J. Bollen, and J. E. Daalder, *Operation of restructured power systems*. USA: Kluwer Academic Publishers, 2001.

[18] V. Quezada and e. al., "Assessment of Energy Distribution Losses for Increasing Penetration of Distributed Generation," *IEEE Transactions On Power Systems,* vol. 21, May 2006.

[19] C. E. Commission, "DG Definition and Cost-benefit Analysis - Policy Inventory," July 2004.

[20] E. Z. Gumerman, R. R. Bharvirkar, K. H. LaCommare, and C. Marnay, "Evaluation Framework and Tools for Distributed Energy Resources," Feb 2003.

[21] J. B. Campbell, T. J. King, B. Ozpineci, D. T. Rizy, L. M. Tolbert, Y. Xu, and X. Yu, "Ancillary Services Provided From DER," National Technology Information Service ORNL/TM-2005/263, December 2005.

[22] M. H. Albadi and E. F. El-Saadany, "A summary of demand response in electricity markets," *Electric Power Systems Research,* vol. 78, pp. 1989–1996, 2008.

[23] M. H. Albadi and E. F. El-Saadany, "Demand Response in Electricity Markets: An Overview," in *IEEE PES 2007 General Meeting (GM' 07)*, Tampa, FL, USA, 2007, pp. 1-5.

[24] A Framework for Developing Collaborative DER Programs: Working Tools for Stakeholders: Report of the E2I Distributed Energy Resources Public/Private Partnership," Palo Alto, CA 2004.

[25] U.S. Combined Heat and Power Association, www.uschpa.org.

[26] Ministry of energy, Ontario, Canada, http://www.energy.gov.on.ca.

[27] Y.-H. Huang and J.-H. Wu, "A transition toward a market expansion phase: Policies for promoting wind power in Taiwan," *Energy,* vol. 34, pp. 437-447, 2009.

[28] European Wind Energy Association (EWEA), *Wind Energy The Facts: A Guide to the Technology, Economics and Future of Wind Power*. London: Earthscan Publications Ltd., 2009.

[29] J. Sawin and C. Flavin, "National policy Instruments: Policy Lessons for the Advancement and Diffusion of Renewable Energy Technologies around the World, World, Thematic Background Paper," in *The International Conference for Renewable Energies* Bonn, Germany, 2004.

[30] B. Lucy and K. Neuhoff, "Comparison of feed in tariff, quota and auction mechanisms to support wind power development," Cambridge University, Dept. Of Applied Economics 2004.

[31] J. A. Lesser and X. Su, "Design of an economically efficient feed-in tariff structure for renewable energy development," *Energy Policy,* vol. 36, pp. 981-990, 2008.

[32] WWEA, "World Wind Energy Report 2008," Bonn, February 2009.

[33] H. Lund and B. V. Mathiesen, "Energy system analysis of 100% renewable energy systems--The case of Denmark in years 2030 and 2050," *Energy,* vol. 34, pp. 524-531, 2009.

[34] Q. Y. Meng and R. W. Bentley, "Global oil peaking: Responding to the case for abundant supplies of oil'," *Energy,* vol. 33, pp. 1179-1184, 2008.

[35] U. Bardi, "Peak oil: The four stages of a new idea," *Energy,* vol. 34, pp. 323-326, 2009.

[36] R. L. Hirsch, "Peaking of word oil production: impacts, mitigation and risk management " 2005.

[37] E. Hau, *Wind turbines: fundamentals, technologies, application, economics* 2nd ed. Berlin: Springer Verlag, 2006.

[38] The Congress of the United States - Congressional Budget Office (CBO), "Prospects for Distributed Electricity Generation," Department of Energy, September 2003.

[39] Danish Wind Industry Association, Guided Tour on wind energy-Economics, http://www.windpower.org/en/tour/econ/.

[40] T. Ackermann, *Wind Power in Power Systems*. Chichester: John Wiley & Sons, 2005.

[41] D. D. Li and C. Chen, "A novel approach to estimate load factor of variable-speed wind turbines," *Power Systems, IEEE Transactions on,* vol. 20, pp. 1186-1188, 2005.

[42] D. S. Zinger and E. Muljadi, "Annualized wind energy improvement using variable speeds," *Industry Applications, IEEE Transactions on,* vol. 33, pp. 1444-1447, 1997.

[43] Vestas Wind Systems A/S, http://www.vestas.com.

[44] M. R. Patel, *Wind and Solar Power Systems*. New York: CRC Press, 1999.

[45] H. Holttinen, "Design and Operation of Power Systems with Large Amounts of Wind Power, first results of IEA collaboration," in *Global Wind Power Conference* Adelaide, Australia 2006.

[46] A. TrueWind, "An Analysis of the Impacts of Large-Scale Wind Generation on the Ontario Electricity System," April 2005.

[47] J. C. Smith, M. R. Milligan, E. A. DeMeo, and B. A. Parsons, "Utility Wind Integration and Operating Impact State of the Art," *IEEE Transactions on Power Systems,* vol. 22, pp. 900-908, 2007.

[48] J. C. Smith, M. R. Milligan, E. A. DeMeo, and B. A. Parsons, "Wind power impacts on Electric Power system operating costs: summary and perspective on work to data," in *the American Wind Energy Association Global WindPower Conference* Chicago, Illinois, 2004.

[49] GE Energy, "Ontario Wind Integration Study, a report prepared for Ontario Power Authority, Independent Electricity System Operator, and Canadian Wind Energy Association," October 6, 2006.

[50] Helimax Energy Inc, "Analysis Of Future Wind Farm Development In Ontario - A report prepared for Ontario Power Authority," March 2006.

[51] ILEX and UMIST, "Quantifying the system costs of additional renewables in 2020," 2002.

[52] E. Corp. and W. Inc, "Characterization of the Wind Resource in the Upper Midwest, Wind Integration Study-Task 1," Sep. 10 2004.

[53] R. Zavadil, J. King, L. Xiadong, M. Ahlstrom, B. Lee, D. Moon, C. Finley, L. Alnes, L. Jones, F. Hudry, M. Monstream, and S. Lai, "Final Report - Wind Integration Study," J. Smith Xcel Energy, Minnesota Department of Commerce, EnerNex Corporation, and Wind Logics Inc. Sep. 2004.

[54] R. Piwko, X. Bai, K. Clark, G. Jordan, N. Miller, and J. Zimberlin, "The Effects of Integrating Wind Power on Transmission System Planning, Reliability, and Operations: Report on Phase 2, Prepared for The New York State Energy Research and Development Authority," March 2005.

[55] The North American Electric Reliability Corporation (NREC), Reliability Standards, http://www.nerc.com.

[56] H. A. Gil and G. Joss, " Integration of Wind Generation with Power Systems in Canada: overview of Technical and economical impacts," CANMET Energy Technology Centre – Varennes CETC 2006-016, February 2006.

[57] M. H. Albadi and E. F. El-Saadany, "The role of taxation policy and incentives in wind-based distributed generation projects viability: Ontario case study," *Renewable Energy,* vol. 34, pp. 2224-2233, 2009.

[58] M. H. Albadi and E. F. El-Saadany, "The Role of Taxation policy and Incentives in Wind-based Distributed Generation Projects Viability: Ontario SOP Case Study," in *IEEE PES 2008 North American Power Symposium (NAPS' 08)*, Calgary, AB, Canada, 2008, pp. 1-6.

[59] M. H. Albadi and E. F. El-Saadany, "Wind Power in Ontario: An Economical Valuation," in *IEEE Canada 2007 Annual Electrical Power Conference (EPC' 07)*, Montréal, QC, Canada, 2007, pp. 496-501.

[60] Ontario Power Authority, "Supply Mix Advice and Recommendations report," 9 December 2005.

[61] Canadian Wind Energy Association (CanWEA), Canada's Current Installed Capacity, www.canwea.ca.

[62] Ontario Power Authority, Renewable Energy Standard Offer Program, http://www.powerauthority.on.ca/sop/.

[63] Bank of Canada, www.bankofcanada.ca.

[64] Canadian Wind Energy Atlas, http://www.windatlas.ca.

[65] K. Thomsen and P. Sorensen, "Fatigue loads for wind turbines operating in wakes," *Journal of Wind Engineering and Industrial Aerodynamics,* vol. 80, pp. 121-136, 1999.

[66] T. Wekken, "Wind farm Development and Operation: A Case Study," Leonardo Energy January 2007.

[67] W. Sullivan, E. Wcks, and J. Luxhoj, *Engineering Economy*. New Jersey: Prentice Hall, 2006.

[68] The California Energy Commission, Economics of Owning and Operating DER Technologies, http://www.energy.ca.gov/distgen/economics/operation.html.

[69] S. Starky, Capital Cost Allowance, Parliamentary Information and Research Service, Parliament of Canada, Ottawa, Ontario, April 2006.

[70] Current Generation Inc., Taxing Wind in Canada: Property Tax Assessment Policies and Practices in Canada, Canadian Wind Energy Association, 2005.

[71] Natural Resources Canada, http://www.nrcan-rncan.gc.ca/com/index-eng.php.

[72] Deloitte Touche Tohmatsu, Deloitte Quick Tax Facts 2007, 24 January 08, http://www.deloitte.com.

[73] M. H. Albadi, E. F. El-Saadany, and H. A. Albadi, "Wind to power a new city in Oman," *Energy,* vol. 34, pp. 1579-1586, October 2009.

[74] M. H. Albadi, E. F. El-Saadany, and H. A. Albadi, "Wind to Power a New City in Oman," in *International Conference on Computer Communication and Power (ICCCP' 09)* Muscat, Oman, 2009, pp. 1-6.

[75] UN Cartographic Section, Map of Oman, January 2004, No. 3730 Rev. 4, http://www.unhcr.org/refworld/docid/460a393b2.html.

[76] Ministry of Tourism - Oman, http://www.omantourism.gov.om.

[77] Ministry of National Economy - Oman, http://www.moneoman.gov.om.

[78] H. Lund, "Renewable energy strategies for sustainable development," *Energy,* vol. 32, pp. 912-919, 2007.

[79] J. A. Carta, P. Ramírez, and S. Velázquez, "A review of wind speed probability distributions used in wind energy analysis: Case studies in the Canary Islands," *Renewable and Sustainable Energy Reviews,* vol. In Press, Corrected Proof.

[80] A. S. S. Dorvlo and D. B. Ampratwum, "Wind energy potential for Oman," *Renewable Energy,* vol. 26, pp. 333-338, 2002.

[81] A. S. Malik and A. Awsanjli, "Energy fuel saving benefit of a wind turbine," in *Proceedings of the 12th IEEE Mediterranean Electrotechnical Conference MELECON 2004.* , 2004, pp. 1041-1044 Vol.3.

[82] Oman Tender Board, http://www.tenderboard.gov.om.

[83] The Authority for Electricity Regulation - Oman, http://www.aer-oman.org.

[84] M. Ilkan, E. Erdil, and F. Egelioglu, "Renewable energy resources as an alternative to modify the load curve in Northern Cyprus," *Energy,* vol. 30, pp. 555-572, 2005.

[85] A. S. S. Dorvlo, "Estimating wind speed distribution," *Energy Conversion and Management,* vol. 43, pp. 2311-2318, 2002.

[86] Y. Himri, S. Rehman, B. Draoui, and S. Himri, "Wind power potential assessment for three locations in Algeria," *Renewable and Sustainable Energy Reviews,* vol. 12, pp. 2488-2497, 2008.

[87] I. AWS Scientific, "Wind Resource Assessment Handbook," Golden, Colorado 1997.

[88] Authority for Electricity Regulation - Oman, Study on Renewable Energy Resources in Oman - Final Report, Muscat, May 2008.

[89] E. Díaz-Dorado, C. Carrillo, J. Cidrás, and E. Albo, "Estimation of Energy Losses in a Wind Park," in *9th International Conference on Electrical power Quality and Utilization* Barcelona, Spain, 2007.

[90] A. Graves, K. Harman, M. Wilkinson, and R. Walker, "Understanding availability trend of operation wind farms," in *AWEA Wind Power Conference* Houston, 2008.

[91] R. Gupta, "Economic implications of non-utility-generated wind energy on power utility," *Computers & Electrical Engineering,* vol. 28, pp. 77-89, 2002.

[92] Energy Information Administration, Short Term Energy Outlook- July 8, 2008 Release.

[93] Energy Information Administration, Oman Energy Data, Statistics and Analysis - Oil, Gas, Electricity, Coal. http://www.eia.doe.gov/emeu/cabs/Oman/NaturalGas.html.

[94] M. H. Albadi and E. F. El-Saadany, "Wind Turbines Capacity Factor Modeling - A Novel Approach," *IEEE Transactions on Power Systems,* vol. 24, pp. 1637-1638, 2009.

[95] M. H. Albadi and E. F. El-Saadany, "New Method for Estimating the CF of Pitch-regulated Wind Turbines " submitted to *Eclectic Power System Research*.

[96] R. D. Prasad, R. C. Bansal, and M. Sauturaga, "Some of the design and methodology considerations in wind resource assessment," *IET Renewable Power Generation,* vol. 3, pp. 53-64, 2009.

[97] Z. M. Salameh and I. Safari, "Optimum windmill-site matching," *IEEE Transaction on Energy Conversion,* vol. 7, pp. 669-676, 1992.

[98] Y. Tai-Her and W. Li, "A Study on Generator Capacity for Wind Turbines Under Various Tower Heights and Rated Wind Speeds Using Weibull Distribution," *IEEE Transaction on Energy Conversion,* vol. 23, pp. 592-602, 2008.

[99] V. G. Rau and S. H. Jangamshetti, "Normalized Power Curves as a Tool for Identification of Optimum Wind Turbine Generator Parameters," *IEEE transaction on Energy Conversion,* vol. 16, p. 283, Sep 2001 2001.

[100] S. H. Jangamshetti and V. G. Ran, "Optimum siting of wind turbine generators," *IEEE Transaction on Energy Conversion,* vol. 16, pp. 8-13, 2001.

[101] S. H. Jangamshetti and V. G. Rau, "Site matching of wind turbine generators: a case study," *IEEE Transaction on Energy Conversion,* vol. 14, pp. 1537-1543, 1999.

[102] E. N. Dialynas and A. V. Machias, "Reliability modelling interactive techniques of power systems including wind generating units," *Archiv Fuer Elektrotechnik* vol. 72, pp. 33 - 41, 1989.

[103] C. G. Justus, W. R. Hargraves, and A. Yalcin, "Nationwide Assessment of Potential Output from Wind-Powered Generators," *Journal of Applied Meteorology,* vol. 15, 1976.

[104] P. Giorsetto and K. F. Utsurogi, "Development of a New Procedure for Reliability Modeling of Wind Turbine Generators," *power apparatus and systems, ieee transactions on,* vol. PAS-102, pp. 134-143, 1983.

[105] R. Pallabazzer, "Evaluation of wind-generator potentiality," *Solar Energy,* vol. 55, pp. 49-59, 1995.

[106] M. H. Albadi and E. F. El-Saadany, "Effect of Power Curve Model Accuracy on CF Estimation of Pitch-regulated Turbines," in *CIGRÉ Canada 2009 Conference on Power Systems* Toronto, ON, Canada, 2009, pp. 1-13.

[107] T.-J. Chang and Y.-L. Tu, "Evaluation of monthly capacity factor of WECS using chronological and probabilistic wind speed data: A case study of Taiwan," *Renewable Energy,* vol. 32, pp. 1999-2010, 2007.

[108] A. N. Celik, "Energy output estimation for small-scale wind power generators using Weibull-representative wind data," *Journal of Wind Engineering and Industrial Aerodynamics,* vol. 91, pp. 693-707, 2003.

[109] J. Bird, *Engineering Mathematics*: Elsevier Newnes, 2003.

[110] M. H. Albadi and E. F. El-Saadany, "Optimum Turbine-Site Matching," submitted to *Energy*.

[111] M. H. Albadi and E. F. El-Saadany, "Novel Method for Estimating the CF of Variable Speed Wind Turbines," in *IEEE PES 2009 General Meeting (GM '09)* Calgary, Alberta, Canada, 2009.

[112] S. H. Jangamshetti and V. Guruprasada Rau, "Height extrapolation of capacity factors for wind turbine generators," *IEEE Power Engineering Review,* vol. 19, pp. 48-49, 1999.

[113] AAER Inc., http://www.aaer.ca.

[114] ENERCON GmbH, http://www.enercon.de.

[115] Gamesa Corporación Tecnológica's, http://www.gamesa.es.

[116] General Electric Company, http://www.ge-energy.com.

[117] Nordex AG, http://www.nordex-online.com.

[118] Siemens Power Generation AG, http://www.powergeneration.siemens.com.

[119] Fuhrlaender AG, http://www.fuhrlaender.de.

[120] National Renewable Energy Laboratory, http://www.nrel.gov/wind.

[121] Personal correspondence with fuhrlaender A. G. sales representative, the cost of different FL2500 tower heights, Sep. 2008.

[122] M. H. Albadi and E. F. El-Saadany, "Overview of Wind Power Intermittency Impacts on Power Systems," *Electric Power Systems Research,* 2009, doi:10.1016/j.epsr.2009.10.035 .

[123] M. H. Albadi and E. F. El-Saadany, "Comparative Study on Impacts of Wind Profiles on Thermal Units Scheduling Costs," submitted to *IET Renewable Power Generation*.

[124] M. H. Albadi and E. F. El-Saadany, "The effects of wind profile on thermal units generation costs," in *IEEE PES 2009 Power Systems Conference and Exposition (PSCE '09)*, Seattle, WA, USA, 2009, pp. 1-6.

[125] P. Meibom, C. Weber, R. Barth, and H. Brand, "Operational costs induced by fluctuating wind power production in Germany and Scandinavia," *IET Renewable Power Generation,* vol. 3, pp. 75-83, 2009.

[126] P. Meibom, C. Weber, R. Barth, and H. Brand, "Operational costs induced by fluctuating wind power production in Germany and Scandinavia, Deliverable D5b - Disaggregated system operation cost and grid extension cost caused by intermittent RESE grid integration," GreenNetEU27, 2006.

[127] N. P. Padhy, "Unit commitment-a bibliographical survey," *IEEE Transactions on Power Systems,* vol. 19, pp. 1196-1205, 2004.

[128] P. A. Ruiz, R. Philbrick, E. Zak, K. W. Cheung, and P. W. Sauer, "Uncertainty Management in the Unit Commitment Problem," *IEEE Transactions on Power Systems,* vol. 24, pp. 642 – 651, May 2009.

[129] U. A. Ozturk, M. Mazumdar, and B. A. Norman, "A solution to the stochastic unit commitment problem using chance constrained programming," *IEEE Transactions on Power Systems,* vol. 19, pp. 1589-1598, 2004.

[130] E. D. Castronuovo and J. A. P. Lopes, "On the optimization of the daily operation of a wind-hydro power plant," *IEEE Transactions on Power Systems,* vol. 19, pp. 1599-1606, 2004.

[131] V. S. Pappala, I. Erlich, K. Rohrig, and J. Dobschinski, "A Stochastic Model for the Optimal Operation of a Wind-Thermal Power System " *IEEE Transactions on Power Systems,* vol. 24, pp. 642 - 651, May 2009.

[132] N. Amjady, "Short-term hourly load forecasting using time-series modeling with peak load estimation capability," *IEEE Transactions on Power Systems,* vol. 16, pp. 798-805, 2001.

[133] F. Bouffard and F. D. Galiana, "Stochastic security for operations planning with significant wind power generation," in *IEEE 2008 Power and Energy Society General Meeting*, 2008, pp. 1-11.

[134] M. A. Ortega-Vazquez and D. S. Kirschen, "Estimating the Spinning Reserve Requirements in Systems With Significant Wind Power Generation Penetration," *IEEE Transactions on Power Systems,* vol. 24, pp. 114-124, 2009.

[135] L. Landberg, G. Giebel, H. A. Nielsen, T. Nielsen, and H. Madsen, "Short-term Prediction - An Overview," *Wind Energy,* vol. 6, pp. 273-280, 2003.

[136] R. Doherty and M. O'Malley, "A new approach to quantify reserve demand in systems with significant installed wind capacity," *IEEE Transactions on Power Systems,* vol. 20, pp. 587-595, 2005.

[137] L. Soder, "Reserve margin planning in a wind-hydro-thermal power system," *IEEE Transactions on Power Systems,* vol. 8, pp. 564-571, 1993.

[138] H. Bludszuweit, J. A. Dominguez-Navarro, and A. Llombart, "Statistical Analysis of Wind Power Forecast Error," *IEEE Transactions on Power Systems,* vol. 23, pp. 983-991, 2008.

[139] A. Fabbri, T. GomezSanRoman, J. RivierAbbad, and V. H. MendezQuezada, "Assessment of the Cost Associated With Wind Generation Prediction Errors in a Liberalized Electricity Market," *IEEE Transactions on Power Systems,* vol. 20, pp. 1440-1446, 2005.

[140] J. A. Gubner, *Probability and Random Processes for Electrical and Computer Engineers*. Cambridge: Cambridge University Press, 2006.

[141] B. Hasche, R. Barth, and D. J. Swider, "Effects of improved wind forecasts on operational costs in the German electricity system," in *EcoMod Conference on Energy and Environmental Modeling* Moscow, Russia, 2007.

[142] M. Lange and U. Focken, *Physical Approach to Short-Term Wind Power Prediction*. Berlin: Springer, 2006.

[143] U. Focken, M. Lange, K. Mönnich, H.-P. Waldl, H. G. Beyer, and A. Luig, "Short-term prediction of the aggregated power output of wind farms--a statistical analysis of the reduction of the prediction error by spatial smoothing effects," *Journal of Wind Engineering and Industrial Aerodynamics,* vol. 90, pp. 231-246, 2002.

[144] K. Methaprayoon, C. Yingvivatanapong, L. Wei-Jen, and J. R. Liao, "An Integration of ANN Wind Power Estimation Into Unit Commitment Considering the Forecasting Uncertainty," *IEEE Transactions on Industry Applications,* vol. 43, pp. 1441-1448, 2007.

[145] S. Takriti, J. R. Birge, and E. Long, "A stochastic model for the unit commitment problem," *IEEE Transactions on Power Systems,* vol. 11, pp. 1497-1508, 1996.

[146] J. Dupačová, N. Gröwe-Kuska, and W. Römisch, "Scenario reduction in stochastic programming," *Mathematical Programming,* vol. 95, pp. 493-511, 2003.

[147] C. W. Yu, L. Wang, F. S. Wen, and T. S. Chung, "Optimal Spinning Reserve Capacity Determination Using a Chance-constrained Programming Approach " *Electric Power Components and Systems,* vol. 35, pp. pages 1131 - 1143 October 2007.

[148] C. Yingvivatanapong, W.-J. Lee, and E. Liu, "Multi-Area Power Generation Dispatch in Competitive Markets," *IEEE Transactions on Power Systems,* vol. 23, pp. 196-203, 2008.

[149] P. M. Subcommittee, "IEEE Reliability Test System," *IEEE Transactions on Power Apparatus and Systems,* vol. PAS-98, pp. 2047-2054, 1979.

[150] C. Grigg, P. Wong, P. Albrecht, R. Allan, M. Bhavaraju, R. Billinton, Q. Chen, C. Fong, S. Haddad, S. Kuruganty, W. Li, R. Mukerji, D. Patton, N. Rau, D. Reppen, A. Schneider, M. Shahidehpour, and C. A. Singh, "The IEEE Reliability Test System-1996. A report prepared by

the Reliability Test System Task Force of the Application of Probability Methods Subcommittee," *IEEE Transactions on Power Systems,* vol. 14, pp. 1010-1020, 1999.

[151] C. Yingvivatanapong, "Multi-area unit commitment and economic dispatch with market operation components," in *Faculty of the Graduate School*. vol. PhD Arlington: The university of texas at Arlington, 2006.

[152] B. C. Ummels, M. Gibescu, E. Pelgrum, W. L. Kling, and A. J. Brand, "Impacts of Wind Power on Thermal Generation Unit Commitment and Dispatch," *IEEE Transaction on Energy Conversion,* vol. 22, pp. 44-51, 2007.

[153] R. Piwko, D. Osborn, R. Gramlich, G. Jordan, D. Hawkins, and K. Porter, "Wind energy delivery issues [transmission planning and competitive electricity market operation]," *IEEE Power and Energy Magazine ,* vol. 3, pp. 47-56, 2005.

[154] B. A. McCarl, *McCarl GAMS User Guide*, Version 22.6 ed.: GAMS Development Corporation, 2008.

[155] P. Meibom, R. Barth, H. Brand, and C. Weber, "Wind power integration studies using a multi-stage stochastic electricity system model," in *IEEE 2007 Power Engineering Society General Meeting*, 2007, pp. 1-4.

[156] E. Denny and M. O'Malley, "Quantifying the Total Net Benefits of Grid Integrated Wind," *IEEE Transactions on Power Systems,* vol. 22, pp. 605-615, 2007.

[157] US Department of Energy, Benefits of Demand Response in Electricity Markets and Recommendations for Achieving them, Report to the United States Congress, February 2006, http://eetd.lbl.gov.

[158] *International Energy Agency, The Power to Choose—Demand Response in Liberalized Electricity Markets, OECD, Paris, 2003.*

[159] K. Herter, P. McAuliffe, and A. Rosenfeld, "An exploratory analysis of California residential customer response to critical peak pricing of electricity," *Energy,* vol. 32, pp. 25-34, 2007.

[160] M. Piette, O. Sezgen, D.Watson, N.Motegi, C. Shockman, Development and Evaluation of Fully Automated Demand Response in Large Facilities, Prepared For California Energy Commission, Public Interest Energy Research (PIER) Program, March 30, 2004 (LBNL-55085).

[161] S. Valero, M. Ortiz, C. Senabre, C. A. A. C. Alvarez, F. J. G. A. F. F. J. G. Franco, and A. A. G. A. Gabaldon, "Methods for customer and demand response policies selection in new electricity markets," *IET Generation, Transmission & Distribution,* vol. 1, pp. 104-110, 2007.

[162] O. Sezgen, C. A. Goldman, and P. Krishnarao, "Option value of electricity demand response," *Energy,* vol. 32, pp. 108-119, 2007.

[163] Y. Tan, D. Kirschen, Classification of Control for Demand-side Participation, University of Manchester, 29 March 2007.

[164] P. Jazayeri, A. Schellenberg, W. D. Rosehart, J. A. D. J. Doudna, S. A. W. S. Widergren, D. A. L. D. Lawrence, J. A. M. J. Mickey, and S. A. J. S. Jones, "A Survey of Load Control Programs for Price and System Stability," *IEEE Transactions on Power Systems,* vol. 20, pp. 1504-1509, 2005.

[165] *C. Gellings, J. Chamberlin, Demand Side Management: Concepts and Methods, The Fairmont Press Inc., US, 1988.*

[166] Charles River Associates, Primer on Demand-SideManagement with an Emphasis on Price-Responsive Programs, Report prepared for The World Bank, Washington, DC, CRA No. D06090, available online: http://www.worldbank.org.

[167] E. Bloustein, School of Planning and Public Policy, Assessment of Customer Response to Real Time Pricing, Rutgers—The State University of New Jersey, June 30, 2005, available online: http://www.policy.rutgers.edu.

[168] D. S. Kirschen, "Demand-side view of electricity markets," *IEEE Transactions on Power Systems,* vol. 18, pp. 520-527, 2003.

[169] L. Goel, W. Qiuwei, and W. Peng, "Reliability enhancement of a deregulated power system considering demand response," in *IEEE 2006 Power Engineering Society General Meeting,* pp. 1-6, 2006.

[170] K. Spees and L. B. Lave, "Demand Response and Electricity Market Efficiency," *The Electricity Journal,* vol. 20, pp. 69-85, 2007.

[171] G. Barbose, C. Goldman, C. Neenan, A Survey of Utility Experience with Real Time Pricing, Lawrence Berkeley National Laboratory Report No. LBNL-54238, December 2004.

[172] D. Caves, K. Eakin, and A. Faruqui, "Mitigating Price Spikes in Wholesale Markets through Market-Based Pricing in Retail Markets," *The Electricity Journal,* vol. 13, pp. 13-23, 2000.

[173] S. Braithwait, K. Eakin, The role of demand response in electric power market design, Laurits R. Christensen Associates, Prepared for Edison Electric Institute, Madison, October 2002.

[174] M. G. Lijesen, "The real-time price elasticity of electricity," *Energy Economics,* vol. 29, pp. 249-258, 2007.

[175] D. S. Kirschen, G. Strbac, P. Cumperayot, and D. de Paiva Mendes, "Factoring the elasticity of demand in electricity prices," *IEEE Transactions on Power Systems,* vol. 15, pp. 612-617, 2000.

[176] A. K. David and Y. Z. Li, "Consumer rationality assumptions in the real-time pricing of electricity," *IEE Proceedings on Generation, Transmission and Distribution,* vol. 139, pp. 315-322, 1992.

[177] E. C. Banda and L. A. Tuan, "Modeling of demand response in electricity markets: effects of price elasticity," in *Power and Energy Systems*, Florida, 2007.